FILIPE ALEXANDRE ALDEIA VERÍSSIMO

IMPACT OF ALBUFEIRA BAY OUTFALL PLUMES IN BATHING WATER QUALITY, A MODELLING APPROACH

UNIVERSIDADE DO ALGARVE

Instituto Superior de Engenharia

2017

FILIPE ALEXANDRE ALDEIA VERÍSSIMO

IMPACT OF ALBUFEIRA BAY OUTFALL PLUMES IN BATHING WATER QUALITY, A MODELLING APPROACH

Mestrado em Ciclo Urbano da Água

Trabalho efetuado sob a orientação de:

Prof. Doutor Flávio Martins (Universidade do Algarve)

Doutor António Martins (Águas do Algarve, S.A.)

UNIVERSIDADE DO ALGARVE

Instituto Superior de Engenharia

2017

IMPACT OF ALBUFEIRA BAY OUTFALL PLUMES IN BATHING WATER QUALITY, A MODELLING APPROACH

Declaração de autoria de trabalho

Declaro ser o autor deste trabalho, que é original e inédito. Autores e trabalhos consultados estão devidamente citados no texto e constam da listagem de referências incluída.

Faro, 11 de junho de 2017

(Filipe Alexandre Aldeia Veríssimo)

ACKNOWLEDGEMENTS

This Master Thesis was accomplished in Instituto Superior de Engenharia (ISE) from the University of Algarve (UALG), in a partnership with Águas do Algarve, S.A. From the present work resulted an oral presentation at the International Symposium on Outfall Systems in Ottawa, May 2016 and an oral presentation at the 17.º ENASB in Guimarães, September 2016.

Firstly, I would like to express my sincere gratitude to my advisor Prof. Flávio Martins for the continuous support of my study and related research, for his patience, motivation, and immense knowledge. His guidance helped me in all the time of research and writing of this thesis. I could not have imagined having a better advisor and mentor for my Master Thesis for the third time. My sincere thanks also goes to João Janeiro, for all the help and support provided during this work. Without his precious support it would not be possible to conduct this research.

I am also thankful to Águas do Algarve, S.A. Administration for their financial and logistical support and for providing necessary guidance concerning this work implementation. I would like to thank my Department Director Joaquim Freire for enabling my participation in this Master Thesis program and providing me with all the necessary tools for the research. I would like to thank all of my work colleagues namely my supervisor Noémia Bento and António Martins for is comments on the papers that resulted from this work. I would like to thank Rita Baptista, Fernando Gabriel and Luís Ponte for the help with the field work.

I also would like to thank the developers and contributors of open source software such as QGis (qgis.org), MOHID (mohid.com), Linux Lite (linuxliteos.com), Cumulus (sandaysoft.com) that indirectly contributed to the elaboration of the present work.

I thank my fellow classmates for the stimulating discussions, for the nights we were working together before deadlines, and for all the fun we have had in the last years.

I would like to thank my family: my parents and to my brother for supporting me spiritually throughout writing this thesis and my life in general.

I would like to thank my daughters for the challenges that put me every day, they gave me the strength to complete this work.

Finally, I must express my very profound gratitude to my spouse Ana, for providing me with unfailing support and continuous encouragement throughout the last years of study and through the process of researching and writing this thesis. This accomplishment would not have been possible without you. Thank you.

RESUMO

O turismo em zonas balneares é responsável por pressões nas infraestruturas do ciclo urbano da água e recursos hídricos, nomeadamente na conceção de sistemas de abastecimento de água e saneamento. O presente trabalho tem como objetivo avaliar o comportamento hidrodinâmico de três emissários submarinos e impacte na qualidade das águas balneares na baía de Albufeira usando uma abordagem de modelação matemática, com base no software MOHID. São investigados os principais processos que controlam a dispersão na baía. Os primeiros desenvolvimentos consistem numa série de campanhas de medição e colheita de dados (parâmetros microbiológicos, caudais, vento, etc.) que fornecem os dados para caracterizar a dispersão neste sistema costeiro. Uma rede de pontos de observação e controlo são definidos para avaliar o impacte das plumas na zona de influência dos emissários submarinos. A aplicação e desenvolvimento do modelo de dispersão proporciona uma melhor compreensão e controlo dos processos de diluição e dispersão na baía. Os resultados da modelação são utilizados para avaliar a necessidade de desinfeção, que pode reduzir custos operacionais e permitirá um aumento da resiliência do sistema em caso de falhas nas infraestruturas de colheita, transporte e de tratamento de águas residuais e proporcionar um melhor funcionamento e gestão de instalações.

Keywords: modelação matemática, emissário submarino, águas balneares, diluição, Albufeira, MOHID

ABSTRACT

Tourism activity in bathing areas is responsible for important pressures on urban water cycle facilities and water resources, especially regarding the design of water supply and treatment systems. The present work aims at evaluating the hydrodynamic and water quality behaviour of three marine outfalls located in Albufeira Bay using a mathematical modelling approach, using the MOHID modelling system to investigate the main processes controlling dispersion in this coast. The first developments consist in a series of measurement campaigns and data collection (microbiological parameters, flow, wind, etc.) providing the data to characterize the dispersion in this coastal system. A net of control observation points and monitoring boxes are be defined to evaluate the impact of the plumes in the coastal areas of interest. The application and development of the dispersion model provides a better understanding and control of dilution and dispersion processes in the bay. The modelling results are used to evaluate the need for disinfection, which can potential reduce costs and enable an increase in the system's resilience in case of failures in the wastewater collection, transport and treatment facilities, providing better operation and management.

Keywords: modelling, submarine outfall, dilution, bathing waters, Albufeira, MOHID

RESUMO ALARGADO

Este estudo foi conduzido numa parceria entre a Universidade do Algarve (Portugal) e a Águas do Algarve S.A., empresa responsável pelos sistemas multimunicipais de abastecimento de água para consumo humano e tratamento de águas residuais na região do Algarve. Ele tem como objetivo avaliar o comportamento hidrodinâmico de três emissários submarinos localizados na baía de Albufeira e o respetivo impacte na qualidade das águas balneares usando uma abordagem de modelação matemática. Para este efeito foi utilizado o modelo hidrodinâmico tridimensional MOHID.

O sistema MOHID Water é um programa de modelação matemática que possibilita a simulação de processos hidrodinâmicos, fenómenos de dispersão (abordagem lagrangeana e euleriana), propagação de ondas, transporte de sedimentos, qualidade da água / processos biogeoquímicos na coluna de água e trocas com o fundo. Para este estudo, o modelo hidrodinâmico resolve as equações primitivas incompressíveis tridimensionais que são acopladas a um modelo de transporte lagrangeano para simular o transporte das plumas de águas residuais descarregadas através de emissários submarinos no campo afastado. A diluição inicial (campo próximo) das águas residuais descarregadas pelos emissários submarinos é calculada acoplando o modelo hidrodinâmico 3D ao modelo MOHIDJet, necessitando apenas das características dos difusores de cada emissário submarino. O sistema MOHID utiliza o método dos volumes finitos para a discretização espacial. O modelo implementado consiste em três modelos acoplados, sendo que o primeiro nível apenas lê os resultados do modelo operacional do Algarve (SOMA). Esta configuração é baseada no método de *downscaling* necessitando de menos requisitos computacionais. A batimetria e malha horizontal foram construídas com base na batimetria do Algarve (resolução ~ 50 m) e o domínio do modelo na zona de influência dos emissários submarinos apresenta uma malha com resolução de 40 m.

A área de estudo encontra-se localizada no Algarve, em Albufeira. O município de Albufeira tem no turismo a sua principal atividade económica e acolhe uma grande fração dos turistas que visitam o Algarve. A qualidade das águas balneares é, portanto, vital para as suas atividades económicas. O transporte e processos de tratamento de águas residuais na região são expostos a diferentes ciclos ao longo do ano à medida que a ocupação turística da região aumenta, aumentando assim a pressão sobre as instalações do ciclo urbano da água. A cidade de Albufeira é servida por uma estação de tratamento de águas residuais com capacidade para 130000 habitantes equivalentes cujo efluente tratado é descarregado por um emissário submarino (Vale Faro) com 1000 metros de comprimento e representa o principal emissário abordado no

presente estudo. As linhas de água da cidade estão secas durante a maior parte do ano, com exceção da Ribeira de Albufeira que recebe o efluente tratado de outra estação de tratamento de águas residuais localizada a 6 km do centro da cidade de Albufeira. Esta ribeira desemboca na praia Peneco, cujo afluente da mesma é descarregado por um emissário submarino (Pluviais) com 800 m de comprimento de modo a evitar a descarga de água na zona balnear. Finalmente um terceiro emissário (Inatel), com 600 metros de comprimento, recolha eventuais descargas de uma pequena linha de água contígua à ETAR de Vale Faro.

A primeira fase do trabalho compreendeu a realização de 3 campanhas de campo que compreenderam a colheita e análise dos efluentes descarregados pelos emissários submarinos e de vários pontos no mar num raio de cerca de 200 m dos difusores dos emissários submarinos. Estas campanhas foram realizadas no mesmo dia das colheitas para controlo da qualidade das águas balneares realizada pela Agência Portuguesa do Ambiente. Os caudais descarregados foram medidos e os dados foram completados usando registos históricos. Os dados obtidos permitiram uma caracterização da área de estudo e das descargas dos emissários submarinos.

Os resultados das campanhas de monitorização, mostraram contaminação de *escherichia coli* no emissário de Pluviais em ambas as campanhas e no emissário do Inatel na segunda campanha, indiciando a descarga de águas residuais nas linhas de água a montante da entrada nos emissários submarinos. No entanto se verificaram concentrações de *escherichia coli* superiores ao valor limite em qualquer das zonas balneares.

Os resultados do modelo implementado mostram soluções realistas que permitem a caracterização da dispersão, a sua eficiência e os processos que a controlam. O modelo foi aplicado na Baía Albufeira, obtendo a variação temporal das correntes, maré, salinidade, e os parâmetros bacteriológicos em pontos estipulados do domínio analisado.

Os resultados obtidos pelo modelo matemático permitem avaliar o impacte ambiental das descargas dos três emissários submarinos com várias condições de vento na baía de Albufeira e zonas balneares adjacentes. As principais condições que promovem a dispersão na baía são o vento e a maré. As concentrações de *escherichia coli* são maiores no início da manhã, diminuindo à medida que se verifica o aumento de radiação solar devido à radiação UV forte e voltam a aumentar no final do dia quando os caudais descarregados são também maiores. As condições de vento simuladas mostram que o risco de contaminação da qualidade das águas balneares é maior nas praias da baía de Albufeira (Peneco, Pescadores, Inatel e Alemães), principalmente com ventos de S e SE, enquanto os ventos N e O afastam as plumas das praias.

Vários cenários ambientais e de descarga foram testados para estudar a sensibilidade do sistema de emissário a estas condições. Os resultados permitem prever as consequências de falhas no sistema e ajudam a entidade gestora do sistema de águas residuais a gerir esses eventos. Os resultados também permitem adaptar o nível de tratamento final (desinfeção) da estação de tratamento de águas residuais, reduzindo custos operacionais nomeadamente no sistema de desinfeção do efluente secundário cujo custo energético representa uma fatia substancial do consumo total da ETAR.

Como sugestão para trabalhos futuros, propõe-se a instalação a título definitivo de uma estação meteorológica na ETAR de Vale Faro e a realização de trabalhos de inspeção vídeo ao emissário submarino de modo a avaliar a condição estrutural do mesmo e condições de descarga pelo difusor.

CONTENTS

LIST OF FIGURES

LIST OF TABLES

LIST OF EQUATIONS

ACRONYMS AND ABREVIATIONS

ADA	Águas do Algarve, S.A.
APA	Agência Portuguesa do Ambiente (Environmental Portuguese Agency)
BOD	Biological Oxygen Demand
CMA	Câmara Municipal de Albufeira (Albufeira Municipality)
COD	Chemical oxygen demand
CORJET	Cornell Buoyant Jet Integral Model
CORMIX	Cornell Mixing Zone Expert System
DGT	Direção Geral do Território (Portuguese Territory Agency)
EU	European Union
FIB	Faecal Indicator Bacteria
FRS	Flux Relaxation Scheme
GOTM	Global Ocean Turbulence Model
HDPE	High-density Polyethylene
INE	Instituto Nacional de Estatística (Portuguese Statistics Institute)
IPAC	Instituto Português de Acreditação (Portuguese Accreditation Institute)
IST	Instituto Superior Técnico
MARETEC	Marine and Environmental Technology Research Center
SOMA	Algarve Operational Modelling and Monitoring System
TSS	Total Suspended Solids
UALG	Universidade do Algarve (University of Algarve)
UV	Ultra Violet
WFD	Water Framework Directive
WS	Weather Station
WWTP	Waste Water Treatment Plant

SYMBOLS

A	Area (m^2)
C_d	Drag coefficient
D_D	Port diameter (m)
g	Acceleration of gravity (m/s^2)
D_D	Port diameter (m)
K_B	Decay rate
p	Pressure (N/m^2)
p_{atm}	Atmospheric pressure (N/m^2)
P	Property
Q_0	Port flow (m^3/s)
S	Salinity (ppm)
T	Temperature (ºC)
T_{90}	Time interval necessary for bacterial concentration decrease by 90%
t	Time (s)
u	Velocity x component (m/s)
v	Velocity y component (m/s)
z	Depth (m)
β_0	Angle between the port normal vector projection in the horizontal plane and the x direction
Δh_0	length of the emitted “cylinder” (m)
Δt	Time step (s)
η	Free surface elevation (m)
θ_m	Angle between the port normal vector and the horizontal plane
ρ	Density (kg/m^3)
ρ_a	Air density (kg/m^3)
ρ_e	Jet Density at the Port exit (kg/m^3)
ρ_0	Reference Density (kg/m^3)

1 INTRODUCTION

1.1 OVERVIEW

This study was conducted as a close partnership between the University of the Algarve (UALG) and Águas do Algarve, S.A. (ADA). ADA is Algarve's Sanitation Multi-Municipal System (Figure 1.1) concessionaire for a thirty years' period (2004…). The Algarve is the southernmost region of Portugal, with an area of 4,997 (DGT, 2014) square kilometres and a resident population of 451,006 (INE, 2012) permanent inhabitants, number that typically triples during the holiday season.

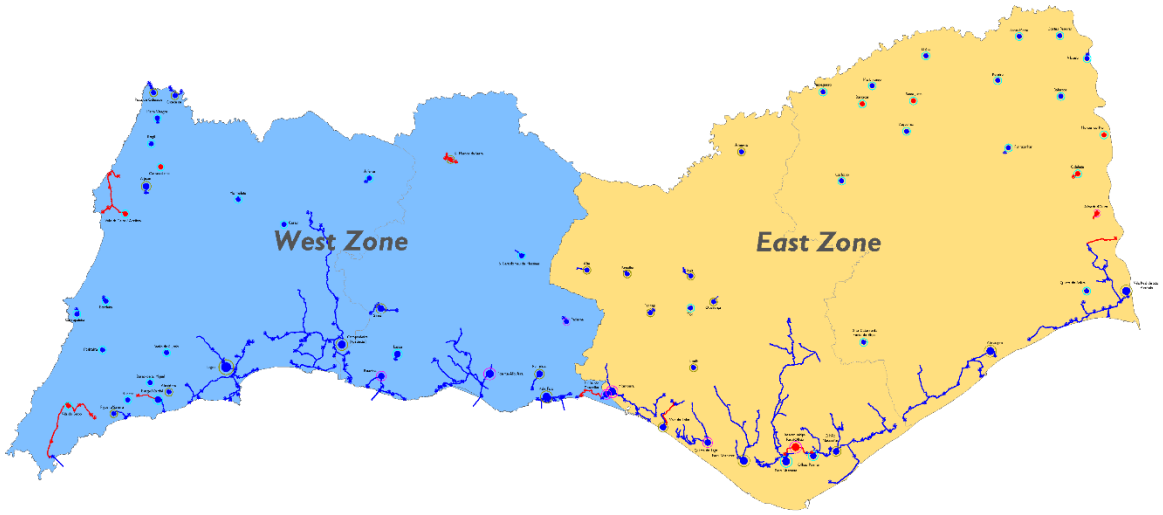

Figure 1.1. Algarve Multi-Municipal Sanitation System

ADA manages the infrastructures intended for interception, treatment and final disposal of waste water collected from the Algarve's sixteen Municipalities. The system has 447.3 kilometres of drainage systems, 175 waste water pumping stations and 66 Waste Water Treatment Plants (WWTP). The waste water volume treated in 2015 was 43.14 cubic hectometres, 88 % of which in WWTP with the secondary treatment level (removal of Biological Oxygen Demand (BOD_5), Chemical Oxygen Demand (COD) and Total Suspended Solids (TSS)) and 11 % with a tertiary treatment level (Phosphorus (P) and Nitrogen (N) removal). About 97 % of the treated effluent was disinfected with Ultraviolet (UV), chlorination systems or in maturation lagoons and 95 % of the treatment capacity are located near sensitive receiving environment, bathing waters or aquaculture production.

The Albufeira municipality has tourism as its main activity, hosting a large fraction of the tourists visiting the Algarve; therefore, bathing water quality is vital for its economic activities. waste water treatment and transport facilities have different cycles throughout the year as the tourist occupation of the region increases in the summer months, thus increasing the pressure

on the urban water cycle facilities and water resources, providing infrastructure management challenges.

Portuguese coastal waters offer hydrodynamic conditions, associated with wind wave action, which are among the most favourable in Europe for dilution and dispersion of treated waste water. To take advantage of this fact some municipalities dispose their urban effluents in these coastal waters through submarine outfalls, after different levels of treatment onshore (Santos *et al.*, 2011). The coast of the Albufeira Municipality hosts six outfalls, from which three are in service at present in the Albufeira Bay (Figure 1.2).

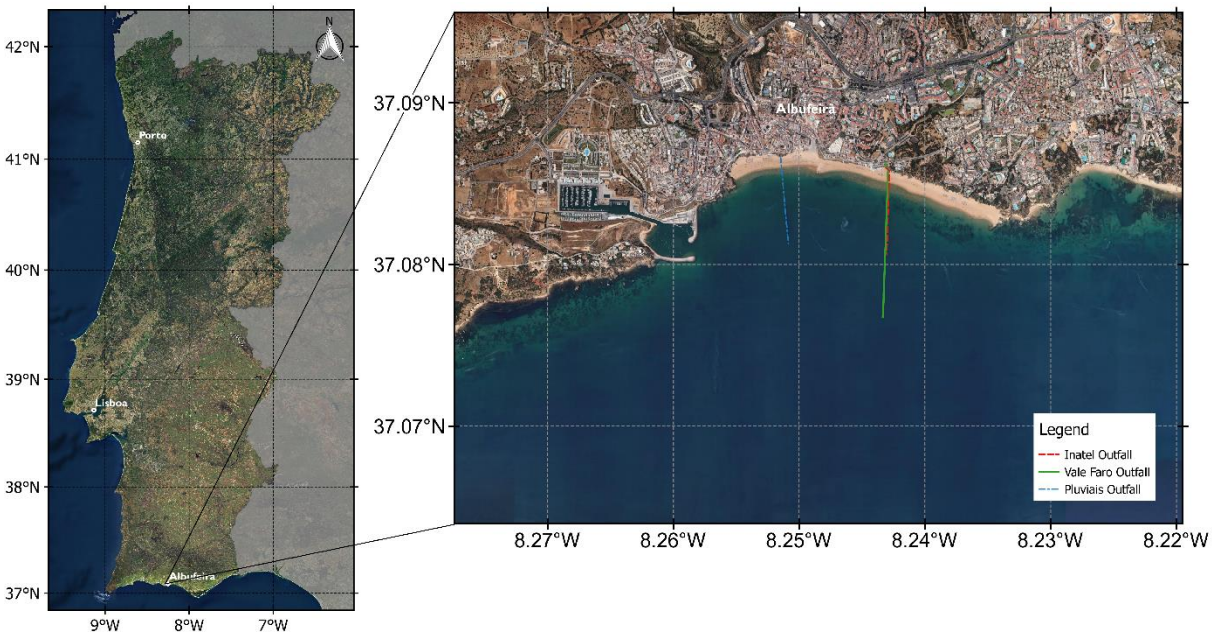

Figure 1.2. Location of Albufeira Bay

The main outfall studied in this work serves the Vale Faro WWTP managed by ADA, while the other two are managed by the Municipality. The effluents discharged by these three outfalls and the bathing waters in their area of influence represent the study area targeted in this work.

The Vale Faro WWTP was built in 1980 and it was subjected to an improvement and expansion in 2002, to allow the removal of nutrients and reusing the treated effluent to produce recycled water. The treated effluent was discharged through a 400-millimetre diameter, 600-metre-long submarine outfall (Inatel outfall) that was replaced in 2005 for a 1000-millimetre diameter outfall 800-metre-long by ADA due to lack of transport capacity of the old outfall. Although the improvement accommodated changes in the process for removal of nutrients, the WWTP discharge license, only requires compliance with the parameters COD, BOD_5 and *Escherichia coli* in treated effluent.

The city's water lines are dry for most of the year, with the exception of the stream "Ribeira de Albufeira" receiving the treated effluent from another WWTP located six kilometres from the city centre. This stream ends at the "Peneco" beach, and the tributary flow is discharged by the 800 metres long "Pluviais" outfall. Finally, the 600 metres long "Inatel" (old Vale Faro WWTP outfall) outfall discharges the effluents of another small stream of water into the bay. This two outfall flows may have punctual contamination of raw sewage due to clogging or contaminated storm water in the city's sewage network.

As referred to in the preceding paragraphs, the Albufeira Bay bathing waters are heavily exposed to the urban occupation of the territory and therefore there is a need to better understand the transport processes of the outfall plumes in the bay. Monitoring is a key factor to achieve good water quality status in bathing waters and mathematical modelling tools can provide a better understanding of the processes controlling the system and the impact of management actions in water infrastructures. Regarding this matter, the European Union (EU) Water Framework Directive (WFD) (2000/60/EC) promotes the use of modelling techniques to monitor water quality for better understanding the transport and fate of microbial pathogens in the coastal waters, and for predicting the effect of changing weather- and discharge conditions on the water quality at the beaches (Eregno *et al.*, 2016; Martins *et al.*, 2009).

1.2 SCOPE AND OBJETIVES

This study aims at evaluating the hydrodynamic behavior of three marine outfalls and impacts of the outfall plumes on the bathing water quality of the beaches located in the Albufeira bay, using a mathematical modeling approach. The MOHID water modelling system was chosen to investigate the key processes controlling the dispersion on this coast. A series of water sampling from the outfalls discharges and ocean samples along with flow measurements were planned and executed helping the validation and comparison of model results with data collected from the field campaigns. The MOHID three-dimensional hydrodynamic model and the Lagrangian tracer transport model were coupled with the near field model MOHIDJET and applied to study the marine outfalls in the Albufeira Bay. Preliminary results of this modelling system will allow the characterization of dispersion in the bay, its efficiency and the identification of the processes controlling it. In a second phase, to get more accurate results and better determination of dynamic characteristics of the discharged effluent in the receiving ambient environment, a nested domain approach was used, linking the initial tested model with the Algarve operational model (Janeiro *et al*., 2012; Janeiro, 2014; Janeiro *et al.*, 2017).

1.3 DISSERTATION OUTLINE

The current chapter aims to present a comprehensive view, very synthetic, focused in the description of each of the major components of this work. The thesis is organized into seven chapters and annexes, including this first chapter with the Introduction.

1 INTRODUCTION - The first chapter presents the general background of the topic discussed, which aims to clarify the nature of the problem and the possible solution found for it.

2 BACKGROUND AND LITERATURE REVIEW - This chapter provides the theory for the realization of this work. It gives a general vision of bathing water quality management, waste water treatment, modelling the dispersion of wastewater submarine outfalls, operational modelling and modelling systems.

3 CASE STUDY - This chapter is intended to provide information of the case study, which describes the general operation of the wastewater treatment plant, the submarine outfalls and their characteristics. The climate conditions of the region and the conditions of the receiving environment are also characterized.

4 METHODOLOGY - This chapter presents the data required for the construction and describes the way the nested hydrodynamic and Lagrangian dispersion models were implemented, which include the coastal area where the Vale Faro, Pluviais and Inatel outfall plumes dispersion occur. The scenarios used in this study are explained and characterized. This chapter also shows a description of the mathematical modelling tool (MOHID Water Modelling System) used in this work as well as the assumptions made. The grids used in the simulations and the initial and boundary conditions imposed on the models are also described.

5 RESULTS - The results are presented in chapter. The first results showed are those obtained in field campaigns followed by the results of the mathematical model for the scenarios considered and its comparison with the field data.

6 DISCUSSION

- In this chapter, the results are analysed and the factors that influence the dispersion of bacterial plumes are discussed.

7 CONCLUSIONS - The last chapter sets out the main conclusions of this work. It also addresses the future work.

2 BACKGROUND AND LITERATURE REVIEW

2.1 URBAN WATER CYCLE

Most of us understand the basics of the hydrologic cycle (condensation, precipitation, transportation, and evaporation). Generally, it is defined as a conceptual model describing the storage and circulation of water between the biosphere, atmosphere, lithosphere, and the hydrosphere. These processes operate on global scales and in natural environments. But on local scales and in engineered environments like cities, a different cycle dominates: the urban water cycle (Figure 2.1). The hydrologic cycle is greatly modified by urbanisation impacts on the environment and the need to provide water services to the urban population, including water supply, drainage, wastewater collection and management, and beneficial uses of receiving waters. Thus, it was noted that the hydrological cycle becomes more complex in urban areas, because of many anthropogenic influences and interventions. (Marsalek, *et al.*, 2006)

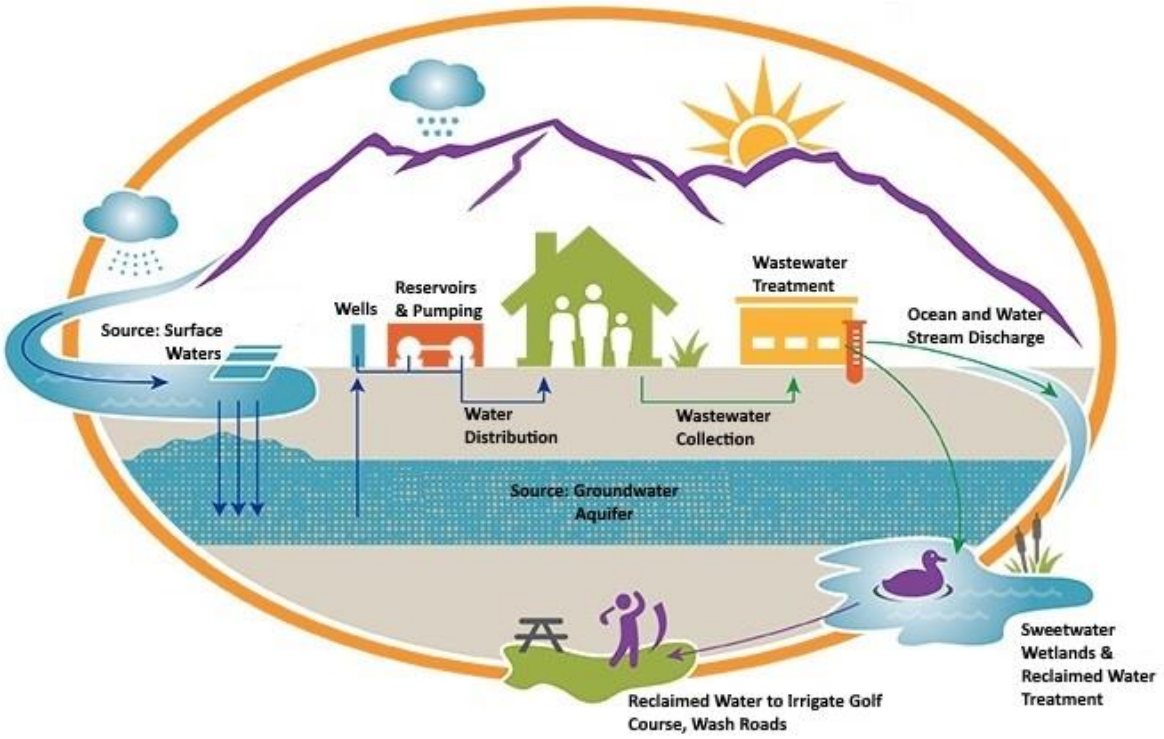

Figure 2.1. The Algarve Urban Water Cycle. Adapted from (Tucson Water, 2017)

Water, of course, is a part of everyday life, from supplying our drinking water to removing our wastes. It is also the largest mass flux into and out of cities, more than food, freight, people, or anything else. Just as water circulates in the global hydrologic cycle, water in our cities flows in an urban water cycle, one of the modern world's fundamental systems (National Geographic, 2017).

Source

Many freshwater sources are found in the environment as a result of geological and meteorological phenomena. Water needed in urban areas may come from groundwater or surface water sources such as lakes, reservoirs, and rivers. It is called untreated or raw water, which is usually transported to a water treatment plant. The degree of treatment depends on the raw water quality and the purpose that this water will be used for (Marsalek, *et al.*, 2006).

Water Treatment

To be suitable for distribution and human use, raw water must be treated to remove contaminants and pathogens. Design of appropriate treatment processes depends on water quality. At a basic level, disinfection is necessary to deactivate harmful microorganisms. More advanced treatment involves a sequence of screening, settling, filtering, disinfection, and chemical adjustments at a water treatment facility (National Geographic, 2017).

Water Distribution

After treatment, finished water is distributed to customers through a pressurized system of pipes, pumps, valves, and storage reservoirs. While much of this infrastructure is buried and invisible, it is an important system that ensures that water is available when and where we need it (National Geographic, 2017).

Use

Water customers use the supplied water for various purposes. Industries use water for manufacturing and cleaning. Businesses and offices use water for daily operations. At home, residents use water for cooking, bathing, laundry, drinking, and landscaping (National Geographic, 2017).

Wastewater Collection

The opposite of distribution, wastewater collection systems (sewers) collect used water and convey it, usually by gravity, to a wastewater treatment facility. This occurs through a network of increasingly large pipes. A typical urban wastewater stream is more than 99% water and less than 1% waste (National Geographic, 2017).

Wastewater Treatment

After use, water quality has been degraded and requires treatment before it can be reintroduced into the environment. The quantity and quality of wastewater is determined by many factors.

Not all humans or industries produce the same amount of waste. The amount and type of waste produced in households is influenced by the behaviour, lifestyle and standard of living of the inhabitants as well as the technical and juridical framework by which people are surrounded. (Henze & Comeau, 2008)

Wastewater treatment uses physical, chemical, and biological processes to remove wastes from the influent and restore water quality. Once treated, the effluent is discharged to the environment and the cycle begins again.

While these six components are typical, the urban water cycle varies among cities, or even among parts of cities. Sometimes an intermediate transmission step conveys raw water from a source to a treatment facility. In one shortcut, treated wastewater can be reused directly as reclaimed water; this can be practical when the effluent quality exceeds the natural source quality.

While not directly included in the cycle, storm water runoff can be transformed from a waste product into a resource by practices of low-impact development. Rainwater harvesting is a shortcut from source to use, where rainwater is collected for outdoor applications such as gardening. A given urban system may combine these methods in varying degrees.

Each component in the urban water cycle brings its own benefits and challenges, and understanding them is the first step to developing sustainable water solutions for our growing population.

(National Geographic, 2017)

2.2 WASTEWATER TREATMENT AND DISPOSAL

WWTP are key facilities for safeguarding public health and the receiving environment. The WWTP are infrastructures composed by a set of processes, with the main objective to remove the contaminant loads in the waste water. There are different types of biological treatment, the treatment process chosen must be fitted to the required quality of treated waste water disposed in the receiving environment. Also, the size and design of the WWTP depends on the waste water flowrate and contaminant loads.

Typically, WWTPs are designed so that flow through the plant is obtained by gravity. The wastewater is frequently carried to the WWTP by gravity and, consequently, it is at a substantial depth below grade at the plant entrance. Thus, a pumping station is required to raise the sewage to an appropriate level to facilitate gravity flow through the plant. Flow measurement is an

essential component of the operation and management of the WWTP. Preliminary treatment typically serves three important functions: removal of untreatable solid materials; protection of subsequent treatment units and improvement of the performance of those units. Preliminary treatment unit operations include: screens, shredders or grinders, grit removal, and flow equalization (Davis, 2010).

The Vale Faro WWTP is equipped with screens, grit and grease removal after an initial pumping station. Sand, gravel, broken glass, egg shells, and other material having a settling velocity substantially greater than the organic material in wastewater is called grit. Grit removal is provided to protect mechanical equipment from abrasion and wear; reduce the formation of deposits in pipelines and channels; and reduce the frequency of digester cleaning that is required because of accumulated grit. A secondary, but none-the-less extremely desirable goal of the grit removal system is to separate the grit from the organic material in the wastewater. This separation allows the organic material to be treated in subsequent processes (Davis, 2010).

The major purpose of conventional secondary treatment is to oxidize the readily biodegradable BOD that escapes primary treatment and to provide further removal of suspended solids. Because of the increasing recognition of the deleterious effects of nutrients, tertiary treatment includes treatment of nitrogen and phosphorus.

The Vale Faro WWTP biological treatment type is activated sludge in oxidation ditch with UV disinfection at the final stage of the treatment. Treatment by activated sludge appeared in 1914, in England, by Arden and Lockett and consists in producing a mass of activated microorganisms capable of aerobic degrading of the organic in a biological reactor (Tchobanoglous *et al.*, 2003). After the biological reactor, there is the need to separate the biomass from the treated effluent, so a secondary sedimentation step is required to accomplish this task. In the biological reactor, microorganisms responsible for waste water treatment are kept in suspension in the form of flakes, being provided the oxygen required for biological oxidation of organic matter.

The conversion of BOD to microbial cells does little to reduce the BOD in the effluent if the cells are discharged. Likewise, suspended solids limits cannot be met if the microbial mass grown in the biological processes is discharged. The conventional secondary treatment technology to remove the biomass is settling. The function of secondary settling tanks is to produce a clarified effluent. Secondary settling tanks that follow activated sludge processes also serve the function of thickening to provide a higher solids concentration for either return activated sludge or wasting and subsequent treatment (Davis, 2010).

In the secondary sedimentation, the flakes settle and are separated from the liquid phase, thus leading to a solid-liquid separation. To ensure the adequate concentration of sludge in the biological reactor, a part of the biological sludge is recirculated from the secondary settling tank bottom to the beginning of the biological treatment. To maintain a correct solids retention time in the system, the excess sludge that formed in the reactor is generally purged from the base of settling tank, and pumped to the solid treatment phase (Tchobanoglous *et al.*, 2003).

The purpose of urban wastewater disinfection is to reduce disease bearing micro-organisms or pathogens concentrations to acceptable levels. This final stage before discharging the treated effluent in the receiving environment is the disinfection trough a Ultra-Violet (UV) system. UV light is produced by a special mercury lamp. The effectiveness of UV radiation depends on the dose received by the micro-organisms and this depends on:

- The intensity of the radiation;
- The path length from the source to the microorganisms;
- The contact time at the required dose; and
- The quality of the wastewater (particularly regarding turbidity).

(EPA Ireland, 1997)

UV systems are energy intensive, and UV disinfection can account for approximately 10% to 25% of total electrical energy use at a municipal WWTP.

2.3 SUBMARINE OUTFALLS

Since long ago that the populations of coastal areas have used launching of effluent into the sea, as the natural dilution and dispersion of organic matter, pathogens and other pollutants is a good solution from an economic point of view. However, this discharge may be harmful to marine flora and fauna, and the population, if done indiscriminately and without control.

The most usual technique involves the use of a submarine outfall (Figure 2.2) consisting of a pipeline that transports waste water, treated waste water or runoff within a certain distance of the coast, promoting their dispersion in marine waters, usually by a series of strategically placed holes in the final section of the outfall (diffuser).

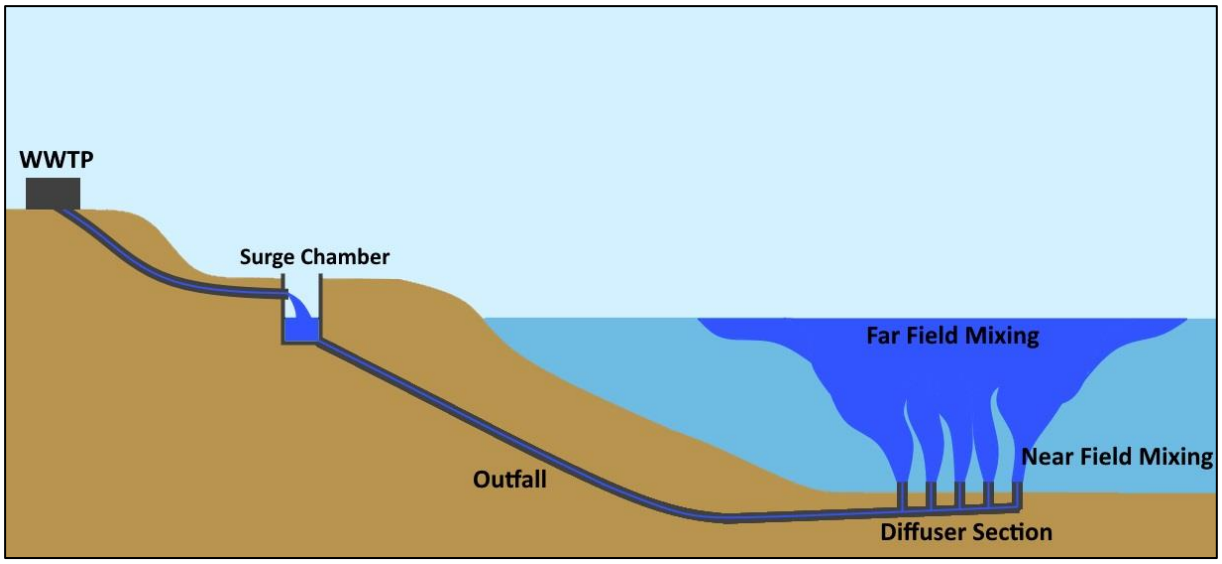

Figure 2.2. A marine wastewater disposal system

Submarine outfalls require minimal operational and maintenance and their reliability are much higher than WWTP, that require high operational and maintenance costs and are subject to malfunctions, especially in developing countries. Submarine outfalls usually range from 1 to 4 kilometres long and discharge into waters 20 to 70 metres deep (Roberts *et al.*, 2010).

The design of a marine outfall focuses on the dilution required to meet the relevant guidelines. Occasionally, guidelines may be met after an appropriate level of wastewater treatment onshore. However, many substances will rely on the dilution with marine waters to meet these guidelines. Dilution depends on:

- Wastewater flowrate;
- Depth of water into which the wastewater is discharged;
- Length of the diffuser;
- Outlet diameter (and whether single or multiple outlets will be used);
- Configuration of the diffuser (e.g., whether T-section outlets or gas-burner type rosettes are used, whether duckbill valves are used);
- Ocean conditions (e.g., currents, stratification of the water column, tides, and ocean turbulence).

Together with cost, the above factors are used to optimize the location and configuration of a submarine outfall. (Tate *et al.*, 2016)

For coastal cities, preliminary treatment followed by discharge through an effective outfall is therefore an affordable, effective, and reliable solution. It is simple to operate and free of negative health and environmental impacts. Many outfalls of this type are successfully

functioning and they have a proven track record in many coastal cities all over the world. A monitoring program should be initiated prior to and continuing after the discharge commences to verify the performance of the outfall and to determine if higher treatment levels are needed. This prevents unnecessary investment in expensive treatment plants, or, even worse, advanced treatment that is unaffordable and results in ‘‘no action,’’ and continued contamination of bathing waters. An outfall system (Figure 2.2), including the outfall and near field, could in fact be considered a treatment plant. It provides a high level of treatment that can be much superior to that which any conventional land-based plant can achieve (Roberts *et al.*, 2010).

Land-based plants can, in extreme cases, remove up to 95%, of BOD and TSS. If the effluent is not disinfected, they remove 50–80% of pathogenic organisms, leaving it with practically the same health risk as raw sewage, although stabilization lagoons can achieve up to 99% pathogens removal with a long detention time. But a well-designed outfall system reduces the concentrations of all contaminants by more than 99% by physical dilution. For pathogenic organisms, even this may be insufficient, but considering their mortality in the marine environment, a well-designed outfall can ensure levels below that which could cause health risks on bathing waters (Roberts et al., 2010).

One can consider two types of jets discharged through submarine outfalls, a positively buoyant jet like the one discharged from a wastewater treatment plant or cooling water from an energy plant and a negatively buoyant jet like the effluent of brine from a desalination plant. In Figure 2.3 it’s possible to identify the two types of jets discharged from a marine outfall.

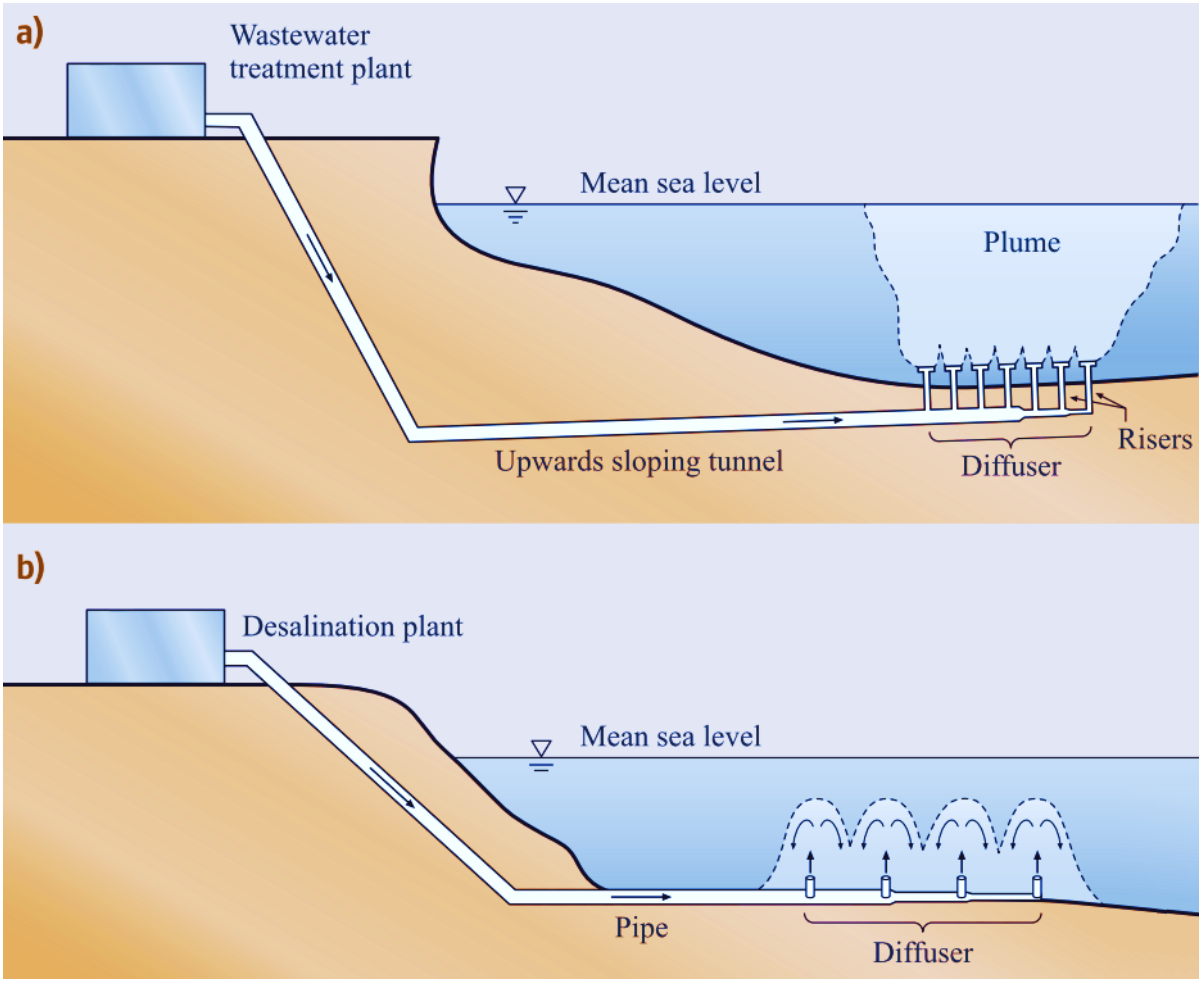

Figure 2.3. Schematics of (a) a positively buoyant jet, and (b) a negatively buoyant jet (Adapted from Tate *et al.*, 2016)

The efficiency of preliminary treatment combined with an effective outfall has been demonstrated in many field studies. Their impacts are small and contained in a limited area. For example, the results of five years of observations of two outfalls in Chile, each consisting of preliminary treatment followed by an effective outfall show that the concentrations at 100 metres from the diffusers for all parameters, except *faecal* and total coliforms, are similar to background values. Although the concentrations of coliforms in the effluents are extremely high, their concentrations are reduced to levels that meet stringent standards about 100 m from the diffusers, and with mortality they quickly fall to background levels beyond this. The study concludes that:

(i) The effect of the outfalls on the ocean water quality is insignificant;

(ii) Heavy metals and micropollutants were below detectable limits around the outfall;

(iii) There were no negative effects on benthic communities.

(Roberts *et al.*, 2010).

2.4 BATHING WATER QUALITY

Water quality can be defined as a set of values of the physical, chemical, biological and microbiological water that allows to evaluate their suitability for certain direct or potential uses.

The first European bathing water legislation, in the form of the 'Bathing Water Directive'[1], was published in 1975, in Portugal, this directive became law in 1998 (DL 236/98, August 1). It was one of the first and most important legislative elements published concerning the European policy on water, its main objectives are to safeguard public health and protect the aquatic environment in coastal and inland areas from pollution (Georgiou & Bateman, 2005). According to Directive 76/160/EEC, bathing water definition is "all running or still fresh waters or parts thereof and sea water, in which: bathing is explicitly authorized by the competent authorities of each member State, or bathing is not prohibited and is traditionally practised by a large number of bathers". According to these assumptions, any place where there is a significant affluence of users is likely to be regarded as bathing area and become subject to periodic analysis to check the quality of its water in accordance with the actual legislation.

Revised European legislation on bathing waters, the New Bathing Water Directive (2006/7/EC) was adopted in 2006, transposed to Portuguese law DL 113/2012, May 23. The revised directive alters the method by which water quality is measured, focusing on the most relevant analytical parameters, which include microbiologic indicators such as intestinal enterococci and *Escherichia coli* instead of *faecal* coliforms. However, the results obtained for *faecal* coliforms with *Escherichia coli* and for *faecal* streptococci with intestinal enterococci are equivalent (Mansilha *et al.*, 2009).

Thus, in accordance with current law, sampling frequency, starts 15 days before the bathing season, as follows:

- Biweekly analysis during the bathing season for bathing waters not showing significant variations in quality. If the bathing waters have shown good quality at least in the two preceding seasons, the frequency can be monthly;
- When systematic quality changes are common, the analysis frequency required is weekly.

[1] Directive 76/160/EEC concerning the quality of bathing water.

The water quality requirements classification (Directive 2006/7/EC) are set according to the values listed on Table 2.1.

Table 2.1. Coastal waters and transitional waters requirements (Directive 2006/7/EC)

Parameter	Excellent quality	Good quality	Sufficient	Reference methods of analysis
Intestinal enterococci (cfu/100 ml)	100*	200*	185**	ISO7899-1 or ISO7899-2
Escherichia coli (cfu/100 ml)	250*	500*	500**	ISO9308-3 or ISO9308-1

* Based upon a 95-percentile evaluation, ** Based upon a 90-percentile evaluation.

All bathing waters must achieve at least "Sufficient" quality classification by the end of the bathing season. To achieve this objective, it should be taken the appropriate measures to increase the number of bathing waters classified as "Good" and "Excellent" quality.

The limit values for each sample, according to the decision of the Technical Monitoring Commission of 12/02/2010 of the Law 135/2009, of 3 June in the version amended by the Law 113/2012, of 23 May are displayed in Table 2.2.

Table 2.2. Biological parameters limit values in bathing waters

Parameter	Limit Value (cfu/100 ml)
Intestinal enterococci	350
Escherichia coli	1,200

Bathing waters are considered "unfit for bathing", understanding that bathing should be discouraged or even forbidden (in the last case if the Health Authority considers relevant risk to bather's health, bans bathing) when the result of the analysed parameters exceeds any of the limit values showed in in Table 2.2.

When the values are equal to or lower than the standard, bathing waters are considered "water suited for bathing", bathing can occur without restrictions related to the quality of bathing water.

The monitoring water quality results that are carried out during the bathing season are made available to the public (http://snirh.pt) and if the results justify, the public are immediately alerted and the red flag is hoisted, banning baths.

The new bathing water directive simplifies management and surveillance methods for bathing water sites. Under the directive, countries also elaborate bathing water profiles for all their bathing water sites and ensure they are available to the public. These bathing water profiles

describe the physical and hydrological conditions of bathing areas and analyses potential impacts on (and potential threats to) their water quality. The bathing water profiles serve both as sources of information for citizens and as a management tool for the competent authorities. The Algarve bathing water profiles can be consulted in the APA web site (www.apambiente.pt/index.php?ref=19&subref=906&sub2ref=910).

A bathing water profile is produced for each of the designated bathing waters. These are intended to provide useful information to the public, and are written in accordance with the requirements of the Bathing Water Directive. Each bathing water profile includes:

- a description, map and photograph of the bathing water;
- information on potential pollution sources and risks to water quality;
- description of actions being taken to improve water quality;
- information on reporting and responding to any pollution incidents;
- local contact details for sources of further information

Waste water is poured into the aquatic environment via several routes: discharges produced under normal operation of the urban water cycle facilities, which include storm overflows, uncontrolled discharges or failures in the system. Modelling the evolution of pollutants and several survey points allows the definition of spatial and temporal variability in the concentration of bacteriological indicators, which are fundamental for the adequate definition of the bathing water profile (López *et al.*, 2013).

2.5 COASTAL HYDRODYNAMICS

The description of hydrodynamic processes in the ocean are based on the momentum conservation law, the mass conservation law and the heat conservation law. The mixing behavior of any wastewater discharge is governed by the interplay of ambient conditions in the receiving water body and by the discharge characteristics.

The ambient conditions in the receiving water body, be it stream, river, lake, reservoir, estuary or coastal waters, are described by the water body's geometric and dynamic characteristics. Important geometric parameters include plan shape, vertical cross-sections, and bathymetry, especially in the discharge vicinity. Dynamic characteristics are given by the velocity and density distribution in the water body, again primarily in the discharge vicinity. In many cases, these conditions can be taken as steady-state with little variation because the time scale for the mixing processes is usually of the order of minutes up to perhaps one hour. In some cases, notably tidally influenced flows, the ambient conditions can be highly transient and the

assumption of steady-state conditions may be inappropriate. In this case, the effective dilution of the discharge plume may be reduced relative to that under stead state conditions (Jirka *et al.*, 1996).

The dynamic processes that exist in the nearshore region are generated by a number of different drivers. Under the influence of these external forces, the fluid motion of the water manifests itself as coastal currents, tides and tidal currents, internal and surface waves, storm surges, tsunamis and others (Horikawa, 1988).

The main difference between coastal waters and deep ocean waters is the presence of two physical constraints (i.e., the sea bottom, at a relatively shallow depth, and the coastline) which somehow determine the motion of the sea water.

The nearshore zone is defined as the region extending from a landward limit associated with storm-wave phenomena (e.g., over wash), to a seaward limit beyond the point where incident waves break, but which depends on the specific context (Horikawa, 1988). Within this zone, several other regions may be distinguished, as shown in Figure 2.4 (Horikawa, 1988). The most relevant of these are the breaker zone, the breaking point, and the surf zone. The former is the zone where incident irregular waves break; the breaking point is where breaking begins and the waves attain maximum height, and the surf zone is defined as the region between the seaward limit of the breaker zone and the area of high turbulence created by the collision of the backrushing water mass and the incoming waves (Horikawa, 1988).

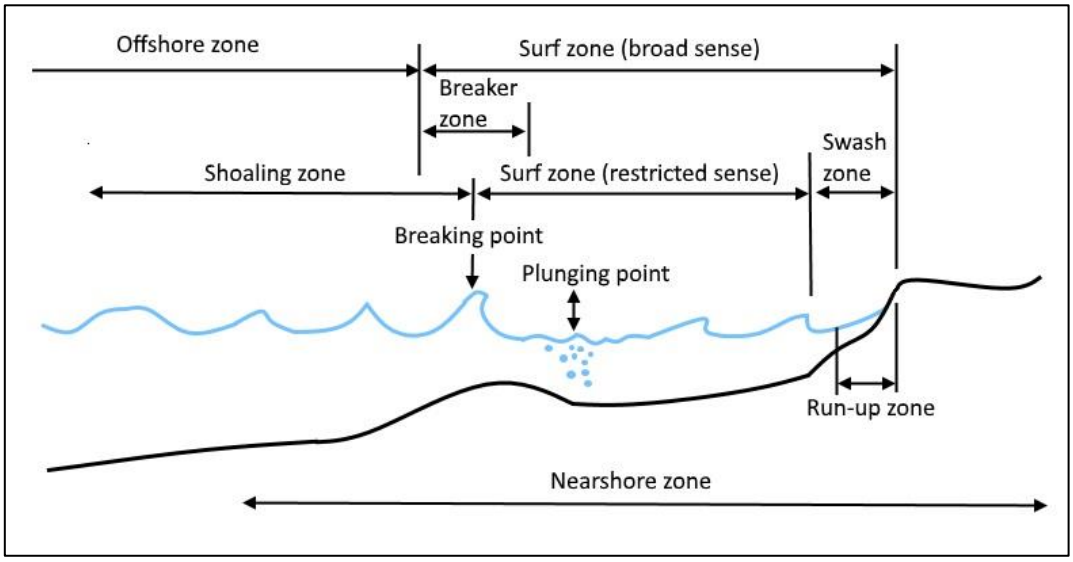

Figure 2.4. Zone division in the nearshore region (Adapted from Horikawa, 1988)

According to Sánchez-Arcilla & Lemos (1990), the relevant phenomena in the surf zone can be classified into four distinct types:

1. Sediment transport and corresponding changes in morphology, with a characteristic time scale of 1 day to 1 month, and a spatial scale between 100 m and 1000 m,
2. Currents (non-oscillatory flow), with time scales between 10 minutes and 1 hour, and spatial scales similar to those of sediment transport,
3. Organised oscillatory flows (i.e., wind waves, infra-gravity waves), with time scales ranging from 10-1 sec to 10 min, and space scales from 1 to 100 m.
4. Random oscillatory flow (turbulence), whose length scales are between 10^{-3} to 10^{1} sec, and with small (10^{-4} to 10^{-1} m) spatial scales.

In a general overview, it can be said that the main features in coastal hydrodynamics are the wind waves, generated by the stress exerted on the ocean surface by the wind. As these waves travel from deep waters into shallower regions, they become more non-linear and dissipative, transferring energy from the peak of the spectrum to higher and lower frequencies. Eventually, the proximity of the sea bottom will induce the breaking of the waves, producing a severe increase in the marine turbulence level, and generating different types of currents, which may extend beyond the surf zone (Prinos, 2016).

However, the study of nearshore hydrodynamics is not an easy task. Wave, current and turbulence scales tend to overlap, thus giving rise to the interaction (to some degree) of these three flow types; since the individual flows are non-linear in nature, their interaction becomes quite complex. The usual procedure followed to derive and understand the governing equations is to decompose all the state variables into contributions from currents, waves and turbulence, and then use time-averaging operators to isolate the desired phenomenon (Prinos, 2016).

2.5.1 Waves

Waves are a common occurrence in everyday life, and can be manifested as, for example, the motion of a plucked guitar string, ripples on a pond, or the billows on the ocean. A definition of wave motion can be stated as a means whereby energy is transported across or through a material without any significant overall transport of the material itself. (Open University, 1999)

All waves can be regarded as progressive waves, in that energy is moving through, or across the surface of the material. Waves which travel through the material are called body waves, for example, sound waves and seismic P- and S-waves. The most familiar surface waves are those which occur at the interface between atmosphere and ocean, caused by the wind blowing over the sea. Tides are also waves caused by the gravitational influence of the Sun and Moon and having periods corresponding to the causative forces. (Open University, 1999)

If two fluids layers having differing speeds are in contact, there is frictional stress between them and there is a transfer of momentum and energy. The frictional stress exerted by a moving fluid is proportional to the square of the speed of the fluid, so the wind stress exerted upon a water surface is proportional to the square of the wind speed. Ate the sea-surface, most of the transferred energy results in waves, although a small proportion is manifested as wind-driven currents. (Open University, 1999)

To simplify the theory of surface waves, it is assumed that the wave-form is sinusoidal and can be represented by the curves shown in Figure 2.5.

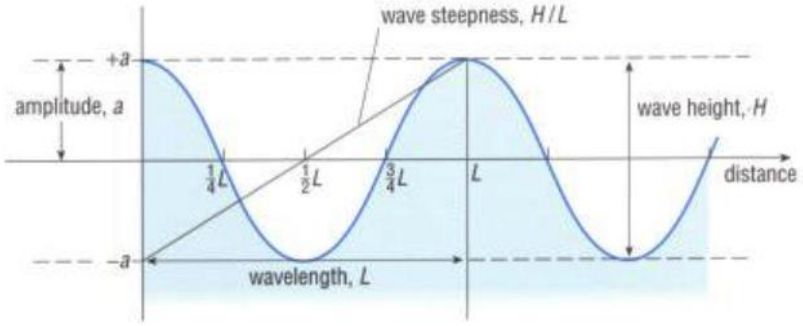

Figure 2.5. Idealized water wave form. Credits: (Open University, 1999)

The **wave height** (H) refers to the overall vertical change in height between the wave crest (or peak) and the wave trough. The wave height is twice the wave **amplitude** (a). **Wavelength** (L) is the distance between two successive peaks. **Steepness** is defined as wave height divided by wave length (H/L), it's not the same thing as the slope of the sea surface between a wave crest and its adjacent trough. The time interval between two successive peaks passing a fixed point is known as the **period** (T), and is generally measured in seconds. The number of peaks which pass a fixed point per second is known as the **frequency** (*f*). (Open University, 1999)

Short waves are waves, generated by the wind that propagate towards the beach. They can be either actively forced by the wind (wind waves) or they can have left their generation area (swell waves). Incident waves are the primary source of energy input to the beach. On their way from deep water towards the shoreline they undergo refraction and shoaling processes. As the waves propagate towards the shoreline, the wave shape becomes increasingly skewed with peaked wave crests and longer, rounded wave troughs, and wave orbital velocities become larger under crests than under troughs. This is a characteristic of fundamental importance to sediment transport, especially seaward of the wave breakpoint as there will be a tendency for the incident waves to push sediment towards the beach. (Mangor, 2008)

The short waves are the single most important parameter in coastal morphology. Wave conditions vary considerably from site to site, depending mainly on the wind climate and on the type of water area. The short waves are divided into:

- **Wind waves**, also called storm waves, or sea. These are waves generated and influenced by the local wind field. Wind waves are normally relatively steep (high and short) and are often both irregular and directional, for which reason it is difficult to distinguish defined wave fronts. The waves are also referred to as short-crested. Wind waves tend to be destructive for the coastal profile because they generate an offshore (as opposed to onshore) movement of sediments, which results in a generally flat shoreface and a steep foreshore.
- **Swell** are waves, which have been generated by wind fields far away and have travelled long distances over deep water away from the wind field, which generated the waves. Their direction of propagation is thus not necessarily the same as the local wind direction. Swell waves are often relatively long, of moderate height, regular and unidirectional. Swell waves tend to build up the coastal profile to a steep shoreface.

The long waves are primarily second order phenomena of shallow water wave processes. The four main types of long waves are:

- **Surf beat** - Natural waves often show a tendency to wave grouping, where a series of high waves follows a series of low waves. This is especially pronounced on open sea-coasts, where the incoming waves may be of different origins and will thus have a large spreading in wave heights, wave directions, and wave periods (or frequencies). Wave grouping will cause oscillations in the wave set-up with a period corresponding to approx. 6 – 8 times the mean wave period; this phenomenon is called surf-beats.
- **Harbour resonance** is forced oscillation of a confined water body (e.g. a harbour basin or a lagoon) connected to a larger water body (the sea).
- A **seiche** is the free oscillation of a water body, probably caused by rapid variations in the wind conditions. Seiche can occur in closed water areas, such as lakes or lagoons, and in semi-closed water bodies, such as bays.
- A **tsunami** is a single wave, which is generated by sub-sea earthquakes; it typically has a period of 5 to 60 minutes. Tsunami waves can travel long distances across the oceans; they are similar to shallow water waves, which means that the speed v is calculated as the square root of the product of the water depth and the acceleration of gravity. Consequently, tsunamis travel very fast in the deep oceans. A tsunami is normally not

very high in deep water, but when it approaches the coastline, the wave will be shoaling and can reach a height of more than 10 m.

Waves are traditionally measured with wave rider buoys. More recently, remote sensing techniques for measuring waves have been developed, see Measuring waves and currents by X-band radar. (Mangor, Waves, 2008)

2.5.2 Tides

Tides are the longest of oceanic waves. So long in fact, that often, we only observe them as a rise and fall of sea level over a period of several hours. Together with wind-generated waves, tides play an extremely important part in coastal processes, geomorphology, flood risk, species zonation and water quality (Prinos, 2016).

The tides of our planet display extremely complex behaviour. For example, in the Mediterranean, the tidal range is very small (<1m), whereas in the Bay of Fundy, Canada, the shape of the bay augments the tidal range to over 15 m. In Europe, the biggest tides can be found in the Severn estuary (12 m) in the UK and near Mont Saint Michel, in France, where the tide goes out 9 km and reputedly comes in faster than a person can run (Prinos, 2016).

The importance of tides around our coasts is often in the currents they generate, which can reach speeds of up to 5 m/s (Bay of Fundy). The rising tide is usually referred to as the flood, whereas the falling tide is called the ebb. The tidal currents of the ebb and flood play a major part in shaping our coasts, transporting large volumes of sediment and moulding estuary environments.

From the earliest times, it has been recognised that there is a connection between the tides and the moon. The most observable effect is that the tidal range is largest when the Moon is full or new (Prinos, 2016).

Today, in contrast to the majority of coastal processes, the tides can be predicted with very good accuracy, for as many as two hundred years into the future. However, there is sometimes a difference between the observed and predicted tide, due to weather induced effects such as the storm surge (Prinos, 2016). The latest version of the FES (Finite Element Solution) tide model developed in 2014-2016 is FES2014, an improved version of the FES2012 model. The new FES2014 model was developed, implemented and validated by the LEGOS, NOVELTIS and CLS, within a CNES funded project (AVISO+, 2017).

FES2014 takes advantage of longer altimeter time series and better altimeter standards, improved modelling and data assimilation techniques, a more accurate ocean bathymetry and a

refined mesh in most of shallow water regions. Special efforts have been dedicated to address the major non-linear tides issue and to the determination of accurate tidal currents.

2.5.3 Currents

An ocean current is a continuous, directed movement of seawater generated by forces acting upon this mean flow, such as breaking waves, wind, the Coriolis effect, cabbeling, temperature and salinity differences, while tides are caused by the gravitational pull of the Sun and Moon. Depth contours, shoreline configurations, and interactions with other currents influence a current's direction and strength. Ocean currents flow for great distances, and together, create the global conveyor belt which plays a dominant role in determining the climate of many of the Earth's regions. More specifically, ocean currents influence the temperature of the regions through which they travel.

Large-scale **surface ocean currents** are driven by global wind systems that are fuelled by energy from the sun. These currents transfer heat from the tropics to the Polar Regions, influencing local and global climate. The warm Gulf Stream originating in the tropical Caribbean, for instance, carries about 150 times more water than the Amazon River. The current moves along the U.S. East Coast across the Atlantic Ocean towards Europe. The heat from the Gulf Stream keeps much of Northern Europe significantly warmer than other places equally as far north. (NOAA, 2011)

Differences in water density, resulting from the variability of water temperature and salinity, also cause ocean currents. This process is known as thermohaline circulation. In cold regions, such as the North Atlantic Ocean, ocean water loses heat to the atmosphere and becomes cold and dense. When ocean water freezes, forming sea ice, salt is left behind causing surrounding seawater to become saltier and denser. Dense-cold-salty water sinks to the ocean bottom. Surface water flows in to replace the sinking water, which in turn becomes cold and salty enough to sink. This "starts" the global conveyer belt, a connected system of deep and surface currents that circulate around the globe on a 1000 year time span. This global set of ocean currents is a critical part of Earth's climate system as well as the ocean nutrient and carbon dioxide cycles. (NOAA, 2011)

Tidal currents are strongest in large water depths away from the coastline and in straits where the current is forced into a narrow area. The most important tidal currents in relation to coastal morphology are the currents generated in tidal inlets. (Mangor, Currents, 2008)

The wind blows across the ocean and moves its waters as a result of its frictional drag on the surface. Ripples or waves cause the surface roughness necessary for the wind to couple with surface waters. If Earth did not rotate, frictional coupling between moving air and the ocean surface would push a thin layer of water in the same direction as the wind. This surface layer in turn would drag the layer beneath it, putting it into motion. This interaction would propagate downward through successive ocean layers, like cards in a deck, each moving forward at a slower speed than the layer above. However, because Earth rotates, the shallow layer of surface water set in motion by the wind is deflected to the right of the wind direction in the Northern Hemisphere and to the left of the wind direction in the Southern Hemisphere. This deflection is known as the Coriolis effect (NASA, 2017).

Using vectors to plot the direction and speed of water layers at successive depths, we can show a simplified three-dimensional current pattern caused by a steady horizontal wind Figure 2.6.

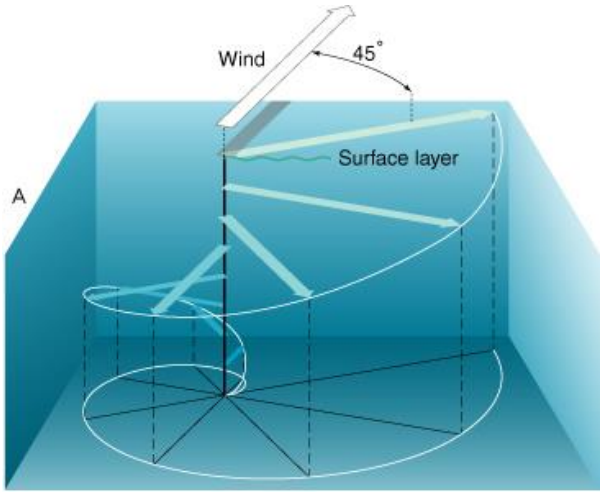

Figure 2.6. Ekman spiral. Credits (NASA, 2017)

This model is known as the Ekman spiral, named for the Swedish physicist V Walfrid Ekman (1874-1954) who first described it mathematically in 1905 (NASA, 2017).

In the Northern Hemisphere, the Ekman spiral predicts net water movement through a depth of about 100 to 150 m at 90 degrees to the wind direction. That is, if one adds up all the vectors in, the resulting flow is at 90 degrees to the right of the wind direction. In the Southern Hemisphere, the net water movement is 90 degrees to the left of the wind direction. This net transport of water due to coupling between wind and surface waters is known as Ekman transport (NASA, 2017).

In some coastal areas of the ocean, the combination of persistent winds, Earth's rotation (the Coriolis effect), and restrictions on lateral movements of water caused by shorelines and

shallow bottoms induces upward and downward water movements. As explained above, the Coriolis effect plus the frictional coupling of wind and water (Ekman transport) cause net movement of surface water at about 90 degrees to the right of the wind direction in the Northern Hemisphere and to the left of the wind direction in the Southern Hemisphere. Coastal upwelling occurs where Ekman transport moves surface waters away from the coast; surface waters are replaced by water that wells up from below (NASA, 2017).

Storm surge current is the current generated by the total effect of the wind shear stress and the barometric pressure gradients over the entire area of water affected by a specific storm. This type of current is similar to the tidal currents. The horizontal current velocity follows a logarithmic distribution in the water profile and has the same characteristics as the tidal current. It is strongest at large water depths away from the coastline and in confined areas, such as straits and tidal inlets. (Mangor, Currents, 2008)

Nearshore mean currents which occur within the surf zone are principally driven by the breaking waves. For purposes of simplification, nearshore mean currents are usually separated into their cross-shore and longshore components: Undertows and rip currents have their principal axes oriented perpendicular to the beach (offshore) while longshore currents act parallel to the beach. These currents are all driven by cross- and/or longshore components of radiation stress gradients that arise through wave breaking. (Mangor, Currents, 2008)

The longshore current is the dominant current in the nearshore zone. The longshore current is generated by the shore-parallel component of the stresses associated with the breaking process for obliquely incoming waves, the so-called radiation stresses, and by the surplus water which is carried across the surf zone towards the coastline. This current has its maximum within the breaker zone. During storms the longshore current can reach speeds exceeding 2.5 m/s. The longshore current carries sediment along the shoreline, the so-called littoral drift. The longshore current is generally parallel to the coastline and it varies in strength approximately proportional to the square root of the wave height and with $\sin 2\alpha_b$, where α_b is the wave incidence angle at breaking. As the position of the breaking line constantly shifts due to the irregularity of natural wave fields and since the distance to the breaker line varies with the wave height, the distribution of the longshore current in the coastal profile will vary accordingly. (Mangor, Currents, 2008)

2.6 HYDRODYNAMIC MODELLING

The rapid development of computing technology has furnished a large number of models to be employed in coastal hydrodynamic problems. A variety of coastal models are available and the modelling techniques have become quite mature. The numerical technique can be based, among others, in the finite element method, finite difference method, boundary element method, finite volume method and Eulerian-Lagrangian method. The time-stepping algorithm can be implicit, semi-implicit, explicit, or characteristic-based. In finite element models the shape functions can be of the first order, second order, or a higher order. The spatial discretization can be based in different spatial dimensions, i.e., a one-dimensional (1D) model, two-dimensional (2D) depth-integrated model, 2D lateral-integrated model, 2D layered model and 3D model (Prinos, 2016).

An analysis of coastal hydraulics and water quality often demands the application of heuristics and empirical experience, and is accomplished through some simplifications and modelling techniques according to the experience of specialists. However, the accuracy of the prediction is to a great extent dependent on open boundary conditions, model parameters, and the numerical scheme. The adoption of a proper numerical model for a practical coastal problem is a highly specialized task. These predictive tools inevitably involve certain assumptions and/or limitations, and can be applied only by experienced engineers who possess a comprehensive understanding of the problem domain. This leads to severe constraints on the use of models and large gaps in understanding and expectations between the developers and practitioners of a model (Prinos, 2016).

2.7 MODELLING THE DISPERSION OF WASTE WATER

According to Chapra (1997), a mathematical model can be defined as "an idealized formulation that represents the response of a physical system to external stimuli".

Essentially all the relevant models for the simulation of coastal and ocean processes deal with the same basic principle of transport by advection and diffusion of a property in a moving medium (water). There are two different approaches to describe that process: the Lagrangian approach and the Eulerian approach. In the Lagrangian approach the focus is on a specified volume of water, called the system, and its evolution is followed through space and time. In the Eulerian approach the focus is on a specified portion of space, the control volume, and the evolution of the properties associated to the water inside the control volume is monitored while fluxes of water are allowed to flow in and out from it (Zhao *et al.*, 2011).

The mixing and dispersion processes of a continuous discharge into a receiving water body are subjected to two types of mixing processes: near-field and far-field. Near field and far field have different dispersion mechanisms, therefore, a 3D pollutant transport model that couples near-field and far-field dispersion processes is required to ensure the conservation of mass and correct description of processes in the transition zone. The accuracy of the modelling results is extremely important and should be carefully evaluated, in order to accomplish this extensive model comparisons and validations against results from experiments and field measurements are required. Error estimations and sensitivity analysis should be conducted (Zhao *et al.*, 2011).

2.7.1 Near-Field dilution

In an outfall the water is released from the bottom with a certain velocity, due to that the initial mixing is controlled up to a certain height by momentum forces. Beyond this point, mixing is mainly caused by the buoyancy forces dictated by density differences until it reaches the surface. This region is called the near-field mixing zone (Naidu, 2013). This region can be defined as the zone in which the mixture of sea water and the effluent depends mainly on the effluent buoyancy mass and momentum transfer between the mass and the surrounding water (Figure 2.7).

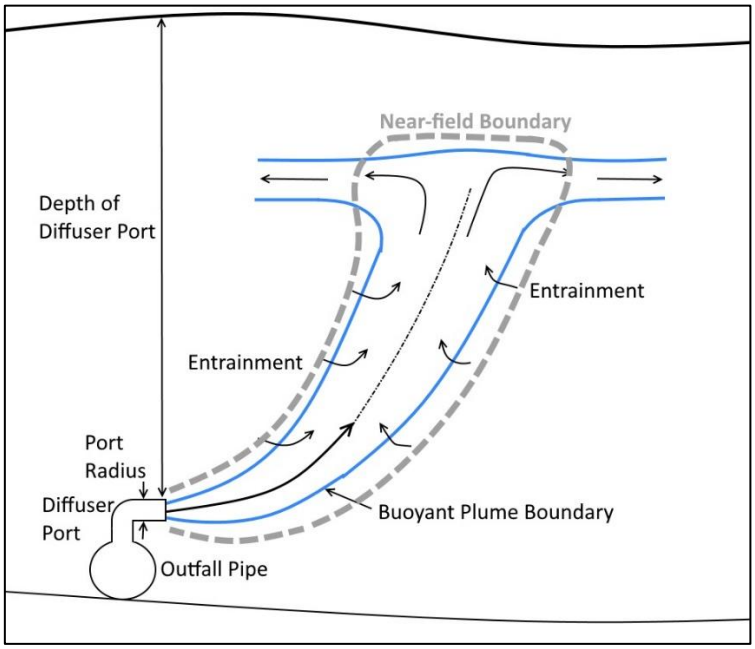

Figure 2.7. Schematic of a buoyant plume Near-field. Adapted from (Owens *et al.*, 2013)

Prediction of near field mixing requires understanding of the dynamics of jets, plumes, and buoyant jets. The discharge conditions relate to the geometric and flux characteristics of the submerged outfall installation. For a single port discharge the port diameter, its elevation above the bottom and its orientation provide the geometry; for multiport diffuser installations the

arrangement of the individual ports along the diffuser line, the orientation of the diffuser line and construction details represent additional geometric features; and for surface discharges the cross-section and orientation of the flow entering the ambient watercourse are important. The flux characteristics are given by the effluent discharge flow rate, by its momentum flux and by its buoyancy flux. The buoyancy flux represents the effect of the relative density difference between the effluent discharge and ambient conditions in combination with the gravitational acceleration. It is a measure of the tendency for the effluent flow to rise or to fall (Jirka et al., 1996).

The parameters that determine the project of an outfall diffuser determine the initial dilution of the effluent and plume geometry at the limit of the near field region.

Initial dilution is the dilution achieved in a plume due to the combined effects of momentum and buoyancy of the fluid discharged from an orifice, and due to ambient turbulent mixing in the vicinity of the plume. The rate of dilution is quite rapid in the first few minutes after exiting the orifice and decreases markedly after the momentum and buoyancy are dissipated (Baumgartner *et al.*, 1994).

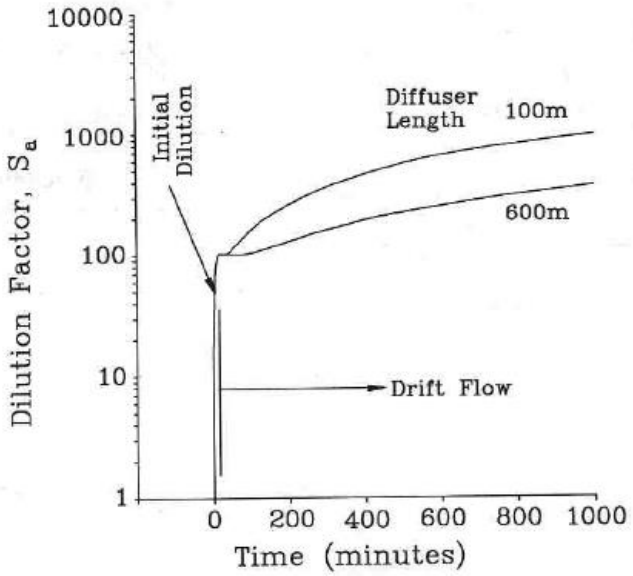

Figure 2.8. Dilution as a function of current speed. Credits: (Baumgartner *et al.*, 1994)

Figure 2.8 schematically represents the relative dilution factors achieved in buoyant plumes and in the subsequent drift flow region under low to moderate current conditions. Ambient currents will also influence the rate of dilution during the buoyant rise of the plume irrespective of jet momentum and buoyancy. As current speed increases so does initial dilution (Baumgartner *et al.*, 1994).

In the near field region, the density variability of sea water from the bottom to the top can cause the stratification of the effluent creating a submerged plume. The project, and the evaluation of the discharge impacts make it necessary to forecast the effluent plume behaviour, in particular their thickness, depth of submersion and initial dilution. It is usual to use as project criteria a value for the minimum initial dilution, defined as the lowest dilution that must be observed in a vertical plane at the limit of the near field region where the effluent behaviour is no longer conditioned by the hydraulic conditions at the exit of the diffuser.

The parameters that determine the dilution values and the geometry of the plume in the near field region are:

- Environmental Parameters
    - Ocean currents speed;
    - Water density and respective vertical gradient;
- Diffuser Parameters
    - Orientation relatively to ocean currents
    - Length
    - Diameter and hole spacing
- Effluent Parameters
    - Flow
    - Density

2.7.2 Far-Field dilution

Once buoyancy forces are no longer in effect, mixing is caused by the prevailing currents of the region. Both advection and diffusion processes are involved in this far-field mixing zone (Naidu, 2013).

This phase is characterized by advective transport, due to ocean currents existing in the environment. When the outfall plume is stabilized (mixture obtained by dilution between the discharged effluent and the receiving medium) the transport becomes independent of its initial conditions. Thus, the trajectory and the dilution of the outfall plume will be controlled by the existing conditions of the surrounding environment, namely the currents and diffusion by oceanic turbulence. According to (Roberts, et al., 2010) it occurs over distances of 100 m to 10 km.

2.7.3 Bacterial decay

Wastewater contains a wide range of microorganisms, some of which are pathogenic. The direct determination of pathogenic organisms requires complex microbiological analysis.

Pathogens are often responsible for the spread of waterborne diseases (Gao *et al.*, 2015). However, due to the difficulties of direct measurement of pathogens, indicator microorganisms have generally been used in water quality management (Chapra, 1997). *Faecal* indicator bacteria (FIB) groups, such as total coliform, faecal coliform, *Escherichia coli* and enterococci, are used commonly around the world to measure the health hazards in bathing and shellfish harvesting waters (Gao *et al.*, 2015). This is due principally to the fact that the faecal indicator bacteria can be easily quantified using laboratory tests and are generally not present in unpolluted waters, and the concentrations of these indicator bacteria tend to be correlated with the contamination level (Gao *et al.*, 2015).

Hydrodynamic and hydrological processes play very important roles on the distribution of faecal bacteria and pathogen concentrations in river, estuarine and coastal waters (Gao *et al.*, 2015).

In the faecal bacteria fate and transport model, the bacteria are normally modelled as a reactive tracer, wherein they will be transported by the flow processes once they enter the model domain and their concentrations are affected by faecal bacteria specific processes (Gao *et al.*, 2015).

The bacterial decay rate is often expressed as T_{90}: time for bacterial concentration to decrease by 90%. Bacterial inactivation in natural waters is driven by a number of interacting processes. The main driver is the intensity of the incident irradiance from sunlight (Kay *et al.*, 2005). In coastal waters the decay rate of faecal bacteria is also affected by salinity (Gao *et al.*, 2015) and temperature (Blaustein *et al.*, 2013).

2.8 OPERATIONAL MODELLING

An operational model can be understood as an infrastructure of coupled models, an input data set (bathymetries and initial conditions) and an automatic monitoring network (including remote sensing, boats, buoys, etc.), all integrated to produce model forecasts. Through a web application, databases for storage of measurements and forecasts, mechanisms and validation tools of the different sources of information, this set of information and results are available in a useful interface to the end users.

The purpose of an operational model is the production of sea state forecasts, marine and their biochemical components for a given period of time. In order to produce these estimates, the system should include systematically, a network of observation/monitoring with systems analysis and real-time data acquisition, numerical models and data assimilation procedures (Pinardi & Flemming, 1998).

The operational model used to nest the Albufeira Bay model is the Algarve Operational Modelling and Monitoring System (SOMA) developed to assist in the decision making in case of oil spills in the southern region of Portugal given its vulnerability do sea oil spills due to intense vessel traffic in the region (Janeiro *et al.*, 2012; Janeiro, 2014; Janeiro *et al.*, 2017).

2.9 MATHEMATICAL MODELLING SYSTEMS

Modelling the total ocean simulation system is extremely complicated and involves many variables and processes, including highly nonlinear interactions. Some of those most widely used for simulations of waste water dispersion in coastal and ocean areas are presented in Table 2.1 showing the features of these modelling packages (Zhao *et al.*, 2011).

Table 2.3. Most widely used modelling systems for simulation of pollutant dispersion processes, adapted from Zhao *et al.*, 2011

Model	Reference	Major functionalities
Jet and plume models		
CORMIX	(Doneker & Jirka, 2007)	Prediction of jet and (or) plume geometry and dilution in the near field; single or multiple jets
OpenFOAM®	(Openfoam.com, 2016; (Jasak *et al.*, 2007))	
VISJET	(Lee and Cheung, 1990; Lee and Chu, 2003)	
Visual PLUMES	(Frick *et al.*, 2003)	
Sophisticated multidisciplinary models		
MIKE 21/3	(DHI, 2016)	Predictions of ocean hydrodynamics; pollutant fate and transport in the far field; water quality; sediment processes
Delft3D	(Deltares, 2016)	
EFDC-Hydro	(Hamrick, 1992; US EPA, 2002)	Predictions of ocean hydrodynamics; Pollutant dispersion in the far field; near-field processes using the embedded jet model JETLAG; suspended sediment transport
MOHID	(Miranda *et al.*, 2000; MOHID, 2016)	Predictions of ocean hydrodynamics; Pollutant dispersion in the far field; near-field processes using the embedded jet model MOHIDJET; suspended sediment transport
HydroQual-ECOMSED	(HydroQual, 2002)	Predictions of ocean hydrodynamics; pollutant fate and transport in the far field; sediment processes
Specialized model – produced water modelling		
DREAM	(Reed *et al.*, 2001)	Predictions of pollutant fate and trans- port in both near field and far field; single or multiple sources
PROTEUS	(Sabeur & Tyler, 2004)	

3 CASE STUDY

3.1 ALBUFEIRA MUNICIPALITY

The Municipality of Albufeira is located in the Algarve, the most southern region of Portugal where the Mediterranean Sea meets the Atlantic Ocean.

Archaeological sites confirm the presence of man in the area of the municipality of Albufeira in the Neolithic and Bronze Age. The Romans settled in the peninsula where there was the primitive urban center of Albufeira. Roman Baltum, little more is known than the fact that it was a fishing center and in Paderne area, existed mining. (ERTA, 2016).

With the Arab conquest, the city gets its name Albufeira. It is a period of prosperity based on agriculture and trade with North Africa, which led to the construction or reconstruction of the castle and defensive walls. After the first Christian occupation, in 1249, the retaking of the Algarve starts by Afonso III. In 1250, all the castles and land are retaken in the Algarve, including Albufeira. A period of decline, resulting from the reduction of trade with the Mediterranean ports, followed by the economic dynamism of the period of the Discoveries (XV/XVI). In the XVIII century, several earthquakes, culminating in the earthquake of 1755, impoverished Albufeira. Only at the end of the XIX century, with the growth of the fishing industry and fish preserves, prosperity is restored. From the 60's, tourism elects Albufeira as one of its international centers and the city grows being raised to city in 1986 ("Visitalgarve", 2016).

The Albufeira Municipality has an area 140.66 km^2 and a population of 40,828 fixed inhabitants. This value increases from two to three times in the summer period. The 20 km coastline of Albufeira is gifted by 25 classified bathing waters with varied morphologies (Figure 3.1), from imposing cliffs overcoming a long stretch of golden sand, to beaches delimited by dunes and a lagoon, passing through the jagged beaches and surrounded by cliffs of different dimensions, including the most famous beaches near urban areas. The bathing season is one of the longest in Portugal, from 15th of May until 18th of October.

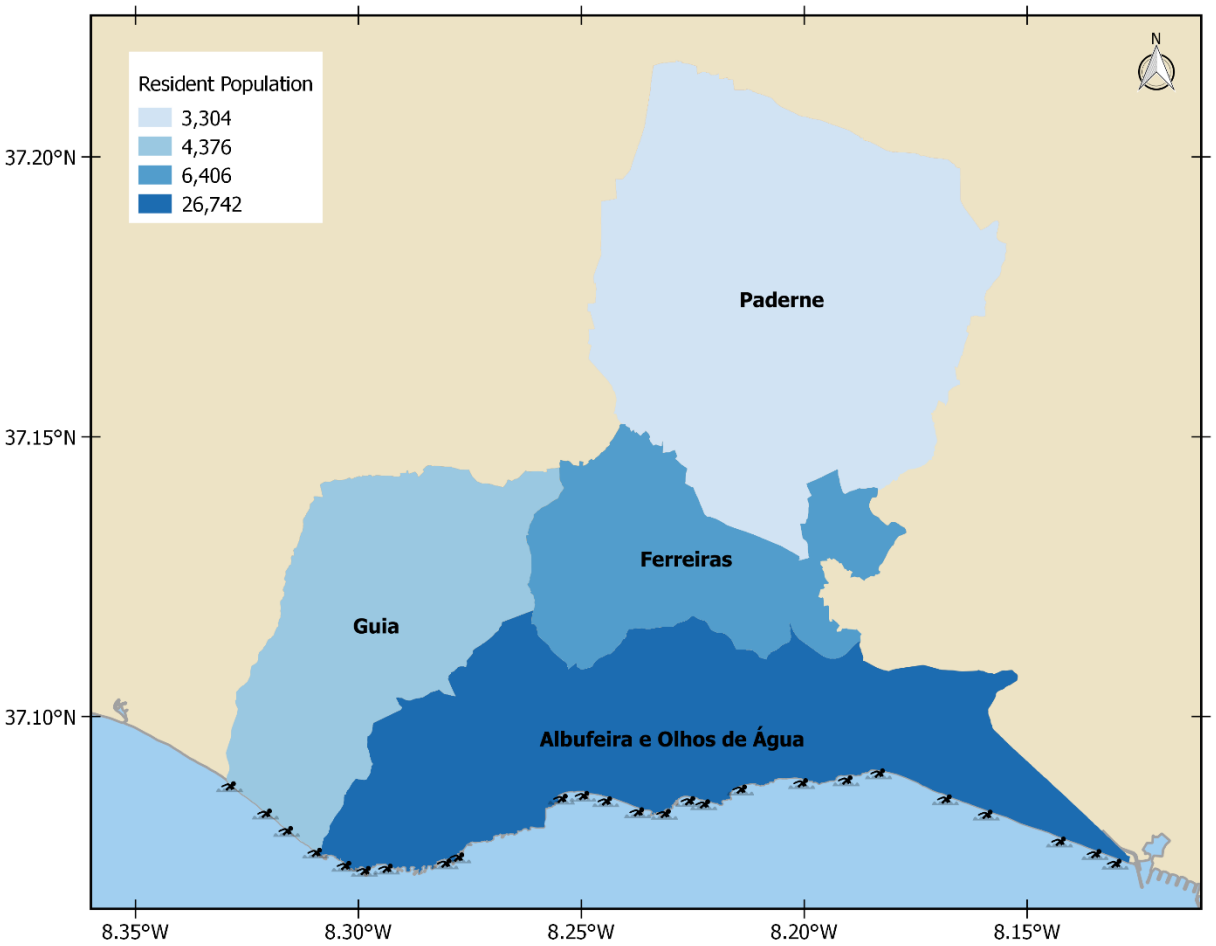

Figure 3.1. Albufeira Municipality areas and 25 classified bathing waters

Tourism activity in bathing areas is one of the major pressures on urban water cycle facilities and water resources, particularly concerning the design of water supply and water treatment systems. This is due to the fact that floating population often doubles the resident population, causing significant pressure on bathing waters quality, especially in the urban areas. As of this fact, the Albufeira Municipality has its resident and tourist population near the litoral an it's responsible for about 40% of tourist occupation of the Algarve Region (Hidra, 2016), posing important pressures and challenges in the management of the urban water cycle facilities in this Municipality, mainly regarding bathing water quality.

The Águas do Algarve Sanitation System serving the city of Albufeira comprises the Vale Faro WWTP and a network of ten pumping stations with 6.5 km of pumping mains, 4.4 km of gravity drains and two submarine outfalls (Vale Faro WWTP and Balaia Pumping Station) totalling 2.6 km (Figure 3.2). This infrastructures were built in the 80's and suffered an update and rehabilitation in 2002 by the Albufeira Municipality before integration in the ADA Algarve Sanitation System in 2005.

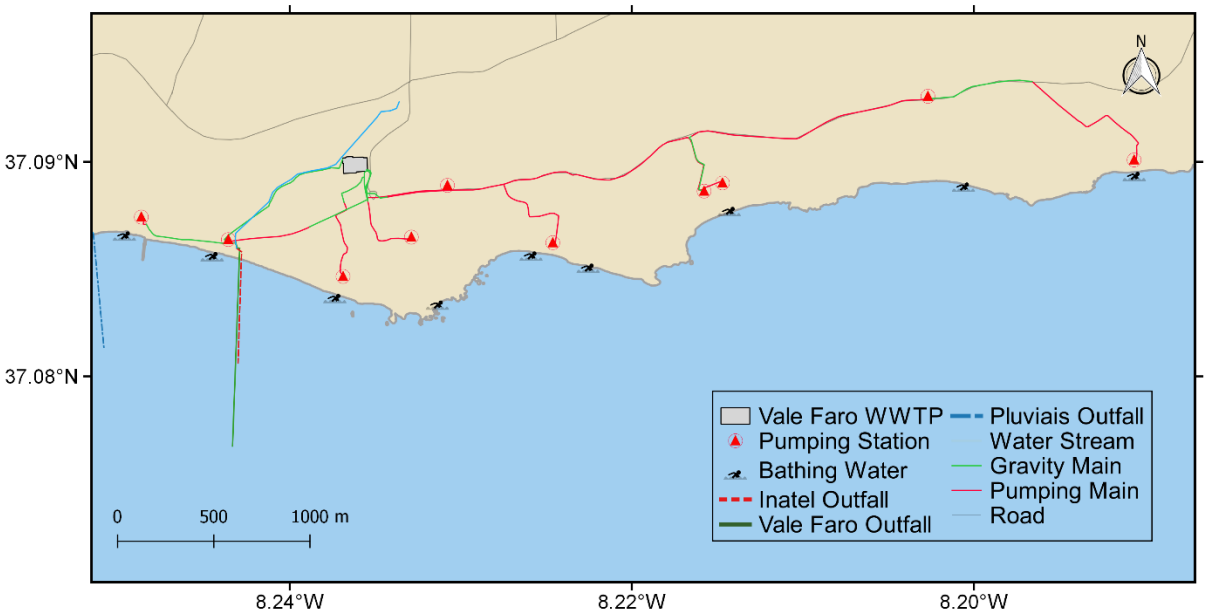

Figure 3.2. Águas do Algarve wastewater collection and treatment system of the city of Albufeira

3.2 CLIMATE AND OCEAN CONDITIONS

According to MAOT (2000), the climate in the Algarve region is heavily influenced by regional factors related to air circulation, the position in the southwest limit of the Iberian Peninsula, on the Atlantic seaboard of the European Continent and by local factors, emphasizing the topographic relief and its displacement. Regarding rainfall, the climate is moderately rainy in most of the region with an average annual rainfall of about 750 mm. The region average air temperature values are situated between 12 ºC in winter and 30 ºC in summer and can be classified as dry with an average relative humidity equal to 65.7 % in the summer and 76.8 % in the winter.

The prevailing winds are on annually average from the North bearing considering records of Sagres, Ameixial and Vila Real de Santo António. In Praia da Rocha the predominant direction is Northeast and East in Faro. In the afternoon there is usually a change in the most frequent directions, becoming Southwest at Praia da Rocha and Faro and Northwest in Ameixial (MAOT, 2000).

The average wind speed usually does not exceed 16 km/h, the highest values are registered in Sagres.

The north wind that is found in the western coast, which is still noticed on the south coast, diminish its intensity eastwards and it is not noticed east of Faro (MAOT, 2000).

The Levante[1] wind is the characteristic wind regime of the Eastern Algarve, blowing from East or Southeast during the spring, summer and early autumn, with associated higher values of air and water temperatures during the summer. The persistence of this winds can usually have a duration up to several days, with daily variations characteristics. The highest wind speeds are achieved in the morning, of about 30 to 40 km/h, decreasing in the afternoon and increasing during the night. Also associated with this winds, and due to its persistence, significant wave height can reach 4 to 5 metres (MAOT, 2000).

The Portuguese coast tide is semi-diurnal with two high tides and two low tides each day. According to the 2015 tide table, published by the Hydrographic Institute, the tide height shows the characteristic values in Lagos showed in Table 3.1.

Table 3.1. Tide characteristics for Lagos 2015

Characteristics	Tide (m ZH)
High Tide – Spring Tide	3.38
High Tide – Neap Tide	2.65
Average Tide	2.00
Low Tide – Neap Tide	1.35
Low Tide – Spring Tide	0.62

[1] Levante is a common weather phenomenon in the Algarve, which can occur once or twice a month and it's characterized by winds from East or Southeast directions.

3.3 VALE FARO WWTP

The Vale Faro WWTP is completely integrated in the urban area beneath a car parking (Figure 3.3).

Figure 3.3. Picture taken from the outside of the Vale Faro WWTP showing the parking lot above the plant

The Vale Faro WWTP was built in 1980 and suffered a major remodelling and expansion in 2002, to allow the removal of nutrients and allow the reuse of the treated effluent for the production of recycled water and increase the treatment capacity. Although the remodelling accommodates changes in the process for removal of nutrients, the discharge regulation for the WWTP only requires compliance with the COD, BOD_5 and *Escherichia* coli parameters in the treated effluent.

The plant has been designed to an average daily flow of 24,310 m^3/day and a population of 130,000 equivalent inhabitants. The various constituent unitary operations and treatment processes of the WWTP can be represented by the flow diagram showed in Figure 3.4.

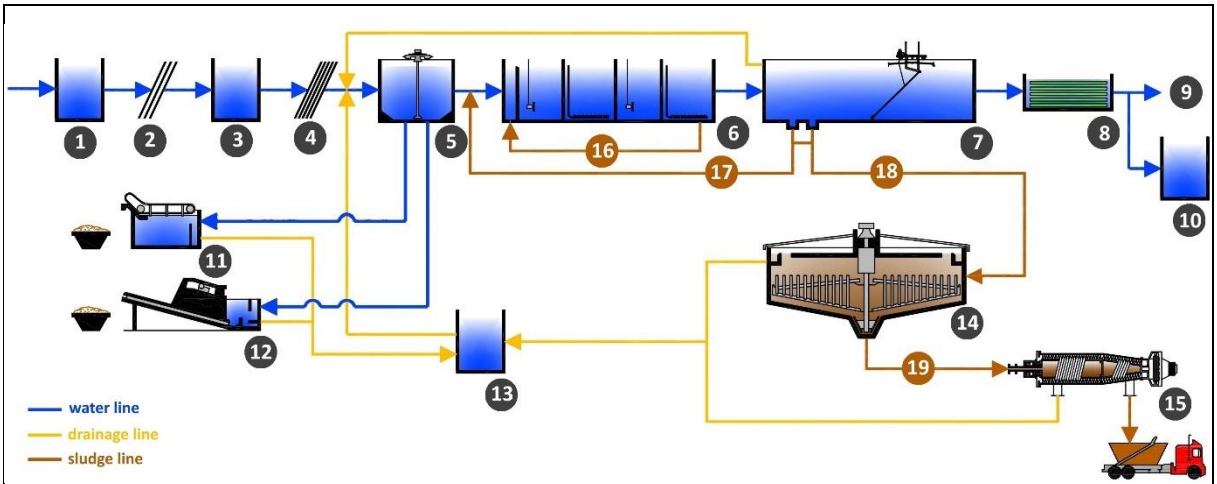

Legend:

1. Raw influent chamber
2. Thick mechanical screening
3. Initial pumping station
4. Fine mechanical screening
5. Grease / Grit tank
6. Oxidation ditch
7. Secondary clarifier
8. UV disinfection
9. To submarine outfall
10. Recycled water reservoir
11. Grease remover
12. Grit remover
13. Drainage pumping station
14. Sludge thickener
15. Centrifugal decanter
16. Recycled nitrates
17. Recycled secondary sludge
18. Secondary sludge extraction
19. Thickened sludge extraction

Figure 3.4. Vale Faro WWTP linear diagram

The adopted treatment solution includes two stages:

1 – Liquid Stage (1 to 13)

The raw influent chamber is equipped with a 20 mm spaced mechanical screen followed by another mechanical fine screen spaced 6 mm. The next step consists in two chambers of grit and grease removal system. These elements are provided at the bottom with electric pumps to lift the sand lying on the bottom and at the surface is equipped with a scraper for the removal of surface grease. Aeration for flotation of grease is carried out by means of three submersible aerators for each chamber.

The removal of grit and grease is followed by the biological treatment by activated sludge in two oxidation ditches with a volume of 10,000 m^3 each, the biological treatment is followed by three rectangular secondary clarifiers. The final step in the liquid phase is the disinfection by ultraviolet radiation (UV) also resulting in recycled water produced for irrigation of green areas, street cleaning and reagent preparation. The UV system accounts for about 8% of the plant energy consumption (Silva *et al.*, 2013).

2 – Solid Stage (14 to 19)

In the solid stage, the secondary sludge's are thickened in two gravity thickeners and the thickened sludge is dewatered in two centrifugal decanters.

The data used for the design of the WWTP can be found in Table 3.2.

Table 3.2. Vale Faro WWTP project parameters

Parameter	Value
Average Daily flow (m^3/d)	24,310
Peak Flow (m^3/h)	4,232
Population (hab)	130,000
TSS (mg/l)	321
BOD_5 (mg/l)	321
COD (mg/l)	802
Nitrogen (mg/l)	50
Phosphorus (mg/l)	12

The quality targets of the Vale Faro WWTP treated effluent required in the discharge permit are presented in Table 3.3.

Table 3.3. Vale Faro WWTP treated effluent discharge permit

Parameter	Limit Value
BOD_5 (mg/l)	25
COD (mg/l)	125
Escherichia coli (MPN/100 ml)	2,000

Currently all flow treated at the Vale Faro WWTP is discharged into the Atlantic Ocean, taking this in consideration, the current regulation doesn't establish a limit value for the removal of phosphorus, so the stage to remove this nutrient is currently out of service. There is the possibility of reusing 5,000 m^3/day of treated effluent in order to use it in the irrigation of green spaces.

The influent flow profile treated at the Vale Faro WWTP is highly affected by the fluctuating population in the Albufeira Municipality due to tourism occupation (Figure 3.5).

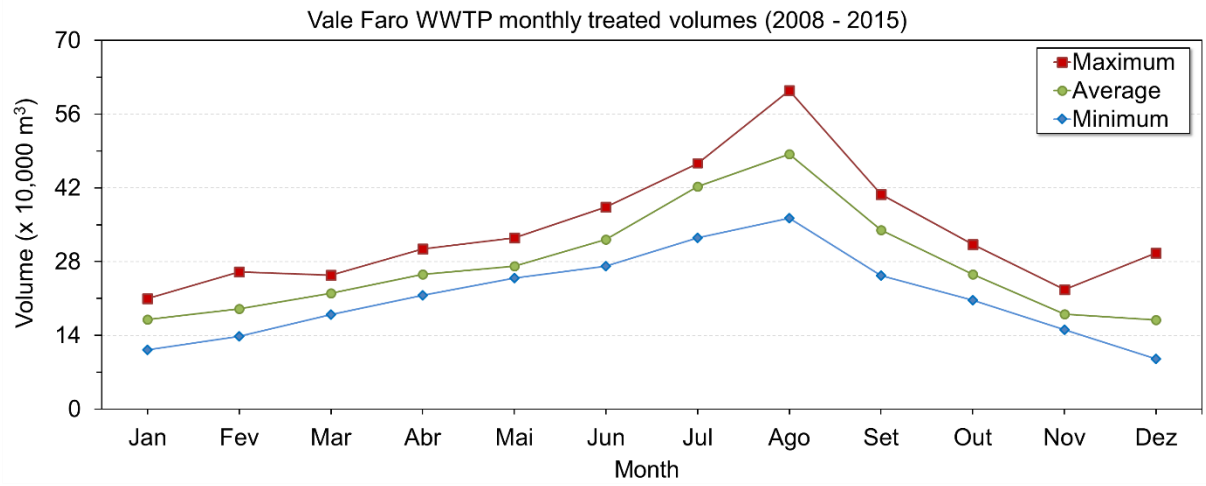

Figure 3.5. Average monthly treated volumes in Vale Faro WWTP from 2008-2015

The influent average monthly treated volumes increase in the summer months, reaching almost three times the treated volumes of the winter months. This constraint have high influence in the maintenance and operational aspect of the Urban Water Cycle facilities in the Albufeira Municipality.

3.4 SUBMARINE OUTFALLS

The coast of the Albufeira Municipality hosts six outfalls, from which three are presently on service in the Albufeira Bay (Figure 3.6). The main outfall studied in this work serves the Vale Faro WWTP managed by Águas do Algarve S.A., while the other two are managed by the Municipality. These three outfalls represent the study area targeted in this work.

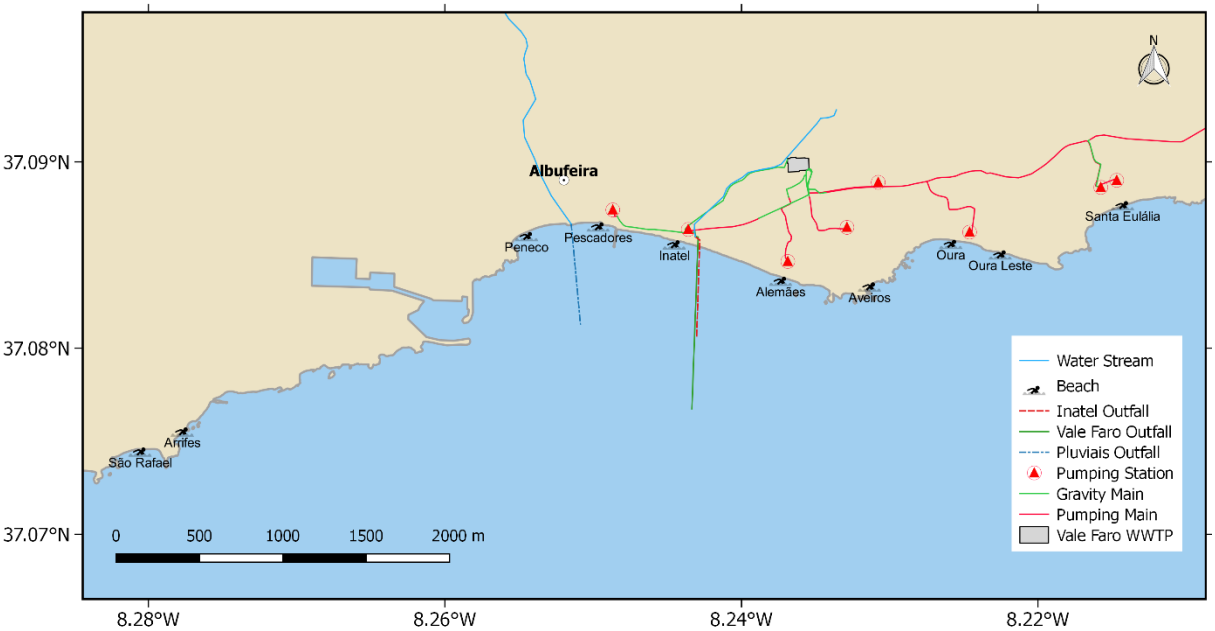

Figure 3.6. Location of the three outfalls in Albufeira Bay (Portugal)

The city's water lines are dry for most of the year, with the exception of the stream "Ribeira de Albufeira" receiving the treated effluent from Ferreiras WWTP located 6 km from the city center. This stream ends at the "Peneco" beach, and the tributary flow is discharged by the 800 meters long "Pluviais" outfall. Finally, the 600 meters long "Inatel" outfall discharges another small stream of water into the bay. This two outfall flows may have punctual contamination of raw sewage due to clogging in the city's sewage network. The outfall characteristics are presented in Table 3.4.

All three outfalls are built in HDPE with pipes welded together and sunk with pre-moulded concrete rings. This method is the most commonly used for HDPE outfalls. Entrenchment, directional drilling, and microtunneling result in greater protection of the outfall, but are usually significantly more expensive than weights or anchors (Roberts, et al., 2010).

Table 3.4. Main characteristics of the three submarine outfalls

Outfall Name	Pluviais	Inatel	Vale Faro
Date	2009	1986	2005
Effluent type	Treated waste water + runoff	Runoff	Treated waste water
Project Flow (m^3/s)	1.00	0.13	1.18
Avg. Flow August 2015 (m^3/s)	0.02141	0.0077199	0.15916
Length (m)	800	600	1000
Material	High-density polyethylene (HDPE)		
Diameter (mm)	1000	400/315	1000
Maximum depth (m HZ)	-8	- 8	- 10.2
Diffusor Type	HDPE, "T" riser with 2 holes ∅ 560 mm with 0º angle with the horizontal plane	HDPE, 10 m, 8 alternated holes ∅ 60 mm with 0º angle with the horizontal plane	HDPE, 160 m, 32 alternated holes ∅ 150 mm 35º angle with the horizontal plane

3.4.1 Vale Faro

The Vale Faro submarine outfall was intended to replace the old outfall; whose capacity is incompatible with the current needs of the city of Albufeira. The design of the new outfall took into account the existing capacity of Vale Faro WWTP. The submarine outfall starts at the Inatel beach in Albufeira, distanced approximately 40 metres to the east of the existing Inatel outfall.

The structural outfall solution consists in a HDPE pipe, of 1,020 metres long, connected upstream to a loading shaft which is constructed in the cliffs and ends downstream with 160 meters long diffuser holding 32 alternated holes with a diameter of 150 mm (Figure 3.7) in a 35º angle with horizontal plane (Figure 3.8).

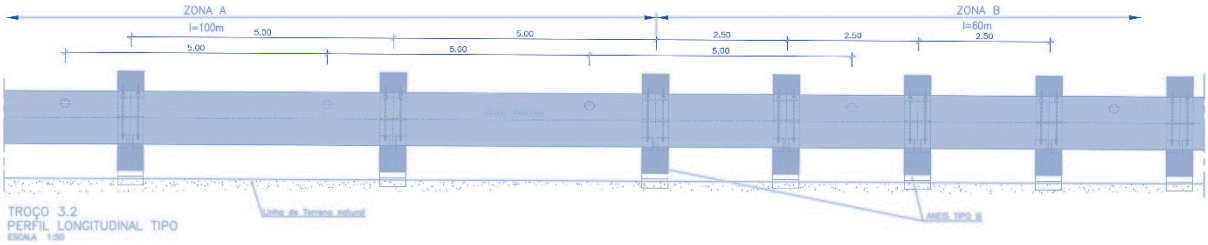

Figure 3.7. Longitudinal profile of the Vale Faro submarine outfall diffuser

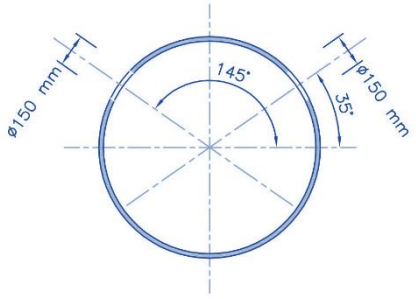

Figure 3.8. Angle of the diffuser holes of the vale Faro Outfall

The pipe has a diameter of 1,000 mm and is embedded in the natural ground portion and supported at the bottom on the remaining length with a 180 degree orientation parallel to the direction of the existing outfall. The stabilization of the section supported directly on the bottom is achieved through the use of reinforced concrete rings.

This outfall, drains a flow rate of 1.18 m^3/s, corresponding to the maximum peak flow capacity of the Vale Faro WWTP. The pipe has an exterior diameter of 1,000 mm and a wall thickness of 47.7 mm that corresponds to the internal diameter of 904.6 mm. The speed for the design flow rate is 1.84 m/s. (Seth, 2004)

3.4.2 Inatel

The Inatel outfall has diameter of 400 mm and is about 634 m long, it started operation in 1986, serving the Vale Faro WWTP with a flow capacity of 0.139 m^3/s being replaced by the new Vale Faro outfall in 2005. Currently is being used to drain runoff in a small water stream to prevent the discharge of effluents in the bathing area. The diffuser is 10 m length with 8 alternating 8 holes of 60 mm diameter in a configuration similar to the new Vale Faro outfall but with the orifices discharging in an angle of 0 degree with the horizontal plane.

The Inatel outfall is the oldest in this study and it has already been subject of repair in 2002 due to hydrodynamic oceanic forces.

3.4.3 Pluviais

The Pluviais outfall is the most recent built outfall in the Albufeira bay. The tunnel that crosses the cliff separating the Peneco and Pescadores beaches receives almost all effluents from the "Av. 25 de Abril" stream (Ribeira de Albufeira channelling) and unitary sanitation network of the corresponding old town, thereby constituting the largest storm water drainage discharged at the beach in Albufeira Bay. The tunnel has an oval upper section, about three meters high. In cases of peak flows during rain events, the flow opens a deep erosion trench at the beach, tearing it with large width and preventing any pedestrian crossing. In the absence of runoff flows, on the contrary, there is a sedimentation of the collector. During the bathing season the final stretch of this tunnel is walled off, and the flow is pumped to the Vale Faro WWTP.

To avoid the pumping and treatment of runoff water this 800 m long and 1000 mm in diameter submarine outfall was built. The outfall has an orientation substantially perpendicular to the overall progress of local bathymetry, although slightly rotated to East, in order to minimize the angle with the tunnel axle.

The piping used consists in HDPE DN1000 PN6, endowed with simple diffuser with two exits of 560 diameter each in a "T" shape (Figure 3.9).

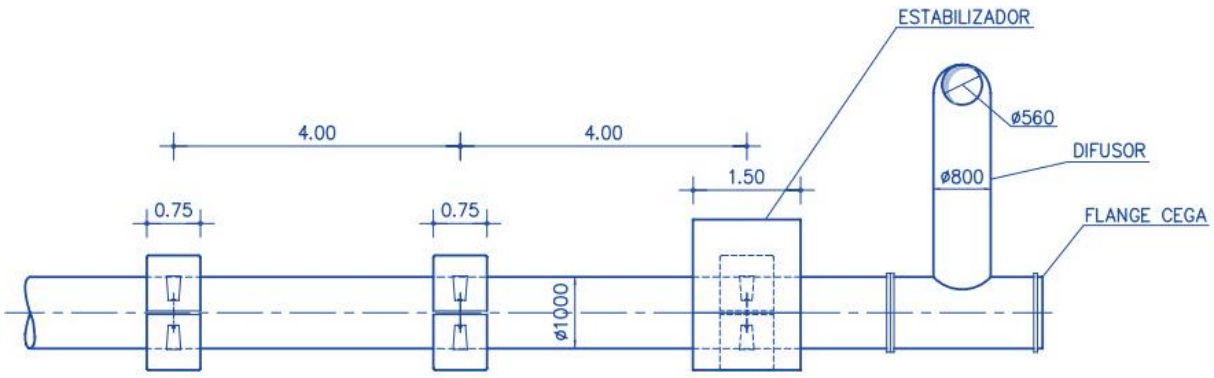

Figure 3.9. Pluviais outfall diffuser

The pipes are welded together and sunk with pre-moulded reinforced concrete rings.

4 METHODOLOGY

4.1 DATA COLLECTING

4.1.1 Flow Measurement

Field campaigns were executed in the bay to characterize properly the study area. The data was completed using historic records. In order to validate the model and replicate the discharge conditions of the marine outfalls the flow rates discharged are necessary to use as Time series input to the mathematical model.

The flow rate of Vale Faro marine outfall was obtained from the WWTP operational treated flow records.

For the flow rate of the Pluviais marine outfall a similar methodology was used, as in the summer period the Ferreiras WWTP, represents all of the influent of the Ribeira de Albufeira discharged by this marine outfall, so the flow rate of Pluviais outfall was estimated based on the Ferreiras WWTP treated flows.

The flow of Inatel outfall was measured for two weeks during the first field campaign (Figure 4.1). The flow for the rest of the periods was inferred based on the flow patterns of the wastewater facilities in the city.

Figure 4.1. Equipment installed during the flow measurement campaign of Inatel outfall

The technology used for the flow measurement was a combined 1 - air-ultrasonic (h – height detection for low levels), 2 - combined water-ultrasonic (v – velocity and h - height) and hydrostatic measurement (P – hydrostatic pressure) as seen in Figure 4.2.

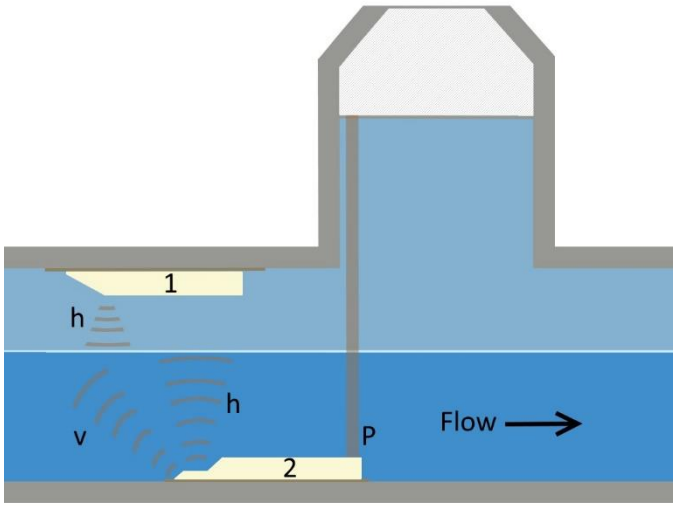

Figure 4.2. Flow measurement technologies used.

4.1.2 Wind conditions

The Albufeira bay hydrodynamics is influenced by tides, by the direct influence of the wind, by wind waves induced coastal currents and by baroclinic coastal currents, wind being a major driver of coastal hydrodynamics in this region. For the characterization of the most frequent wind speed and directions the data available from the Faro Airport WS, Paderne WS, Algoz WS and Loulé WS were collected and analysed, and the respective wind roses were plotted. Table 4.1 shows the wind stations locations.

Table 4.1. Wind Stations location

Weather Station	Location (Lat; Long)
Algoz	37°8'20.05"N; 8°17'53.11"W
Loulé	37°8'45.78"N; 8°0'18.52"W
Paderne	37°10'1.68"N; 8°12'32.06"W
Faro Airport	37°1'8.80"N; 7°58'15.88"W
Vale Faro	37°5'22.24"N; 8°14'10.86"W

As part of this work, in June 2016 a weather station was installed in the Vale Faro WWTP Figure 4.3.

Figure 4.3. Vale Faro WWTP weather station

The Vale Faro weather station has a rain gauge, anemometer and temperature according to the specifications of Table 4.2.

Table 4.2. Weather station outdoor sensors specifications

Transmission distance in open field	100 m
Frequency	868 MHz (Europe)
Temperature range	-40°C … 65°C
Temperature Resolution	0.1 °C
Measuring range rel. humidity	10 … 90 %
Rain volume display	0 … 9999 mm
Rain Resolution	0.1 mm (if rain volume < 1000 mm)
	1 mm (if rain volume > 1000 mm)
Wind speed	0…240 km/h
Measuring interval thermo-hygro sensor	48 s
Water proof level	IPX3

The weather station records data from all the sensors in the PC database with a 5-minute interval and it's connected to the internet with the main web site available in https://goo.gl/obz0IX. The data are also public available in the following website https://goo.gl/XuX9p3.

4.1.3 Tide

The water level was obtained from the data recorded in the tide gauge of the port of Lagos (Figure 4.4) provided by "Direção-Geral do Território" (DGT) (ftp://www.igeo.pt/Lagos/marégrafo) as is compared with the water level obtained by the model during the validation Run.

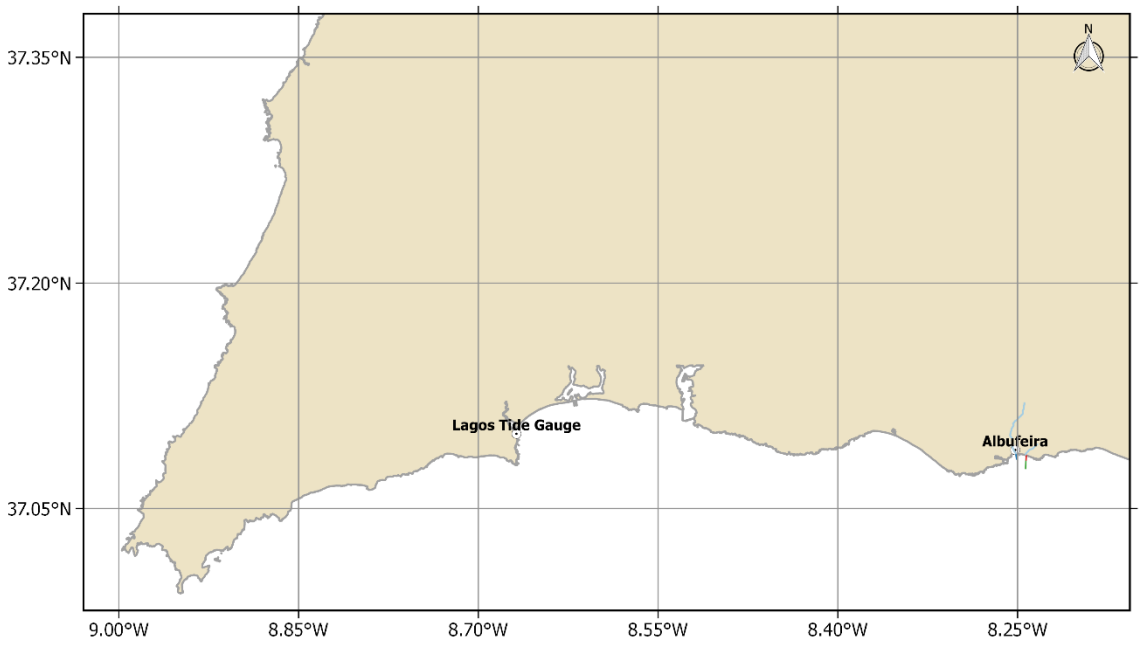

Figure 4.4. Lagos tide gauge (Lat. 37°05.93´N; Long. 8°40.10´W).

4.1.4 Bacteriological Field Campaigns

Three field campaigns were conducted to evaluate the impact of the outfall discharges. Water samples were collected offshore, close to the outfall discharges, in three field campaigns. The field campaigns were executed in the same day (27 Jul 2015, 24 Aug 2015 and 22 Aug 2016) of the compulsory beach sampling executed by the Portuguese Environmental Agency (APA). The results of the bathing water quality monitoring are made available in www.snirh.pt by the APA. Thirteen samples were collected in each field campaign. A sample representing undiluted outfall discharge was collected onshore at the beginning of each outfall and 10 water samples were collected offshore at the ocean surface in a radius of 200 meters from the outfall diffusers (Figure 4.5). The measurements for the biological parameters of these samples were made in the ADA laboratory which is accredited since 2006 by the Portuguese Accreditation Institute (IPAC) according to the NP EN ISO/IEC 17025:2005 standard.

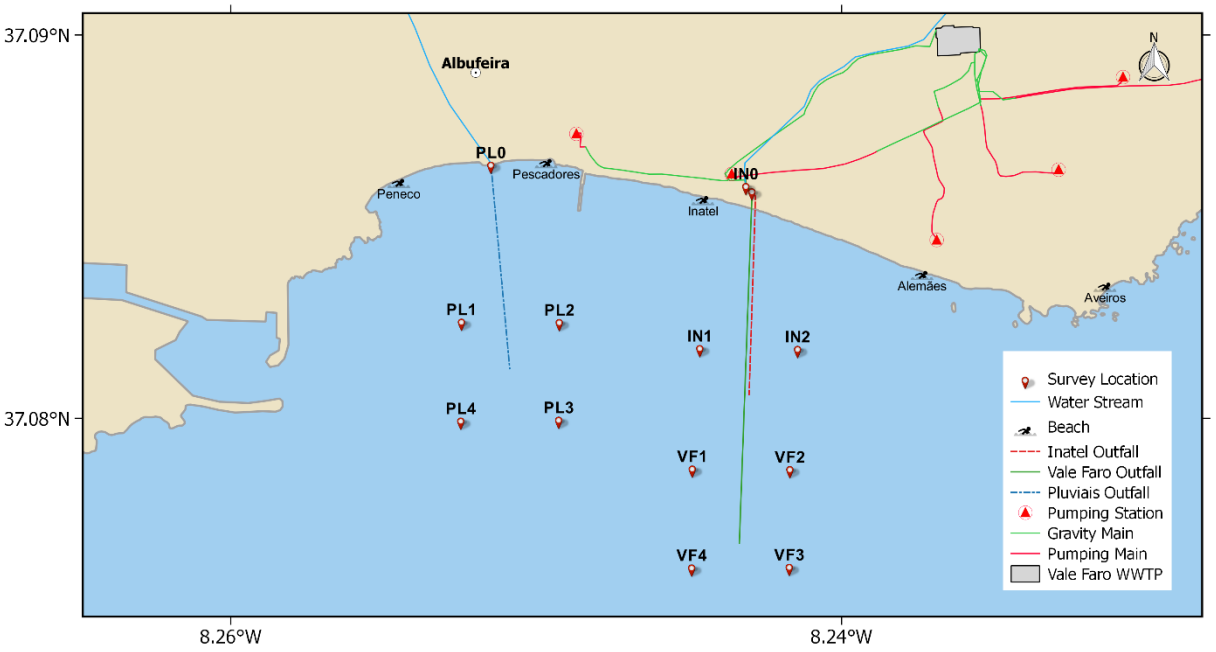

Figure 4.5. Survey point location

4.2 MOHID MODELLING SYSTEM

The MOHID Water Modeling System (Miranda *et al.*, 2000; MOHID, 2016) and the MOHID Studio GUI (www.actionmodulers.pt) were the mathematical modelling tools used in this work.

MOHID started as a simple 2D hydrodynamic model in 1985, developed by MARETEC (Marine and Environmental Technology Research Center), at Instituto Superior Técnico (IST), Universidade de Lisboa. Currently MOHID Water Modeling System is a modeling system using the finite volume method, written in ANSI FORTRAN 95 and using an object oriented programming philosophy, integrating various numerical models and graphical user interfaces. The MOHID system allows the adoption of an integrated modeling philosophy, integrating processes (physical and biogeochemical) and also different scales and systems (estuaries and watersheds), due the adoption of a object oriented programming philosophy.

The components of the MOHID system used in this work were the free surface three dimensional baroclinic hydrodynamic module, the Eulerian transport module, the Lagrangian transport module, the turbulence module and the near field jet model. The hydrodynamic model solves the three-dimensional incompressible primitive equations as in Martins *et al.*, 2001, hydrostatic equilibrium is assumed as well as Boussinesq approximation. The model uses a finite volume approach, making the solution independent of the mesh geometry, thus allowing the use of a generic vertical mesh. The turbulence module uses the well-known General Ocean Turbulence Model (GOTM, www.gotm.net). The model also solves a transport equation for salinity and temperature in order to compute the density. The Eulerian transport module used

to transport these properties is based in the same finite volume method of the hydrodynamic model and is independent of the property transported.

MOHID Water allows the simulation of hydrodynamic processes, simulation of dispersion phenomenon (Lagrangian and Eulerian approaches), sediment transport, water quality / biogeochemical processes in the water column and exchanges with the background (Figure 4.6).

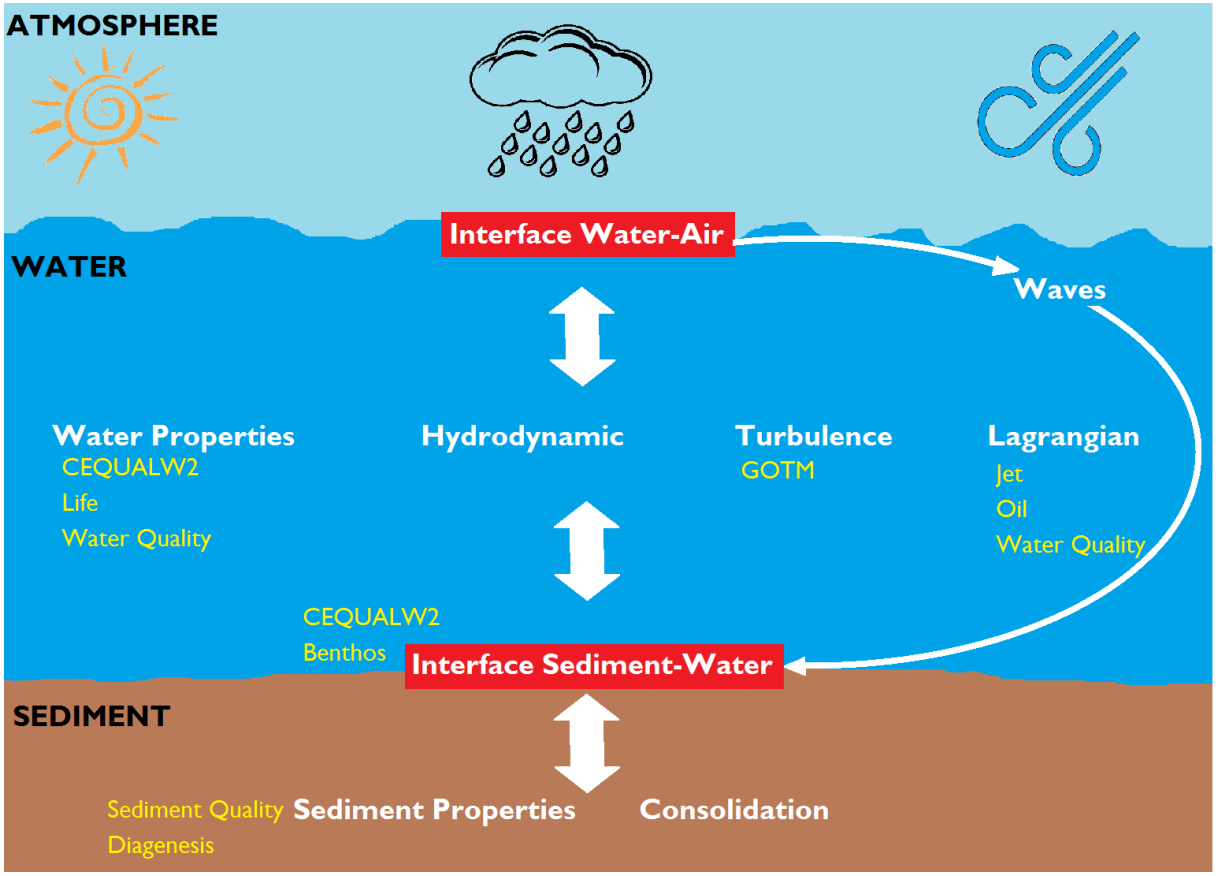

Figure 4.6. MOHID Water processes (adapted from MOHID, 2016)

MOHID uses an object-oriented programming approach together with the potential of FORTRAN 95, allows for a modular organization interconnected in order to determine the objectives pursued in each field of application. Presently MOHID is composed by over 40 modules which complete over 150 thousand code lines. Each module is responsible to manage a certain kind of information. The main modules are those listed in Table 4.3.

Table 4.3. Main modules in MOHID modelling system

Module name	Module description
Model	Manages the information flux between the hydrodynamic module and the two transport modules and the communication between nested models
Hydrodynamic	Full 3D dimensional baroclinic hydrodynamic free surface model. Computes the water level, velocities and water fluxes.
Water Properties (Eulerian transport)	Eulerian transport model. Manages the evolution of the water properties (temperature, salinity, oxygen, etc.) using an eulerian approach.
Lagrangian	Lagrangian transport model. Manages the evolution of the same properties as the water properties module using a lagrangian approach. Can also be used to simulate oil dispersion.
Water Quality	Zero-dimensional water quality model. Simulates the oxygen, nitrogen and phosphorus cycle. Used by the eulerian and the lagrangian transport modules.
Oil Dispersion	Oil dispersion module. Simulates the oil spreading due thickness gradients and internal oil processes such as evaporation, emulsification, dispersion, dissolution and sedimentation.
Turbulence	One-dimensional turbulence model. Uses the formulation from the GOTM model
Geometry	Stores and updates the information about the finite volumes.
Surface (InterfaceWaterAir)	Boundary conditions at the top of the water column.
Bottom (InterfaceSedimentWater)	Boundary conditions at the bottom of the water column.
Open Boundary	Boundary conditions at the frontier with the open sea.
Atmosphere	Atmospheric conditions (wind, solar radiation, precipitation, air temperature)
Discharges	River or Anthropogenic Water Discharges
Jet	Auxiliary module to calculate the initial dilution associated to submarine outfalls
Waves	Radiation stress and wave conditions

4.2.1 Spatial Discretization - Geometry module

Vertical discretization is accomplished using the Geometry module. In vertical discretization it is common to use coordinate transformation in order to optimize the grid accuracy. This

methodology also allows the development, with little effort, of different types of alternative vertical coordinates that best fit a specific situation (Martins F. , 1999). The finite volume models allow great flexibility in spatial discretization, since the geometry is introduced explicitly through the areas and volumes of each cell (Fernandes, 2005). This versatility allows the subdivision of the domain both horizontally and vertically, in zones with different discretization's.

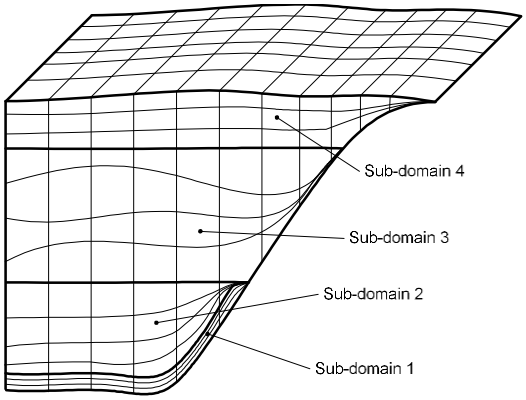

Figure 4.7. Illustrative grid showing the potentialities of the vertical discretization of the MOHID system

The flexibility of the MOHID system concerning vertical discretization allows it to be used in oceanic environments, flow systems, water dam reservoirs or even in small scale processes such as the dispersion of thermal plumes.

The horizontal resolution of the MOHID system can be variable in its extension, allowing for more detailed simulations in specific areas of the calculation grid.

4.2.2 Boundary Conditions

4.2.2.1 Free surface – Module Atmosphere

The atmosphere module is responsible for meteorological data needed to compute processes occurring at the water-air interface, such as computing wind shear stress, radiation balances, latent and sensible heat fluxes. Air temperature is used for latent heat, sensible heat and downward longwave radiation computation (in the atmosphere-water interface). Heat flux with solar origin hitting the water surface. Solar radiation is used to compute radiation that enters the water surface (after reflection). One method for cloud cover computation also uses radiation as input.

Wind is described by its velocity decomposed on x and y components. If not available it can be computed from wind modulus and wind direction. Wind is used to compute latent heat, sensible heat and wind stress (in the water-atmosphere interface).

Specific humidity is the ratio of water mass present in the atmosphere against the air mass. Moisture mixture is the ratio of water mass against that of dry air. Relative humidity can be computed from specific humidity, pressure and air temperature when not given.

Relative humidity is a term used to describe the amount of water vapour that exists in a gaseous mixture of air and water. The relative humidity of an air-water mixture is defined as the ratio of the partial pressure of water vapour in the mixture to the saturated vapour pressure of water at a given temperature. Relative humidity is used for latent heat computation (in the water-atmosphere interface).

Cloud cover is used for downward long wave radiation computation (in the atmosphere-water interface). One method in solar radiation computation (if no data available) uses cloud cover as input.

All advective fluxes across the surface are assumed to be null. This condition is imposed by assuming that the flux of the vertical component of the water velocity *W* at the surface is null:

$$Wflux|_{surface} = 0 \qquad \text{Eq. 4.1}$$

Diffusive flux of momentum is imposed explicitly by means of a wind surface stress, $\vec{\tau}_W$.

$$v\frac{\partial \vec{v}_H}{\partial z}\bigg|_{surface} = \vec{\tau}_W \qquad \text{Eq. 4.2}$$

Wind stress is calculated according to a quadratic friction law:

$$\vec{\tau}_W = C_d \rho_a \overrightarrow{W}\left|\overrightarrow{W}\right| \qquad \text{Eq. 4.3}$$

where C_d is a drag coefficient that is function of the wind speed and surface rugosity, ρ_a is the air density and $\overrightarrow{W}$ is the wind speed at a height of 10 m over the sea surface.

Temperature and salinity advective fluxes are imposed null. Other fluxes of heat and freshwater are introduced as source/sink terms in the transport equations (described in Water Properties Module).

4.2.2.2 Open Boundaries

Open boundaries are usually used to define the interaction of the hydrodynamic module with other bodies of water.

Open boundary conditions can be divided into two types:

1. Passive boundary conditions depend on the internal solution and have as main objective to release disturbances generated within the domain. An example of this type of boundary condition are the boundaries, used in various types of applications, such as wind waves, and oceanic and coastal flows.

Active boundary conditions are imposed and not calculated by the model. One example is the imposition of a tidal curve to simulate the hydrodynamics of an estuary or the imposition of a river flow to simulate a salt wedge.

The methodology for defining open boundary conditions is extremely versatile. One way the user has to ensure the simulation does not diverge from the known solution is by defining an external (or reference) with module Assimilation. Module Assimilation is responsible for handling information used in relaxation schemes. Relaxation schemes are used in MOHID Water to relax computed solutions to a reference solution. In MOHID Water, the reference fields and the relaxation time scales are read and handled by Module Assimilation. The relaxation algorithm itself is implemented in Module Hydrodynamic and Module WaterProperties to apply the relaxation scheme to properties such as velocity U, velocity V, water level, temperature, salinity, etc. It is normally applied in the boundary condition computation, usually when nesting models or using a climatological reference field, via the definition of a "sponge layer" around the open boundary. However it can also be applied to the entire simulation domain. It mainly reads the reference fields and the relaxation coefficients fields used to relax the solution to the reference solution.

Another way is to define the solution at given points, and the hydrodynamic module during the Run to interpolate the solution at the boundary points. This is the methodology used to impose tide. The information may be given in the form of a time series or in the form of harmonic components in the case of the tide. Otherwise, it is also possible to use the hydrodynamic module to calculate the reference solution using the concept of nested models. This is the methodology used in this study for the high resolution model. In this method, a large-scale model with a rough space step was defined, where it was relatively easy to define the boundary conditions, followed by the implementation of nested models, to the study area, gradually reducing the spatial step of the grid until the desired precision is obtained, resulting in a set of 3 nested models.

4.2.2.3 Closed Boundaries

Closed boundaries are used to define the coastline and the processes of covering and uncovering in intertidal zones.

Closed boundaries can be divided into:

1. Fixed - Used to define the coastline;
2. Mobile - Useful for defining coverage and discovery processes in intertidal zones.

Physically there are momentum exchanges between the coast and flows in lateral friction. However, this process is negligible in relation to bottom friction due to the difference between the horizontal and vertical space step.

4.2.3 Module WaterProperties

The water properties module computes the evolution of the water properties in the water column, using an Eulerian approach. This includes the transport due to advective and diffusive fluxes, water discharges from rivers or anthropogenic sources, exchange with the bottom (sediment fluxes) and the surface (heat fluxes and oxygen fluxes), sedimentation of particulate matter and the internal sinks and sources (water quality).

Temperature and salinity can be constant values or change over time due to the effect of transport, the point discharge flows, surface flows, heat exchanges in the case of temperature (solar radiation, infrared radiation, latent heat and sensitive) and mass exchanges in the case of salinity (evaporation / precipitation).

The transport of a given property due advective and diffusive fluxes A, is resolved by the following equation:

$$\partial_t A = -\partial_x(uA) - \partial_y(vA) - \partial_z(wA) + \partial_x(v'_H \partial_x A) + \partial_y(v'_H \partial_y A) + \partial_z((v'_t + v'_A)\partial_z A) \quad \text{Eq. 4.4}$$

where *u*, *v* and *w* are the velocity in *x*, *y* and *z* direction, v'_H and v'_t the horizontal and vertical eddy diffusivities, and v'_A the molecular diffusivity. The temporal evolution of A is the balance of advective transport by the mean flow, turbulent mixing and the possible sinks or sources the property may have.

The density ρ is calculated as a function of temperature and salinity by a simplified equation of state (Leendertsee *et al*. 1978):

$$\rho = (5890 + 38T - 0.375T^2 + 3S)/\left((1779.5 + 11.25T - 0.0745T^2\right) - (3.8 + 0.01T)S + 0.698(5890 + 38T - 0.375T^2 + 3S)) \quad \text{Eq. 4.5}$$

That is an approximation for shallow water of the most widely used UNESCO equation (UNESCO 1981).

At present the MOHID model can simulate 24 different water properties: temperature, salinity, phytoplankton, zooplankton, particulate organic phosphorus, refractory dissolved organic phosphorus, non-refractory dissolved organic phosphorus, inorganic phosphorus, particulate organic nitrogen, refractory organic nitrogen, non-refractory organic nitrogen, ammonia, nitrate, nitrite, biological oxygen demand, oxygen, cohesive sediments, ciliate bacteria, particulate arsenic, dissolved arsenic, larvae and faecal coliforms. In the water quality module, the nitrogen, oxygen and phosphorus cycle can simulate the terms of sink and sources.

Any new property can be added very easily, due to the object orientated programming used within the MOHID model.

4.2.4 Module Hydrodynamic

The MOHID hydrodynamic model solves the three-dimensional incompressible primitive equations as in Martins *et al*., 2001, hydrostatic equilibrium is assumed as well as Boussinesq approximation. The model uses a finite volume approach, making the solution independent of the mesh geometry, thus allowing the use of a generic vertical mesh.

The turbulence module uses the well-known General Ocean Turbulence Model (GOTM, www.gotm.net). The model allows the consideration of open or closed boundary conditions.

The momentum balance equations for mean flow horizontal velocities are, in Cartesian form:

$$\partial_t u = -\partial_x(uu) - \partial_y(uv) - \partial_z(uw) + fv - \frac{1}{\rho_0}\partial_x p + \partial_x\left((v_H + v)\partial_x u\right) + \partial_y\left((v_H + v)\partial_y u\right) + \partial_z\left((v_t + v)\partial_z u\right) \quad \text{Eq. 4.6}$$

$$\partial_t v = -\partial_x(vu) - \partial_y(vv) - \partial_z(uw) - fu - \frac{1}{\rho_0}\partial_y p + \partial_z\left((v_H + v)\partial_x v\right) + \partial_y\left((v_H + v)\partial_y v\right) + \partial_z\left((v_t + v)\partial_z v\right) \quad \text{Eq. 4.7}$$

Where u, v and w are the components of the velocity vector in the x, y and z directions respectively, f is the Coriolis parameter, v_H and v_t the turbulent viscosities in the horizontal and

vertical directions, v is the molecular kinematic viscosity (equal to 1.3×10^{-6} m^2 s^{-1}), p is the pressure. The temporal evolution of velocities (term on the left hand side) is the balance of advective transports (first three terms on the right hand side), Coriolis force (fourth term), pressure gradient (fifth term) and turbulent diffusion (last three terms).

The vertical velocity is calculated from the incompressible continuity equation (mass balance equation):

$$\partial_x u + \partial_y v + \partial_z w = 0 \qquad \text{Eq. 4.8}$$

by integrating between bottom and the depth z where w is to be calculated:

$$w(z) = \partial_x \int_{-h}^{z} u dx + \partial_y \int_{-h}^{z} v dy \qquad \text{Eq. 4.9}$$

The free surface equation is obtained by integrating the equation of continuity over the whole water column (between the free surface elevation $\eta(x,y)$ and the bottom $-h$):

$$\partial_t \eta = \partial_x \int_{-h}^{\eta} u dz - \partial_y \int_{-h}^{\eta} v dz \qquad \text{Eq. 4.10}$$

The hydrostatic approximation is assumed, which reduces the vertical momentum equation to:

$$\partial_z p + g\rho_x = 0 \qquad \text{Eq. 4.11}$$

where g is gravity and ρ is density. If the atmospheric pressure p_{atm} is subtracted from p, and density ρ is divided into a constant reference density ρ_0 and a deviation ρ' from that constant reference density, after integrating from the free surface to the depth z where pressure is calculated :

$$p(z) = p_{atm} + g\rho_0(\eta - z) + g\int_z \eta\rho' \, dz \qquad \text{Eq. 4.12}$$

This relates pressure at any depth with the atmospheric pressure at the sea surface, the sea level and the pressure anomaly integrated between that level and the surface. By using this expression and the Boussinesq approximation, the horizontal pressure gradient in the direction xi can be divided in three contributions:

$$\partial_{x_i} p = \partial_{x_i} p_{atm} - g\rho_0 \partial_{x_i} \eta - g \int_z \eta \partial_{x_i} \, dz \qquad \text{Eq. 4.13}$$

The total pressure gradient is the sum of the gradients of atmospheric pressure, of sea surface elevation (barotropic pressure gradient) and of the density distribution (baroclinic pressure gradient).

The density is obtained from the salinity and from the temperature, which are transported by the water properties module.

4.2.5 Module Lagrangian

The Lagrangian module is used to simulate processes in the far field. The Lagrangian transport model tracks the trajectories of selected water masses using the transport fields from the hydrodynamic model in an explicit procedure. Dispersion is computed using the results from the turbulence model. The Lagrangian transport models are based on the simulation of tracer movement in a Lagrangian referential. They use the concept of tracer and are usually referred to as particle tracking models. The main feature is to avoid the explicit resolution of the advective term of the transport equation, avoiding problems of instability. The great advantage of Lagrangian transport models is that they may be used in the presence of very high gradients, since the Lagrangian approach does not suffer from the numerical diffusion problems characterizing the Eulerian transport models.

At the present stage, the model is able to simulate oil dispersion, water quality evolution and sediment transport. To simulate oil dispersion the Lagrangian module interacts with the oil dispersion module, to simulate the water quality evolution the Lagrangian module uses the features of the water quality module. Sediment transport can be associated directly to the tracers using the concept of settling velocity.

4.2.5.1 Tracer Movement

MOHID's Lagrangian module uses the concept of tracer. The most important property of a tracer is its position (*x, y, z*). A tracer can be a water mass, a sediment particle or a group of sediment particles, a molecule or a group of molecules, or spot phytoplankton cells in a tracer (at the bottom of the food chain) as well as a shark (at the top of the food chain), which means that a model of this kind can simulate a wide spectrum of processes. The movement of the tracers can be influenced by the velocity field from the hydrodynamic module, by the wind from the surface module, by the spreading velocity from oil dispersion module and by random

velocity. The tracers are characterized by their spatial coordinates, volume and a list of properties (each with a given concentration). The properties can be those described in the water properties module or properties specific to the Lagrangian model such as coliform bacteria. Each tracer has associated a time to perform the random movement. The tracers are "born" at origins. The major factor responsible for particle movement is generally the mean velocity. The spatial coordinates are given by the definition of velocity:

$$\frac{dx_i}{dt} = u_i(x_i, t) \qquad \text{Eq. 4.14}$$

where *u* stands for the mean velocity and *x* for the particle position. Eq. 4.14 is solved using a simple explicit method:

$$x_i^{t+\Delta t} = x_i^t + \Delta t \cdot u_i^t \qquad \text{Eq. 4.15}$$

Velocity at any point of space is calculated using a linear interpolation between the points of the hydrodynamic model grid. The Lagrangian module permits to divide the calculation of the trajectory of the tracers into sub-steps of the hydrodynamic time step.

Turbulent transport is responsible for dispersion. The effect of eddies over particles depends on the ratio between eddies and particle size. Eddies bigger than the particles make them move at random.

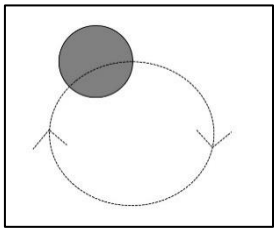

Figure 4.8. Random movement forced by an eddy larger than the particle

Eddies smaller than the particles cause entrainment of matter into the particle, increasing its volume and it's mass according to the environment concentration.

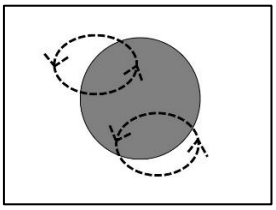

Figure 4.9. Random movement forced by an eddy smaller than the particle

The random movement is calculated following the procedure of Allen (1982). The random displacement is calculated using the mixing length and the standard deviation of the turbulent velocity component, as given by the turbulence closure of the hydrodynamic model. Particles retain that velocity during the necessary time to perform the random movement, which is dependent on the local turbulent mixing length. The increase in volume is associated with small-scale turbulence and is reasonable to assume it as isotropic. In these conditions, small particles keep their initial form and their increase in volume is a function of the volume itself.

4.2.5.2 Near-Field Module MOHIDJET

The plume dispersion of the submarine outfalls in the near field is calculated using the MOHIDJET dispersion module. This module aims at simulating the initial dilution associated with submarine outfall jets, defining the initial conditions for the far field Lagrangian model. The initial dilution is simulated using the evolution of a tracer with a cylindrical geometric shape, using a Lagrangian referential for spatial discretization (Leitão, 2004), The Lagrangian approach used in the MOHIDJET is similar to the one used in the JETLAG model, as in, Lee and Cheung, 1990. In simple terms, the trajectory and volume variation of a tracer with a cylindrical geometry is simulated. For the entrainment parametrization the work of Jirka, 1999 was used, similar to the methodology used in CORJET (Cornell Buoyant Jet Integral Model), the buoyant jet model of CORMIX (Cornell Mixing Zone Expert System).

The initial condition of the jet at the exit of the port holes is conditioned by the diameter and orientation relative to the current of the receiving environment and by the flow rate and density difference between the effluent and the receiving environment. The properties shown in Table 4.4 are used to describe each jet at the outlet of the diffuser orifices.

Table 4.4. Jet properties at the port exit

Property	Description
Δh_0	The length of the emitted "cylinder"
D_D	Port diameter
Q_0	Port flow
ρ_e	Jet Density at the Port exit
θ_m	Angle between the port normal vector and the horizontal plane
β_0	Angle between the port normal vector projection in the horizontal plane and the *x* direction

In this way, the MOHID model is able to simulate the dispersion of outfall plumes in the near-field (MOHIDJET module) and in the far-field (Lagrangian module) in an integrated way.

4.2.5.3 Bacterial Decay Rate

The decay rate depends on the processes that produce or destroy each property. As a general case a water quality or an ecological model represents these processes. In case of properties not produced in the environment, such as bacteria coming from urban sewage outflows, the following equation can be used.

$$\frac{dC}{dt} = -K_B C \quad ^{\wedge} \quad K_B = \frac{ln10}{T_{90}} \qquad \text{Eq. 4.16}$$

C – concentration;
K_B – decay rate
T_{90} – time interval necessary for bacterial concentration decrease by 90%

To resolve numerically the equation Eq. 4.16, an implicit method is used to prevent negative number of coliforms in $t+\Delta t$ (K_B is always positive).

The microbiological properties of the discharge varies due to dilution and mortality and bacteriological decay rate is conditioned by a wide variety of influences (Monteiro, 1995) such as solar radiation, temperature, salinity, predation by the biota of the receiving environment, nutrient concentration, toxic substances, sedimentation after discharge, resuspension of contaminated sediments and growth rate of the microorganisms in the receiving environment. Of all these factors, the condition that has a bigger impact in bacteriological decay rate is solar radiation. In an environment without light, the process of bacteriological decay rate can take at least two orders of magnitude more than the same process exposed to solar radiation.

MOHID Water modelling system has two options for the mortality law for faecal coliforms, in the present work the formula proposed by Chapra (1997) is used. It considers the effects of radiation, temperature, and salinity to compute the T_{90}.

4.3 MODEL SETUP

4.3.1 Spatial Discretization

The MOHID system employs a finite-volume approach for spatial discretization. The implemented model consists in three nested models, as shown in Figure 4.10. this configuration is based on the downscaling method (Leitão *et al.*, 2005) using less computational requirements. This method is used to manage the conditions in the open boundary, allowing the use of large-

scale operational model's solutions in local models with higher spatial resolution (Kenov *et al.*, 2014).

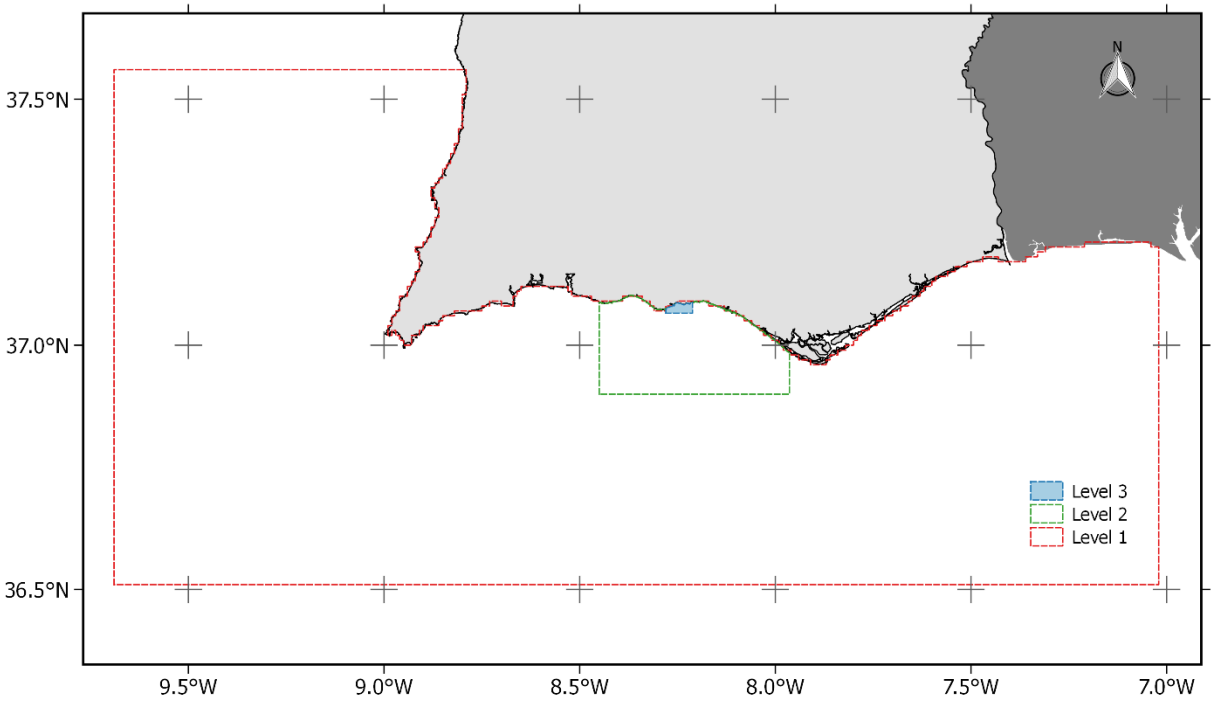

Figure 4.10. Nested model's implementation

The first level consists in reading the results obtained in the operational model SOMA, described in Janeiro *et al.*, 2012 and Janeiro, 2014 that provides tide results, velocity fields, density, temperature and salinity for the entire coast of the Algarve.

From the top level (SOMA reading results), two sub models are implemented, where the grid spacing is being lowered to reach the desired accuracy. The grid spacing transition between the three levels cannot be too abrupt and therefore a transition with a ratio of 1:5 it is considered as described in Leitão (2002). The spatial resolution values of each level are described in Table 4.5.

Table 4.5. Spatial resolution of the implemented model levels

Levels	Spatial Resolution		Origin		Size
	(m)	(º)	(Lat.)	(Long.)	(cells)
Level 1*	1000	0.00878	36.510 N	-9.69 W	267 × 105
Level 2	200	0.00176	36.900 N	-8.45 W	270 × 114
Level 3	40	0.00035	37.065 N	-8.28 W	190 × 65

*SOMA Results

Level 3 is the local model which aims to simulate the dilution and dispersion of the plume caused by the discharge of the marine outfalls.

The three levels use the same vertical geometry. A generic vertical mesh configuration is used with 28 layers, from which the bottom 17 are Cartesian and the top 11 are sigma. The sigma layers occupy the top 20 meters of the water column encompassing the outfall influence zone. This arrangement is advantageous for the simulation of barotropic flows in the shallower part of the domain, maintaining a good baroclinic description in deeper regions (Martins *et al.*, 2001).

4.3.2 Bathymetry and vertical geometry

The bathymetry of the first level is the bathymetry used in the operational model SOMA. The bathymetry of levels 2 and 3 were implemented for this work using a xyz points file with the bathymetry data; a grid and a polygon with information of the coastline. Data with information of the bathymetric values were obtained from Luís (2014). With the three listed files and using tools implemented in MOHID Studio graphical user interface, values of the bathymetric data were interpolated to the desired level resolution in each grid. The obtained bathymetries are represented in Figure 4.11, Figure 4.12 and Figure 4.13.

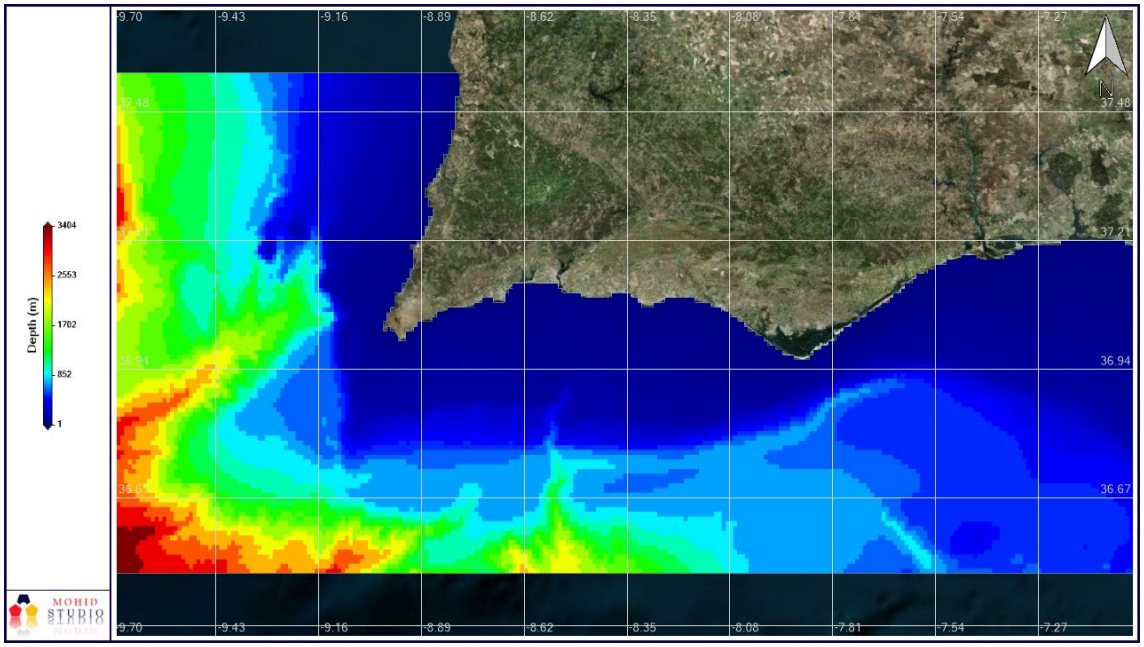

Figure 4.11. Level 1 Bathymetry

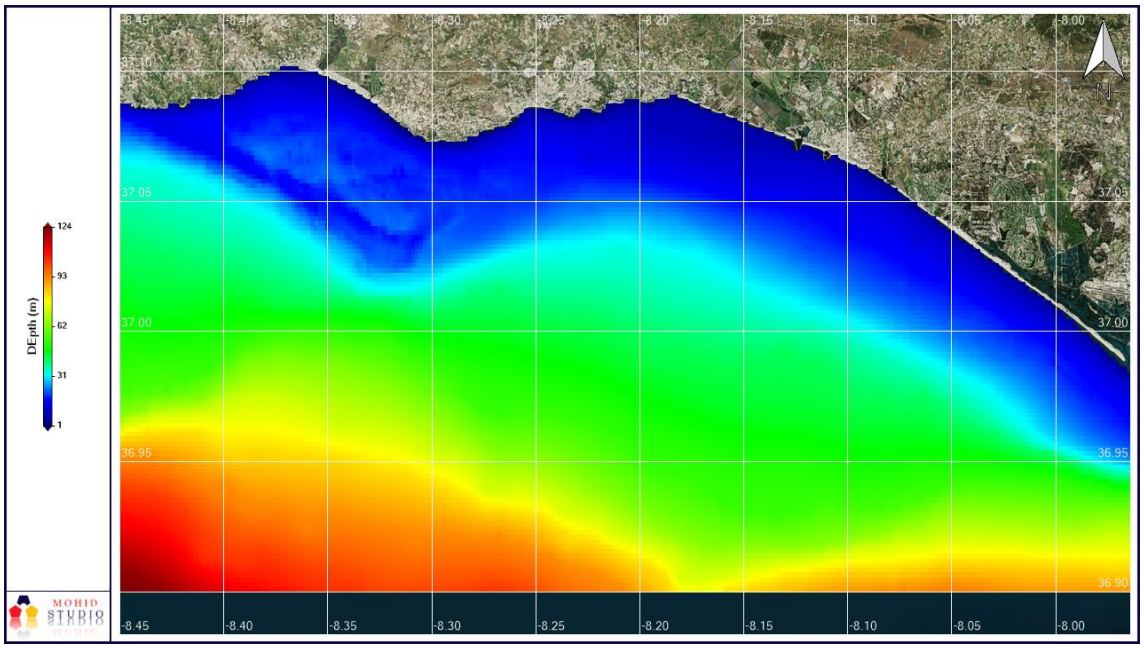

Figure 4.12. Level 2 Bathymetry

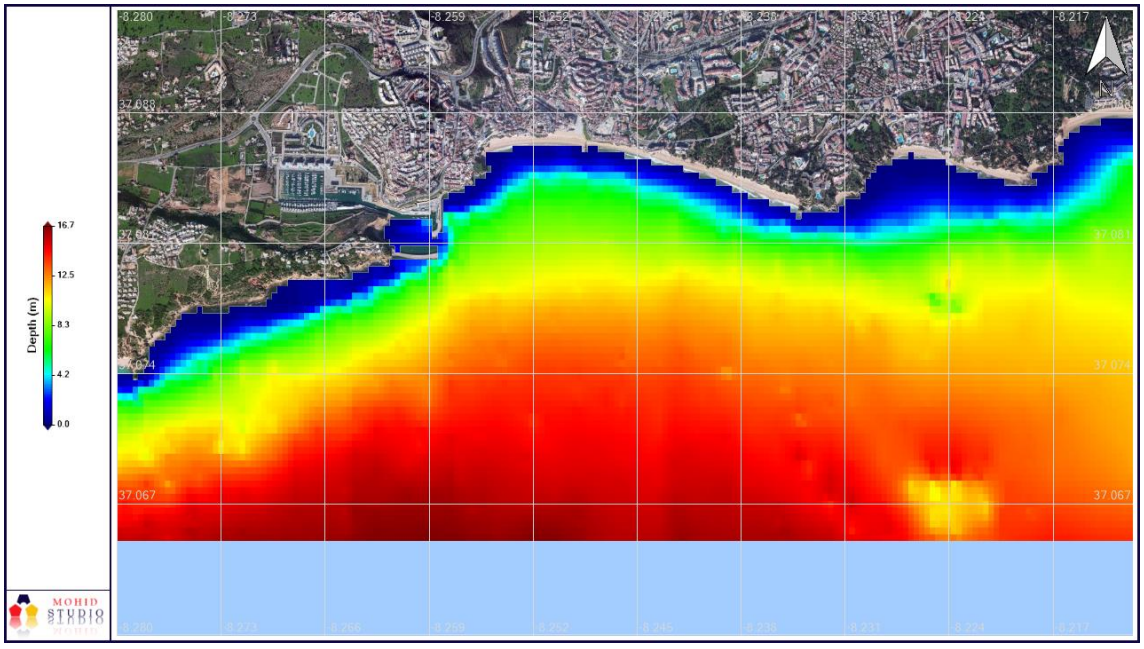

Figure 4.13. Level 3 Bathymetry

4.3.3 Boundary Conditions

At the surface the flow is normally bordered by an air-water interface, hence the flows intended to simulate have a free surface. Contrary of the earth-water interface, air-water interface always works as a source of turbulent cinematic energy and as source or sink of movement quantity, depended on wind direction relatively to Flow. In this case, water is considered stopped relatively to air. In this case the wind shear forces depend on wind speed and free surface roughness which can be calculated. (Leitão, 2002). At the bottom the boundary works as a sink

of momentum due to the effect of the frictional force which is proportional to the square of the water velocity.

In the first level the surface boundary conditions are not imposed because this level is just a reading window of the SOMA results. In the other two levels, at the surface, properties such as wind shear, heat fluxes, radiation, latent heat and sensible heat are imposed. The shear stress exerted by the wind is calculated, using a friction coefficient of 0.0025. The weather data required to enforce heat and motion fluxes to the water surface, were obtained from the SKIRON weather forecast system (Kallos & the SKIRON group, 1998) being interpolated to the grids of levels 2 and 3 (Figure 4.14). The frictional force exerted at the bottom is calculated, assuming a roughness factor equal to 0.0025 m for all levels.

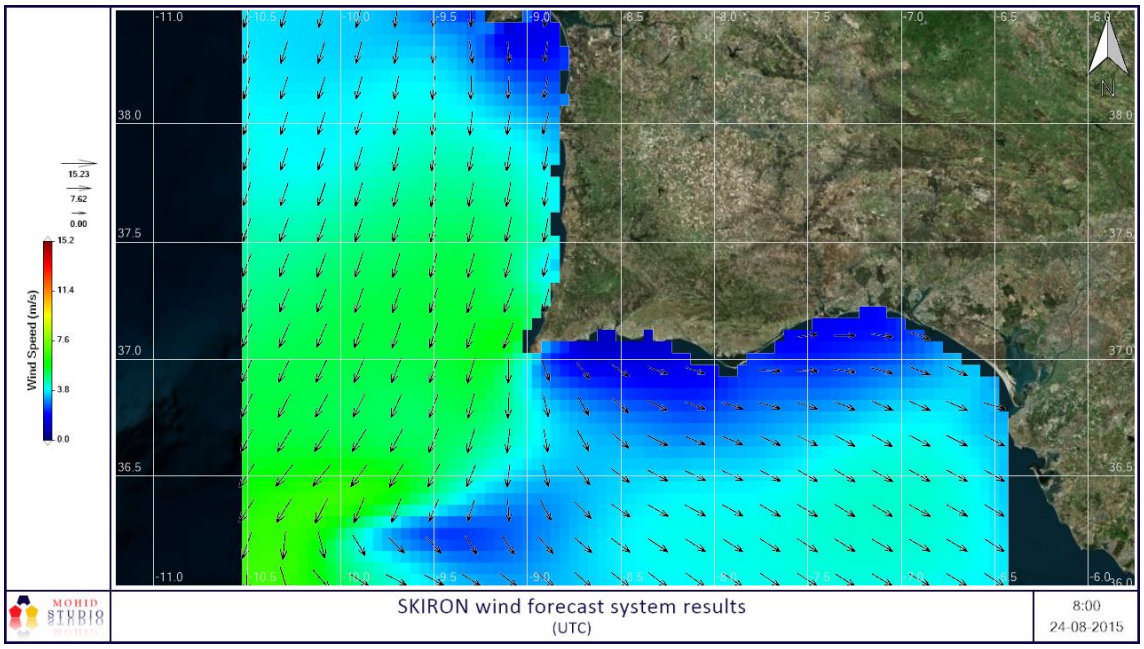

Figure 4.14. SKIRON wind forecast system results for a given instance

Salinity is assumed constant due to the low depth of the diffusers. Density is obtained from Temperature and Salinity using the UNESCO formulation (UNESCO, 1981), being used in the baroclinic forcing and to compute the plume buoyancy.

The horizontal open boundary corresponds to the horizontal boundary with other water masses, it is the definition of this boundary that allows to confine the domain to the study area. The values of the variables in the open boundary of the studied region are obtained by the method of nested models which allows the calculation of an exterior solution. The methodology of nested models is to implement smaller scale models from larger scale ones, for which the information is interpolated. The communication between the models is "one way", the results

of each top-level model are provided to the respective lower-level model in the open horizontal boundary but the opposite does not happen.

To create the conditions in the open boundary, given by each top-level model to the respective lower-level model, radiation methods and/or relaxation methods can be used (Riflet, 2010). For the temperature, salinity and to the velocity's, the condition in the open boundary is applied through a flux relaxation scheme (FRS). A FRS scheme allows that in a layer of 10 cells (sponge layer), at the boundary, the solution is relaxed to the outer solution. The Flather type radiation condition is applied in all levels in the boundary points, which enables to radiate the difference between the reference solution and the model solution with a higher resolution grid (Riflet, 2010).

Outfall plumes are simulated using the far field Lagrangian transport model coupled with the near field MOHIDJET model to simulate the initial dilution. The following inputs were used in the simulations: effluent density of 1000 kg/m^3; seawater density of 1026.70 kg/m^3.

4.3.4 Simulations

To access the impact of Vale Faro outfall in the bathing waters, the wind data was analyzed, and two wind events were chosen for the simulations. The events represent three of the main wind directions observed in the study during the bathing season. The values for Escherichia coli concentration in the discharge simulated were based on Henze & Comeau (2008) for scenario S1, S2 and S3 (Table 4.6).

Table 4.6. Main characteristics of the scenarios simulated

Run	Scenario / Objectives	Flow conditions	*Escherichia coli* (MPN/100ml)	Wind
S0	Real conditions. Validate the model using the finest approximation of the ground conditions during the field campaign of 24-08-2015	Measured flows (Chapter 5.1, page 65)	Pluviais: 2.4×10^5 Inatel: 2.4×10^6 Vale Faro: 8.0	SKIRON forecasts
S1.1	Bathing waters impact. Accessing the impact of the failure of the Vale Faro WWTP initial pumping station during different wind conditions	Vale Faro project maximum medium daily flow of 24,310 m^3/d. Pluviais an Inatel with 5 times the flows measured in the field campaigns.	Pluviais: 2.4×10^5 Inatel: 2.4×10^6 Vale Faro: 5.0×10^8	Constant 4.3 m/s from SE
S1.2				Constant 4.3 m/s from W
S1.3				Constant 4.3 m/s from E
S1.4				Constant 4.3 m/s from S
S2.1	Vale Faro WWTP discharge impact. Accessing the impact of the discharge of Vale Faro WWTP considering different bacteriological concentrations	Vale Faro project maximum medium daily flow of 24,310 m3/d.	Vale Faro: 2,000	Constant 4.3 m/s from S
S2.2			Vale Faro: 10,000	
S2.3			Vale Faro: 44×10^4	

5 RESULTS

5.1 FLOW MEASUREMENT

Figure 5.1 shows the results of the measuring field campaign of the Inatel outfall for a period of two weeks used to estimate the Inatel outfall hourly flowrate for the month of august (Figure 5.4).

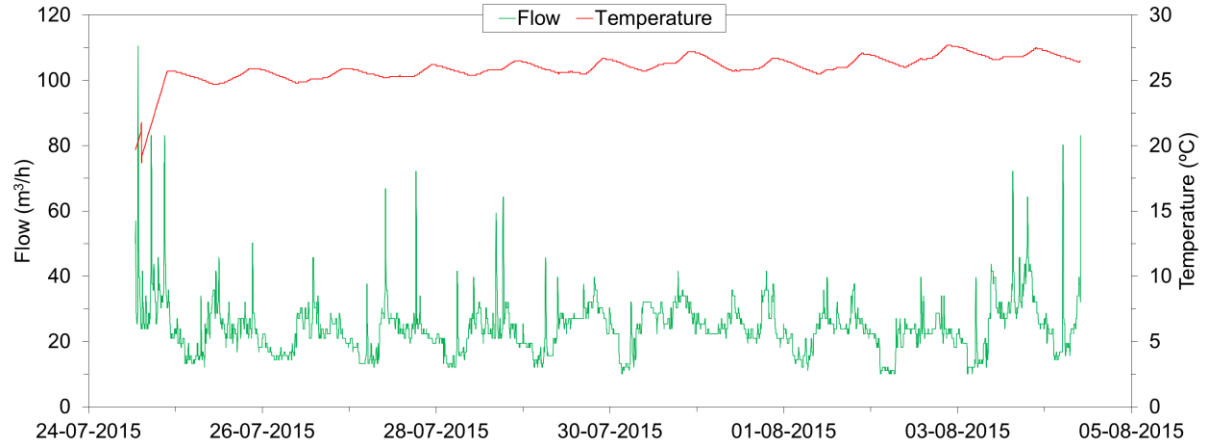

Figure 5.1. Inatel outfall measuring campaign results

Figure 5.2 to Figure 5.4 display the outfall flows results for the entire month of August 2015 used in the simulations as time series.

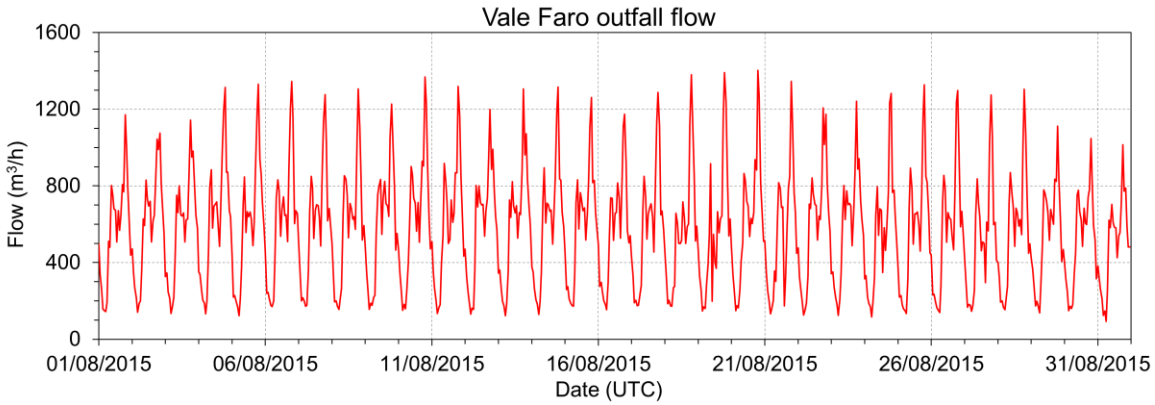

Figure 5.2. Vale Faro outfall hourly flowrate in August 2015

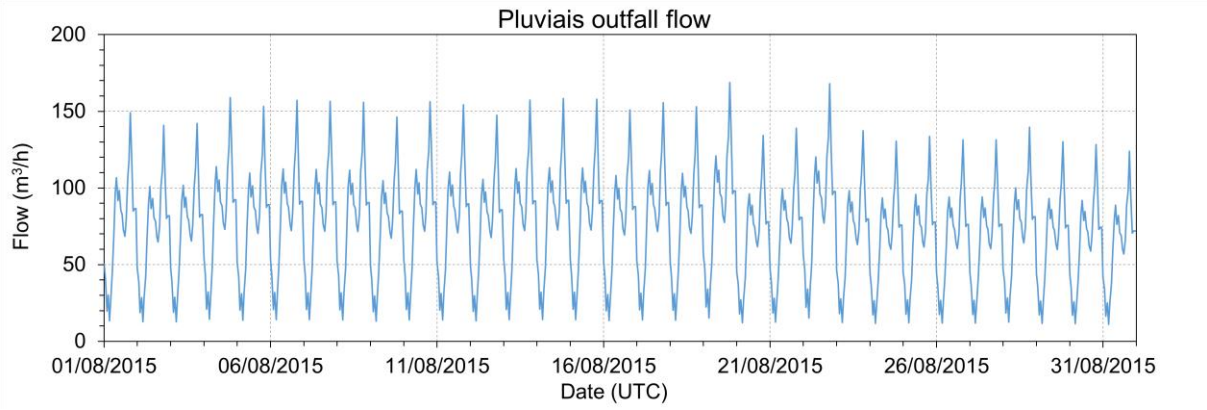

Figure 5.3. Pluviais outfall hourly flowrate estimated for August 2015

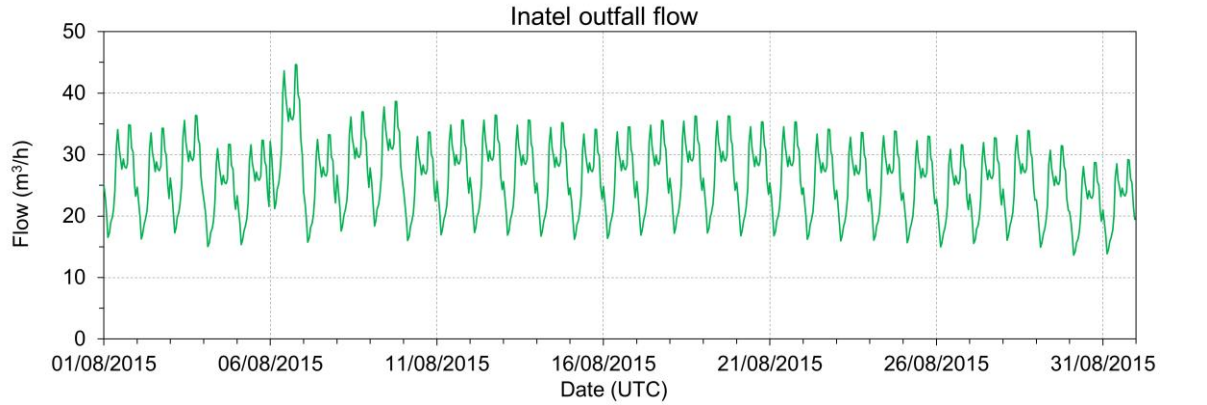

Figure 5.4. Inatel outfall hourly flowrate estimated for August 2015

Figure 5.5 to Figure 5.7 displays the outfalls flows for the simulations during the field campaign of 24th of August 2015.

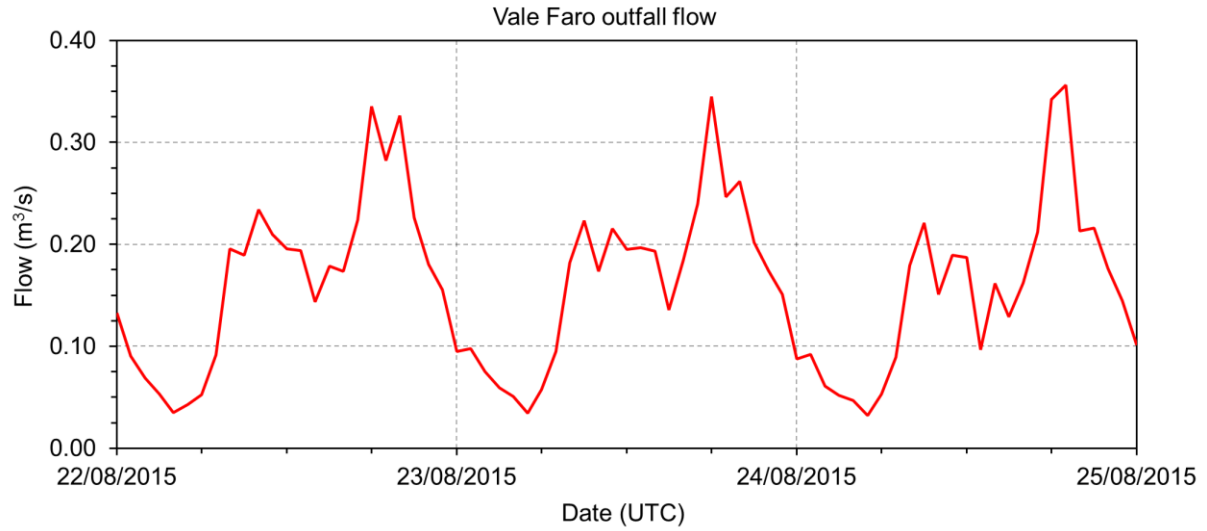

Figure 5.5. Vale Faro outfall hourly flowrate during the field campaign of 24th of August 2015

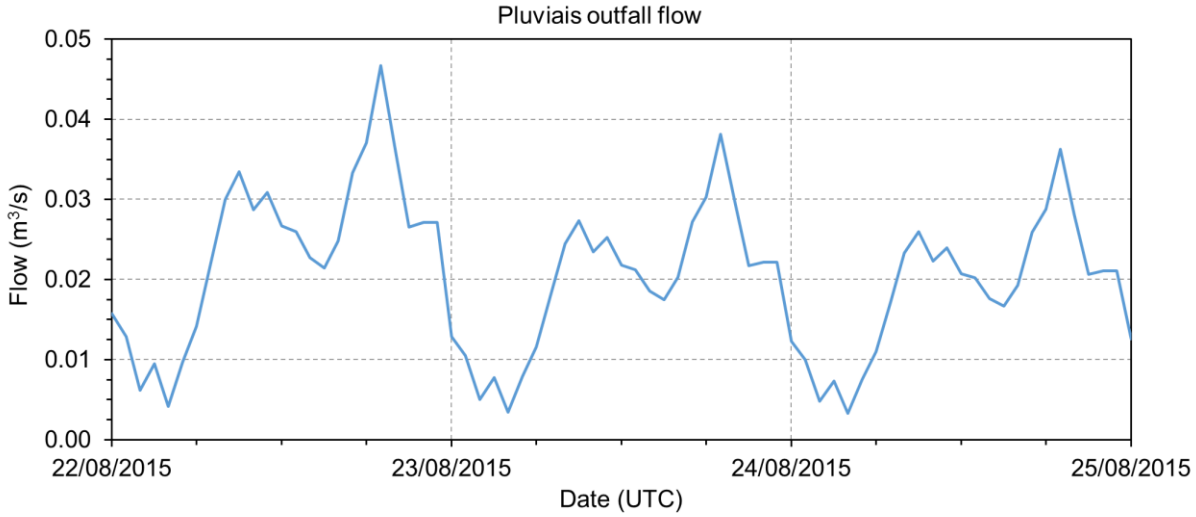

Figure 5.6. Pluviais outfall hourly flowrate during the field campaign of 24th of August 2015

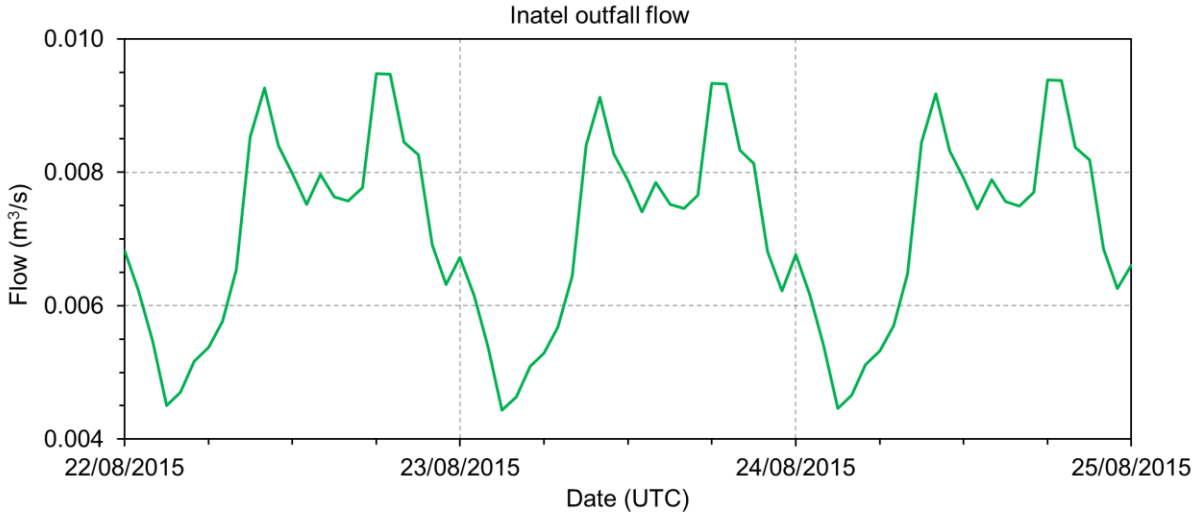

Figure 5.7. Inatel outfall hourly flowrate during the field campaign of 24th of August 2015

5.2 WIND

In Table 5.1 the data collected in the wind stations near the outfalls is presented.

Table 5.1. Characteristics of wind data collected

Weather Station	Records Interval (min)	Analysis Period (Start) (End)	Duration (days)	Expected Records (N.º)	Missing / Discarded Records (%)
Algoz	60	01/02/2001 17:00 08/01/2010 09:00	3262.6	78304	1.1
Loulé	60	15/03/2001 11:00 07/01/2010 15:00	3220.1	77284	1.2
Paderne	60	04/07/2001 16:00 07/01/2010 16:00	3109.0	74616	7.2
Faro Airport	60	10/07/2013 17:00 31/12/2015 23:00	904.2	21702	7.7
Vale Faro	60	05/07/2016 22:05 03/01/2017 09:14	181.4	4355	8.7

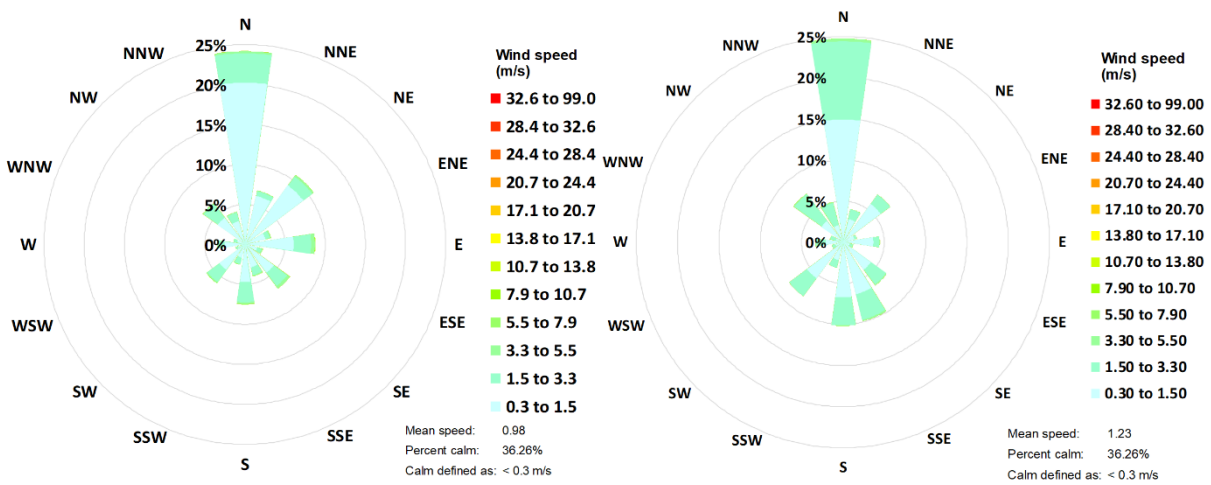

Figure 5.8. Wind direction and speed frequency out of the bathing season (left) and during the bathing season (right) for Algoz WS.

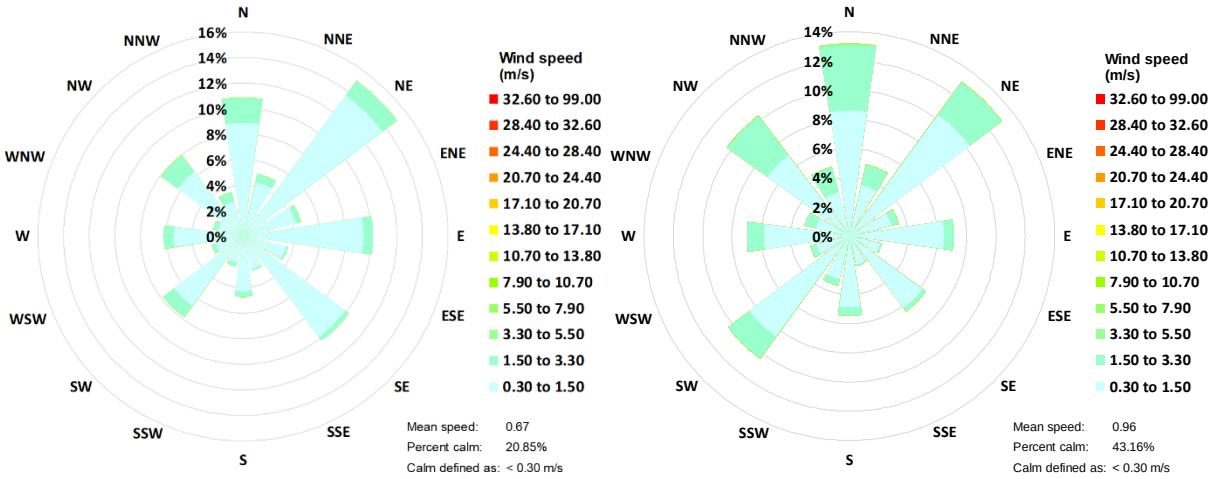

Figure 5.9. Wind direction and speed frequency out of the bathing season (left) and during the bathing season (right) for Loulé WS.

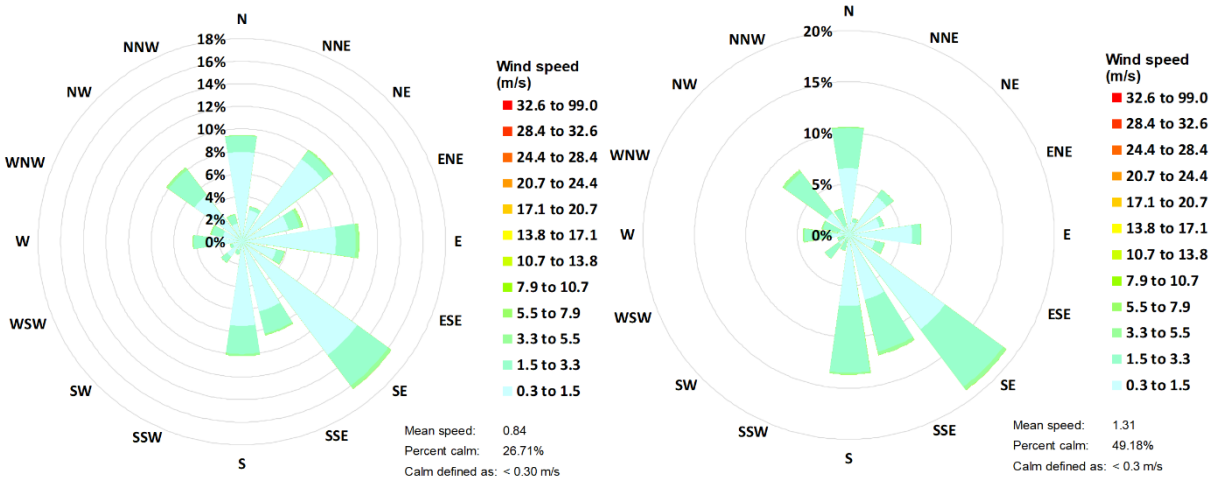

Figure 5.10. Wind direction and speed frequency out of the bathing season (left) and during the bathing season (right) for Paderne WS.

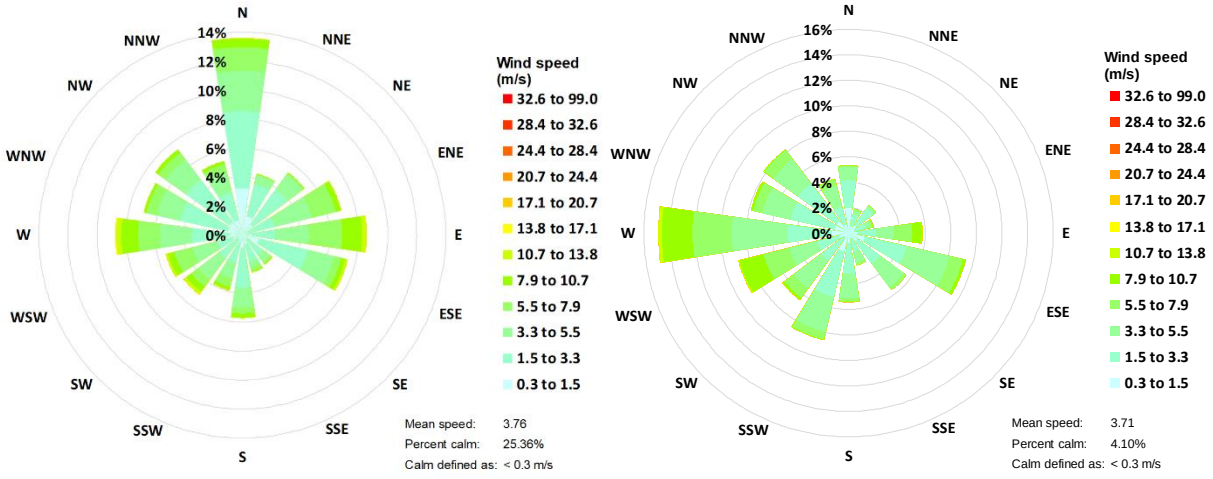

Figure 5.11. Wind direction and speed frequency out of the bathing season (left) and during the bathing season (right) for Faro Airport WS.

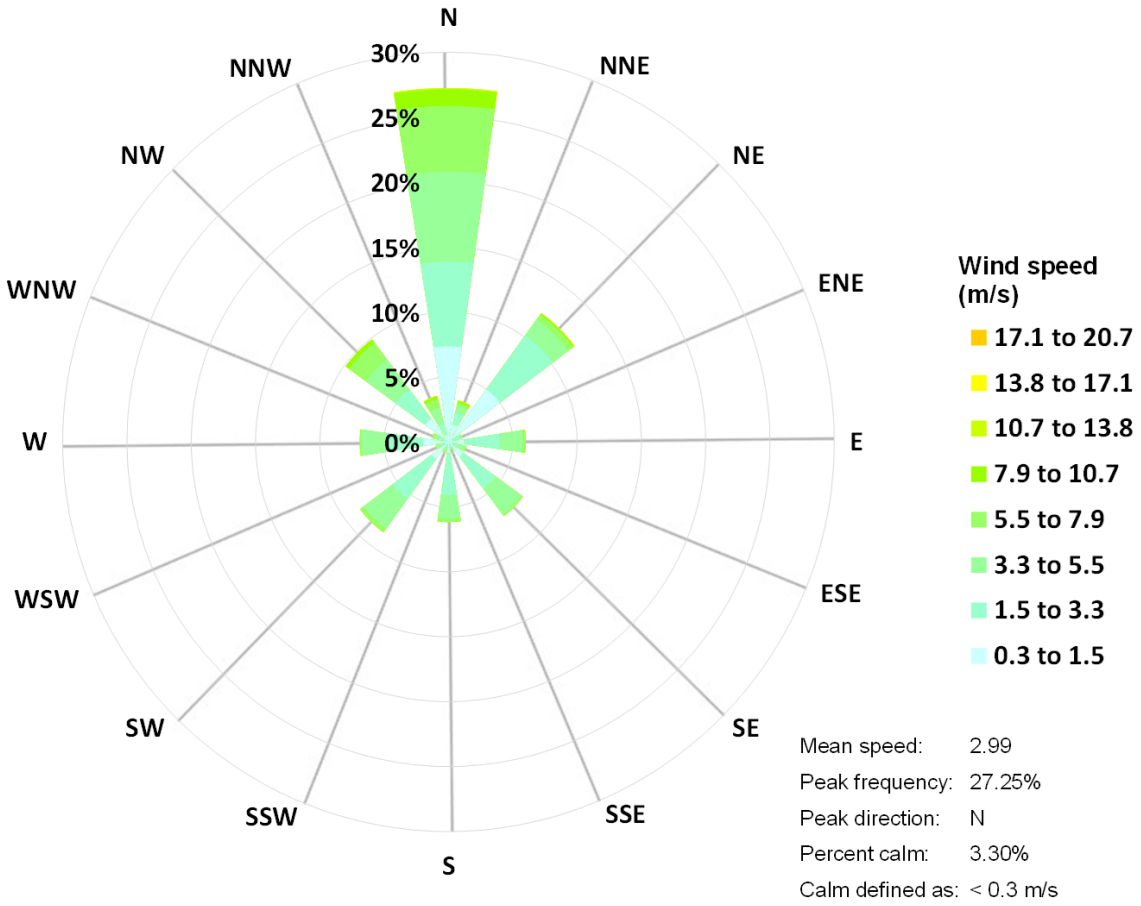

Figure 5.12. Wind direction and speed frequency for Vale Faro WS

5.3 TIDE

Tide data collected from the Lagos tide Gauge from 15th of August to 25th August 2015 is displayed in Figure 5.13.

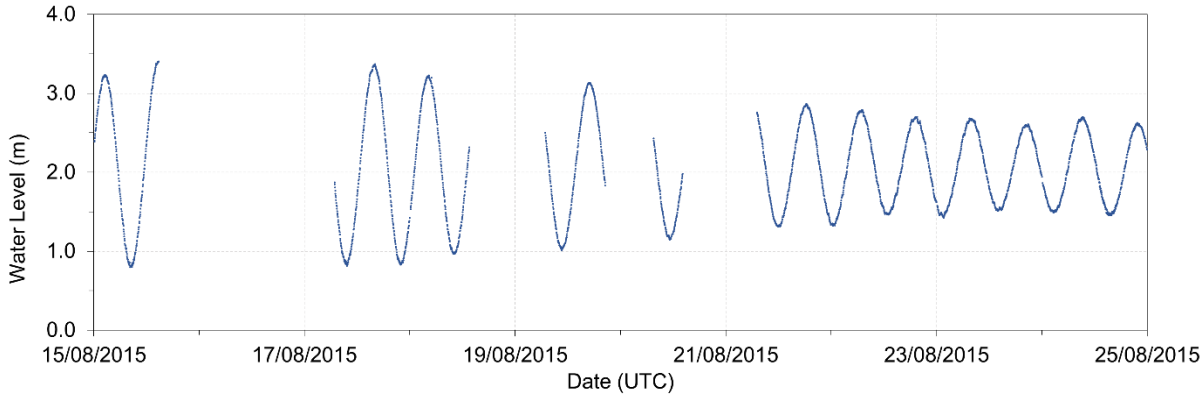

Figure 5.13. Water level obtained from Lagos Tide Gauge

Figure 5.14 displays the measured water level in the Lagos Tide Gauge during August 24th, 2015 field campaign.

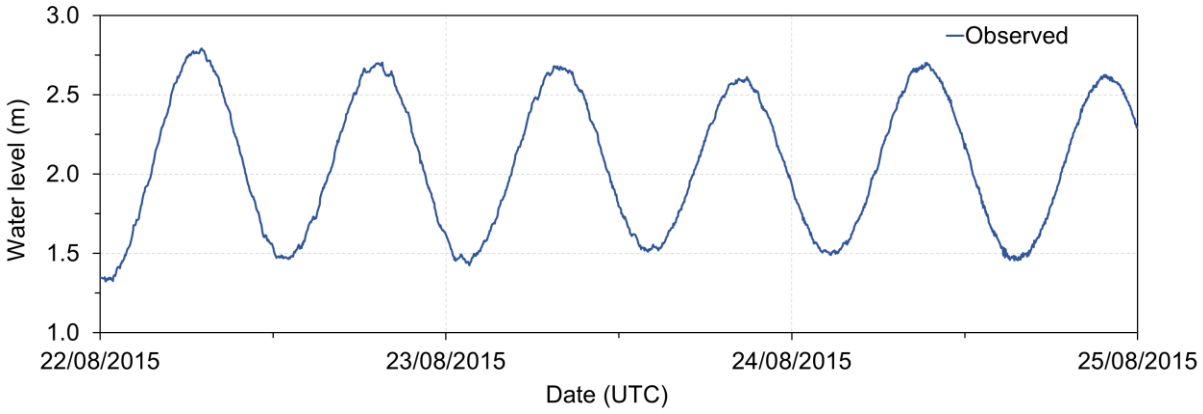

Figure 5.14. Water level obtained from Lagos Tide Gauge during the field campaign of August 24th, 2015

5.4 BACTERIOLOGICAL FIELD CAMPAIGNS

The field campaigns sampling were made by two teams; one in land to collect water samples from the discharges of the marine outfalls PL0, IN0 and VF0; another team to collect the water samples in the ocean around the outfalls diffusers PL1, PL2, PL3, PL4, IN1, IN2, VF1, VF2, VF3 and VF4, using a boat (Figure 4.5). Figure 5.15 shows the trajectory of the boat during the sampling done at sea during the field campaign of august, 22nd of 2016.

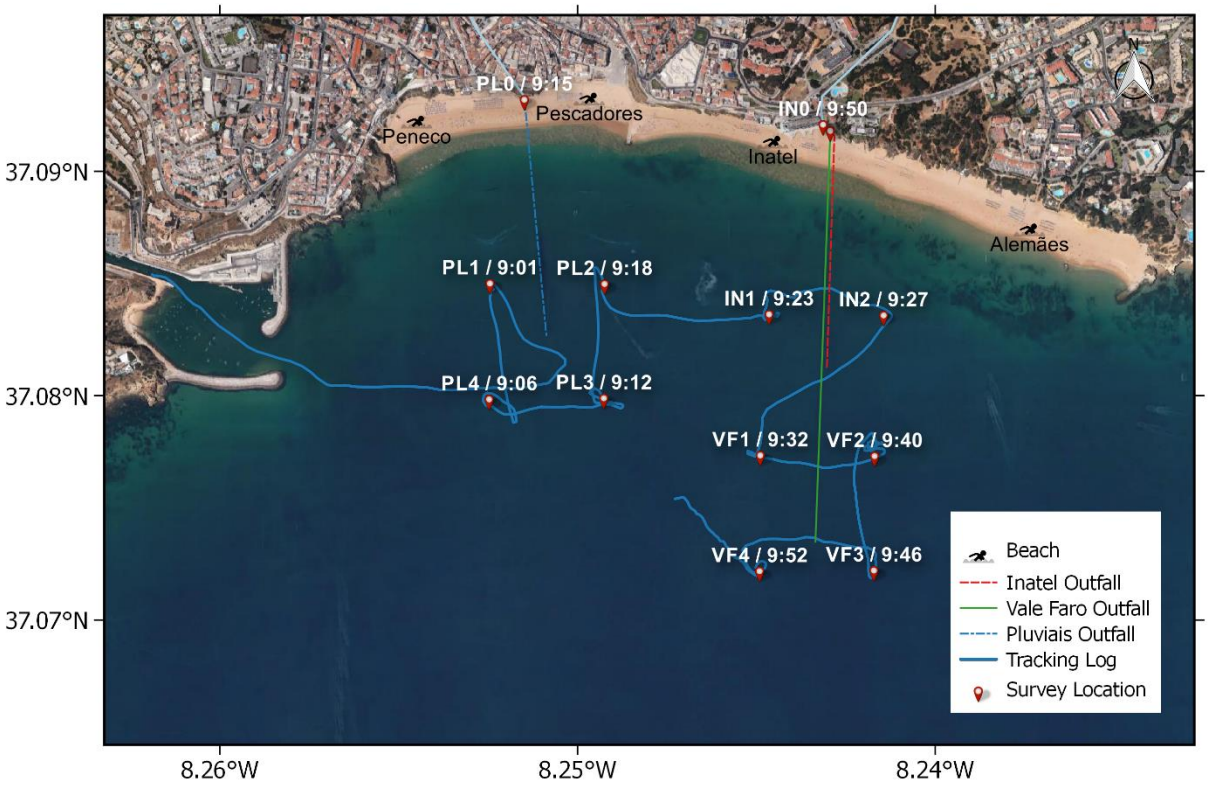

Figure 5.15. Boat tracking log during field campaign (UTC)

The bacteriological measurements results (Table 5.2) were processed according to the ISO 9308-2 and ASTM D6503-99 (2009) standards for *Escherichia coli* and Enterococci respectively and were executed in the ADA accredited Laboratory.

Table 5.2. July 27th, 2015 field campaigns results

Station Name	Time (UTC)	*Escherichia coli* (MPN/100 ml)	Intestinal enterococci (MPN/100 ml)	Temperature (ºC)
PL0	08:55	24×10^4	13×10^3	21.4
PL1	08:29	3	6	15.9
PL2	08:37	70	3	15.5
PL3	08:40	60	3	15.5
PL4	08:47	110	7	15.5
VF0	08:40	32	61	29.3
VF1	09:05	0	5	15.6
VF2	09:01	0	7	15.7
VF3	08:56	0	13	15.9
VF4	08:52	1	2	15.2
IN0	08:35	0	0	24.6
IN1	09:12	120	10	15.6
IN2	09:16	0	3	15.6
Peneco	08:48	< 15	< 15	-
Pescadores	08:56	15	< 15	-
Inatel	09:09	< 15	< 15	-
Alemães	09:16	< 15	< 15	-

Table 5.3. August 24th, 2015 field campaigns results

Station Name	Time (UTC)	*Escherichia coli* (MPN/100 ml)	Intestinal enterococci (MPN/100 ml)	Temperature (ºC)
PL0	09:20	$>24\times10^3$	$>24\times10^3$	20.5
PL1	08:49	210	6	18.5
PL2	08:55	100	6	18.2
PL3	08:59	100	3	18.2
PL4	09:03	110	4	18.3
VF0	08:45	8	53	28.3
VF1	09:09	2	2	18.4
VF2	09:13	2	1	18.4
VF3	09:18	2	0	18.3
VF4	09:25	0	0	18.3
IN0	09:00	$>24\times10^5$	20×10^4	23.4
IN1	09:32	3	4	18.4
IN2	09:35	$>24\times10^3$	13	18.2
Peneco	09:54	61	15	-
Pescadores	10:01	110	61	-
Inatel	10:15	15	15	-
Alemães	10:22	30	< 15	-

Table 5.4. August 22nd, 2016 field campaigns results

Station Name	Time (UTC)	*Escherichia coli* (MPN/100ml)	Intestinal enterococci (MPN/100 ml)	Temperature (ºC)
PL0	09:15	24×10^5	49×10^3	20.7
PL1	09:01	< 10	< 10	22.7
PL2	09:18	10	10	22.4
PL3	09:12	< 10	< 10	22.5
PL4	09:06	30	10	22.4
VF0	09:50	44×10^4	37×10^3	29.4
VF1	09:32	40	20	22.4
VF2	09:40	110	< 10	22.3
VF3	09:46	< 10	< 10	23.0
VF4	09:52	< 10	< 10	23.1
IN0	09:40	> 24×10^3	> 24×10^3	26.6
IN1	09:23	340	110	22.6
IN2	09:27	< 10	< 10	22.7
Peneco	08:26	61	< 15	-
Pescadores	08:16	61	< 15	-
Inatel	08:09	77	15	-
Alemães	07:55	77	< 15	-

5.5 MATHEMATICAL MODELLING

5.5.1 S0 – Validation

The model results obtained for the water level were compared with those obtained from the data recorded in the tide gauge of the port of Lagos (Figure 5.16).

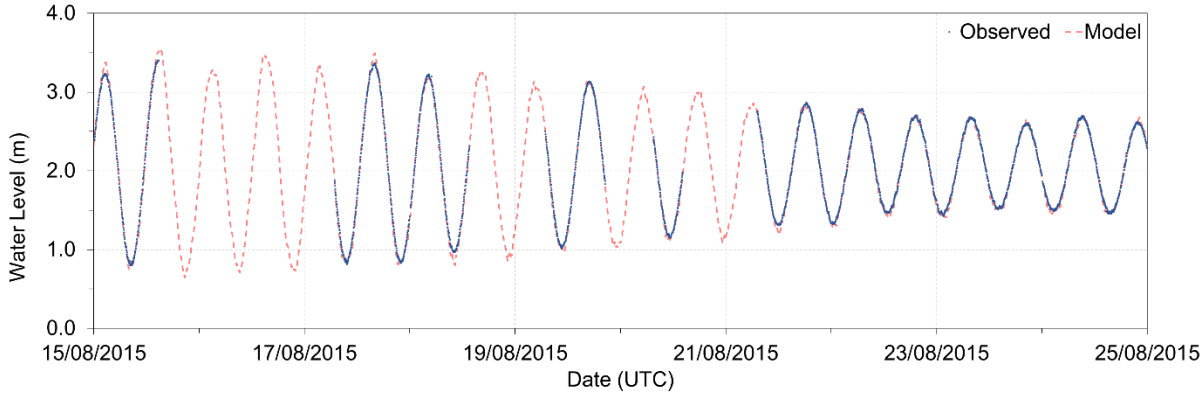

Figure 5.16. Water level measured compared with model results

Figure 5.17 displays the comparison of the water level measured in the tide gauge with tide results from the validation simulation period.

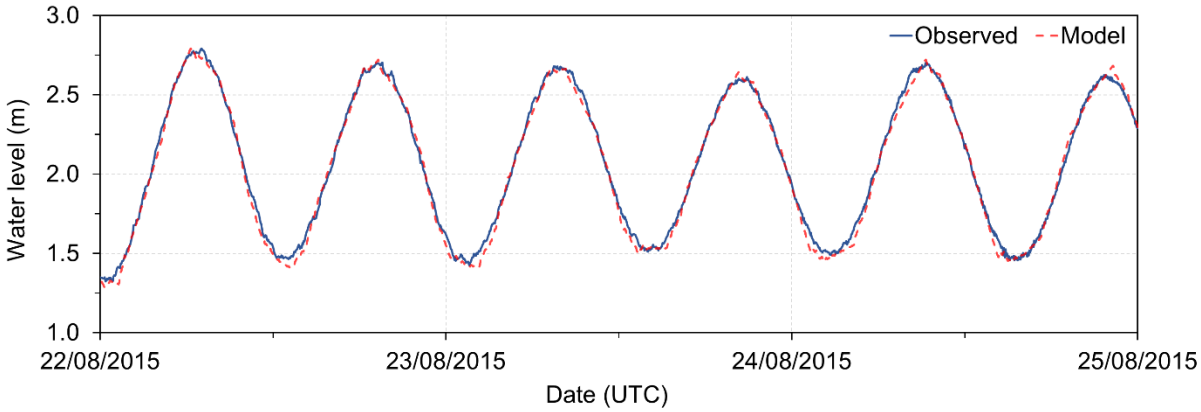

Figure 5.17. Water level measured compared with model results, validation simulation

The root mean square error (RMSE) of the two datasets is 44 mm, with a correlation coefficient of 0.997.

Figure 5.18, Figure 5.19 and Figure 5.20 shows the initial dilution given by the MOHIDJET (near-field) module used as an initial condition of Lagrangian tracer's module (far-field).

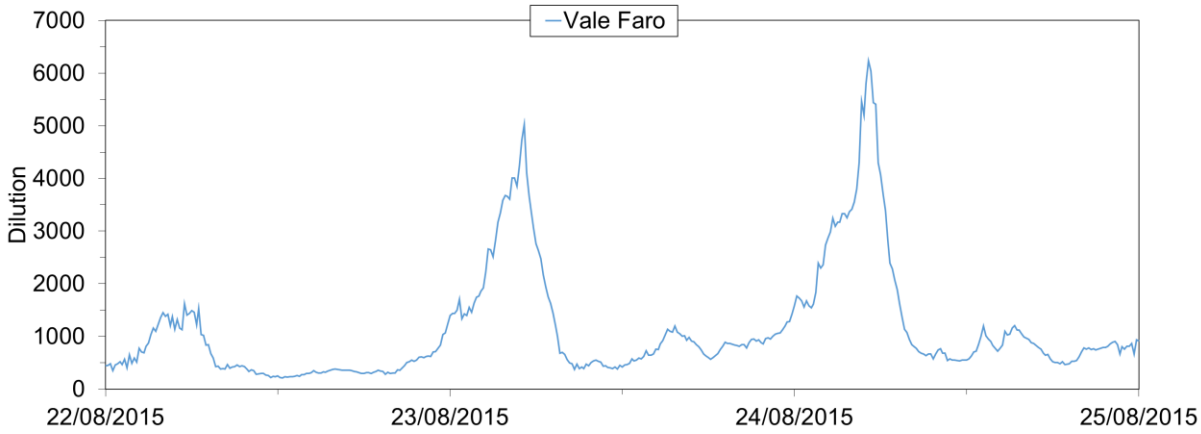

Figure 5.18. Vale Faro outfall initial dilution

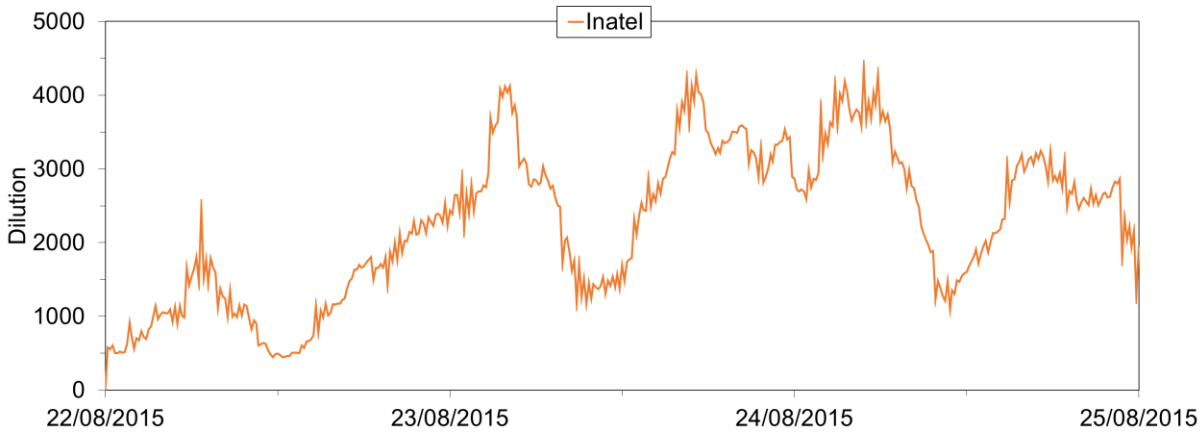

Figure 5.19. Inatel outfall initial dilution

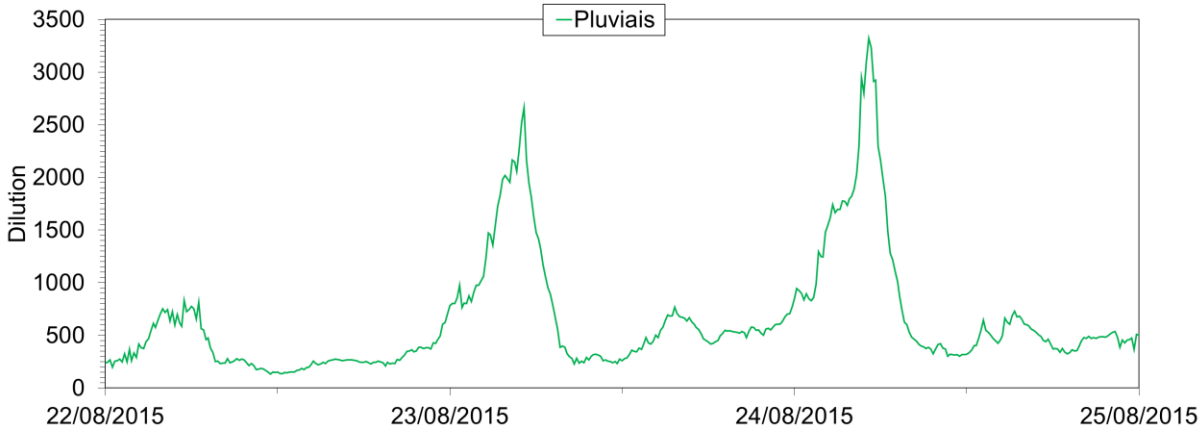

Figure 5.20. Pluviais outfall initial dilution

(Figure 5.21, Figure 5.22 and Figure 5.23 show the results of the hydrodynamic model for all Levels in a specific time instant.

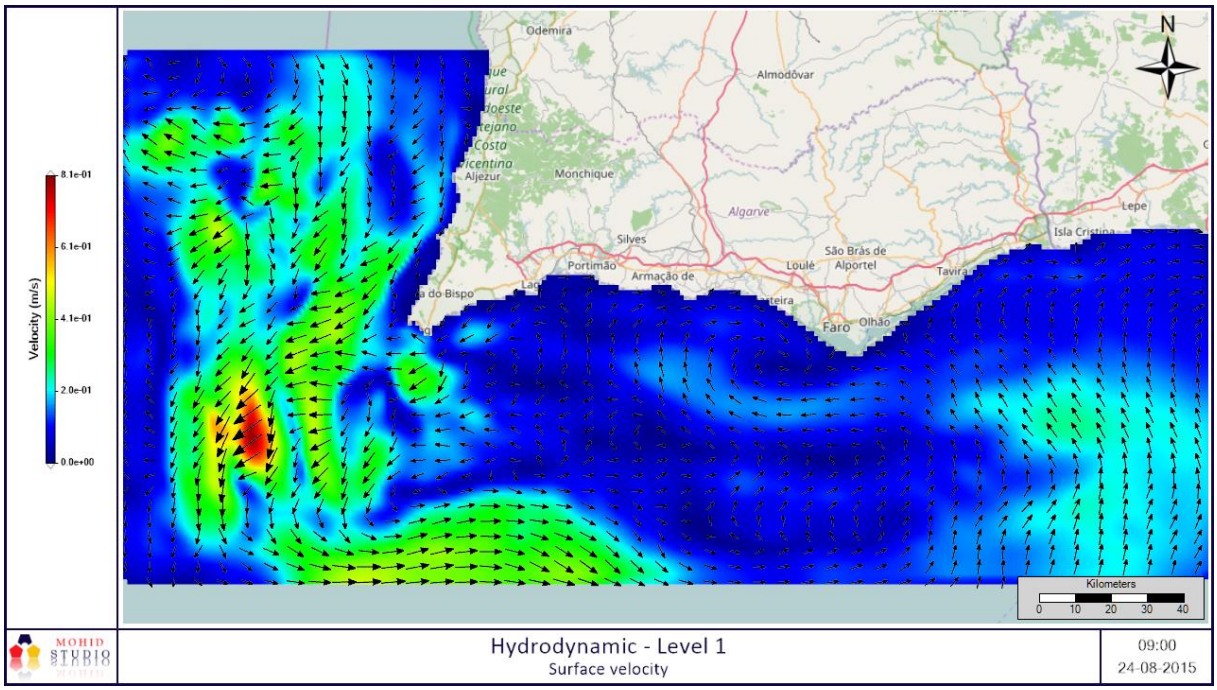

Figure 5.21. Hydrodynamic model results for Level 1

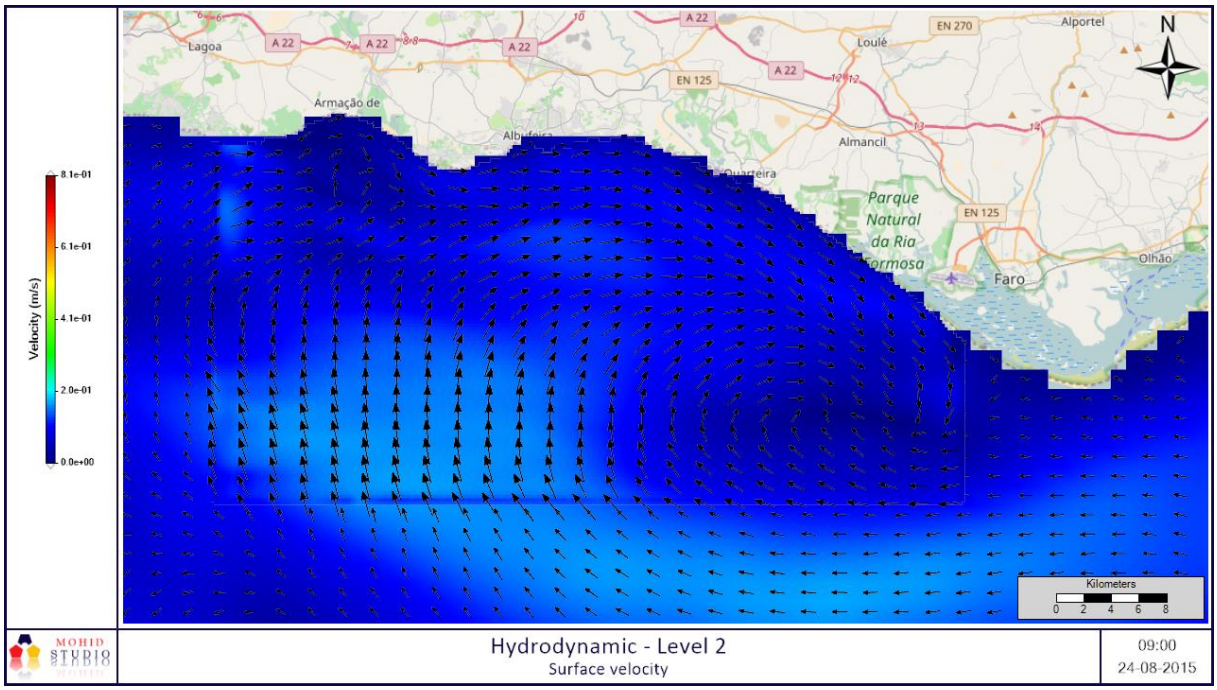

Figure 5.22. Hydrodynamic model results for Level 2

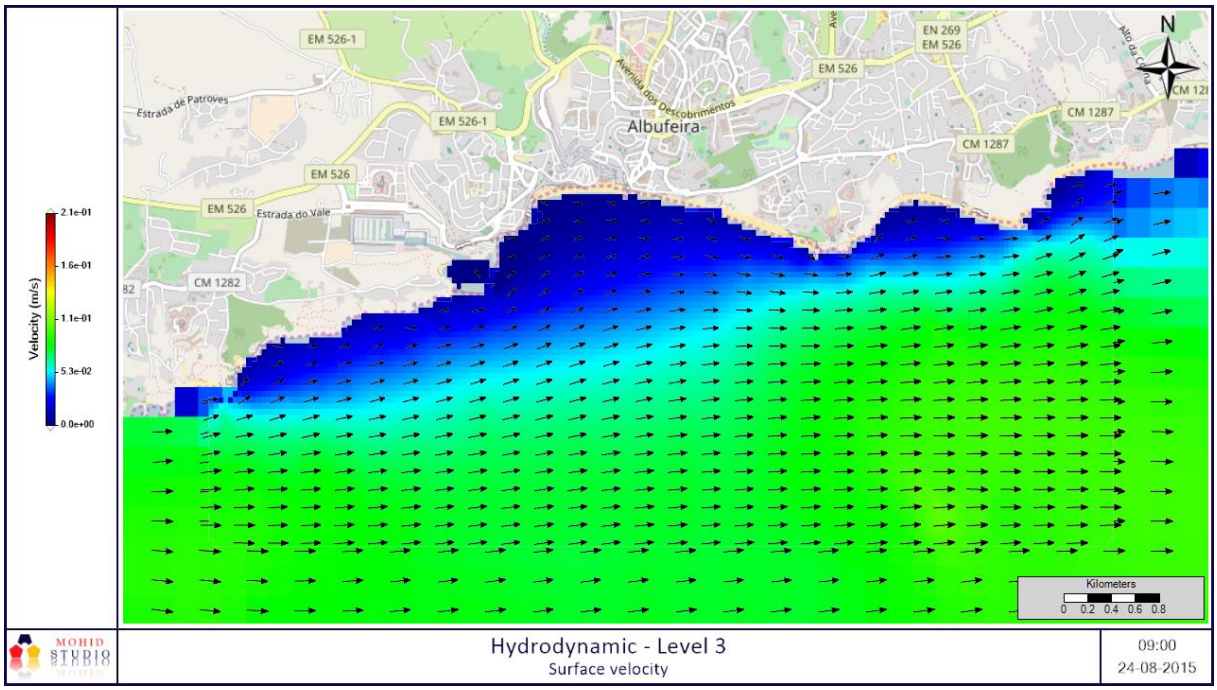

Figure 5.23. Hydrodynamic model results for Level 3

Figure 5.24 show the results of the velocity modulus at the bottom layer near the diffuser of each outfall during simulation S0.

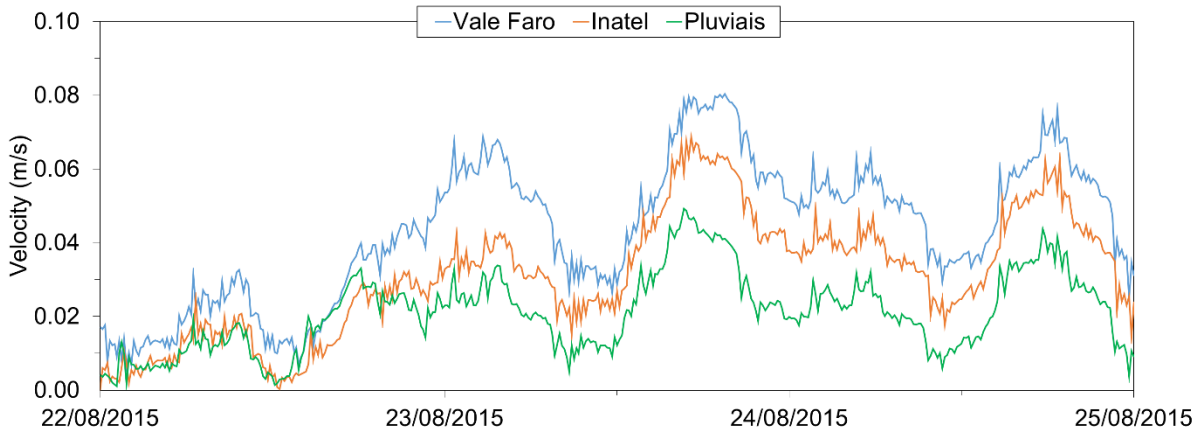

Figure 5.24. Velocity modulus near the outfall diffusers

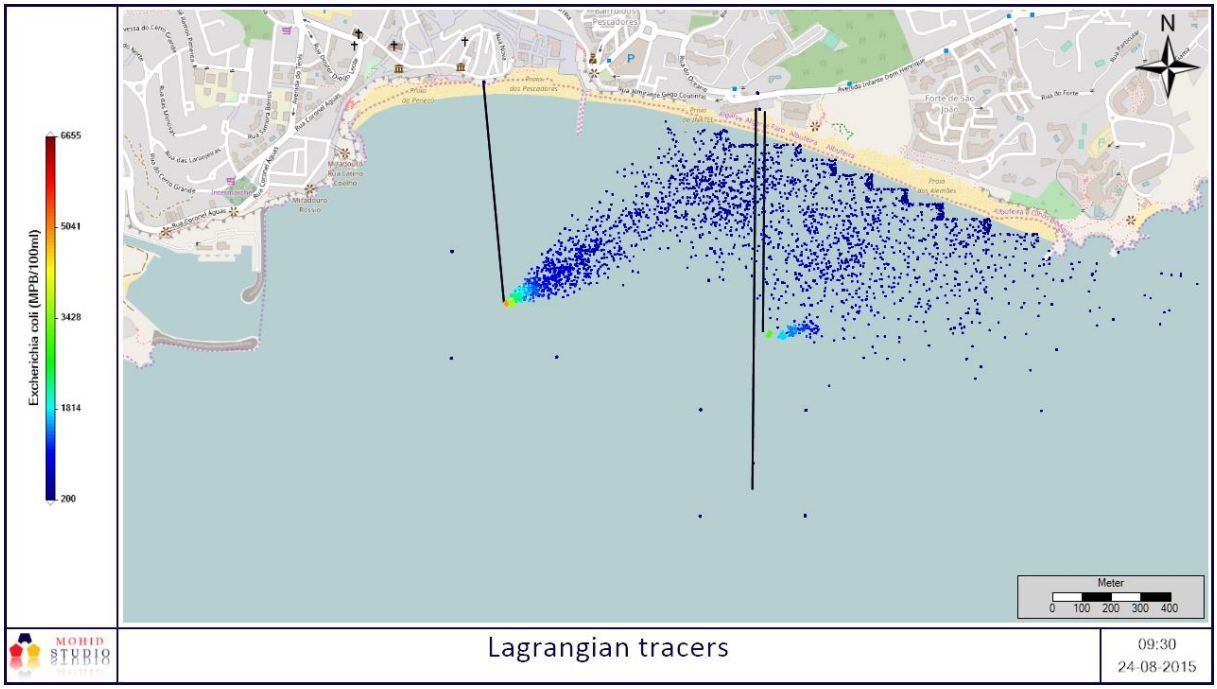

Figure 5.25. Lagrangian tracers results for the time instance of the field campaigns

Figure 5.26 to Figure 5.35 shows the *escherichia coli* concentration in each survey location cell during the entire run S0.

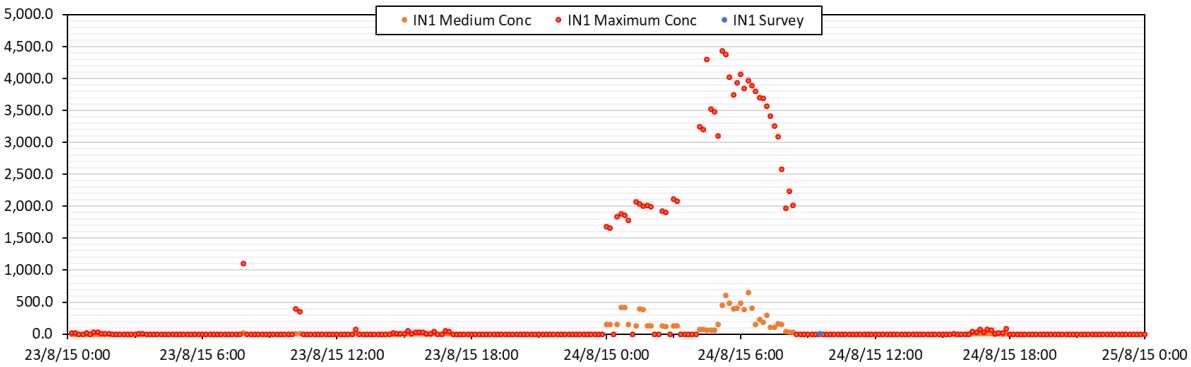

Figure 5.26. Temporal variation of *escherichia coli* concentration in survey point IN1

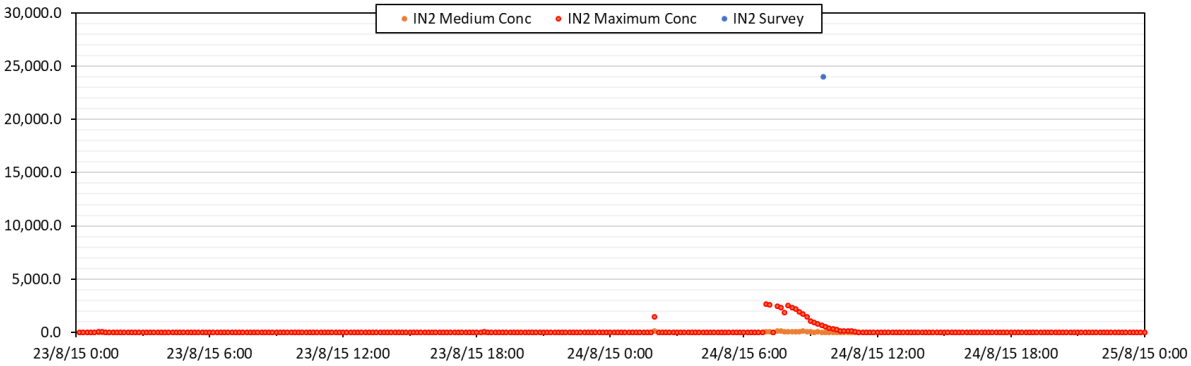

Figure 5.27. Temporal variation of *escherichia coli* concentration in survey point IN2

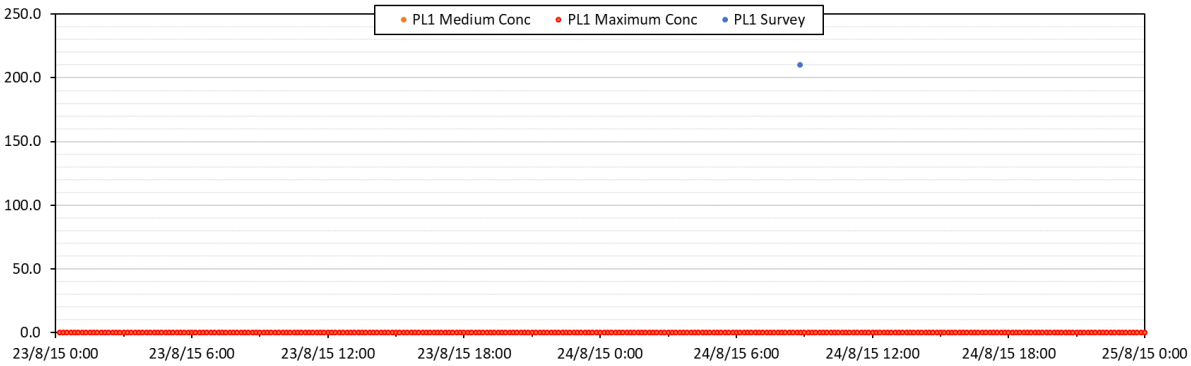

Figure 5.28. Temporal variation of *escherichia coli* concentration in survey point PL1

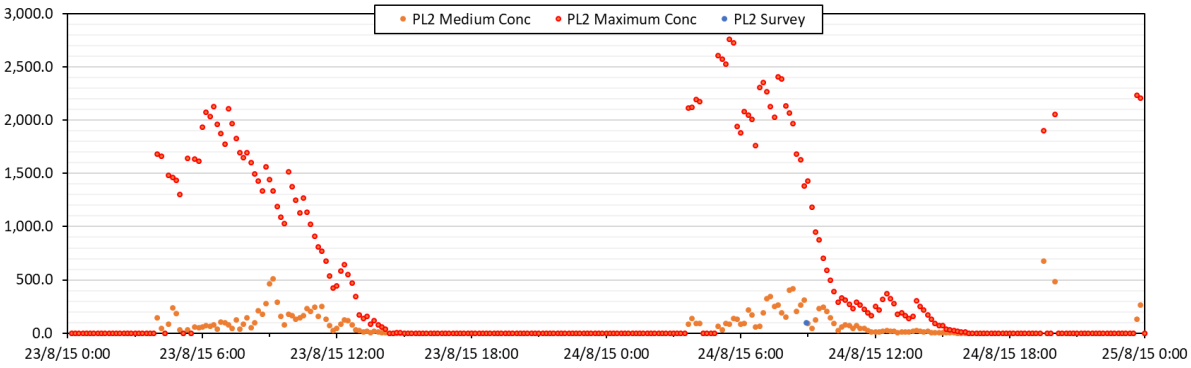

Figure 5.29. Temporal variation of *escherichia coli* concentration in survey point PL2

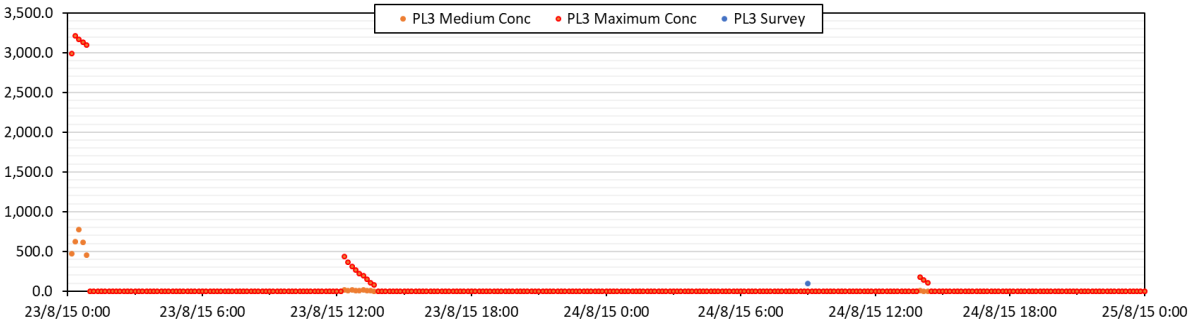

Figure 5.30. Temporal variation of *escherichia coli* concentration in survey point PL3

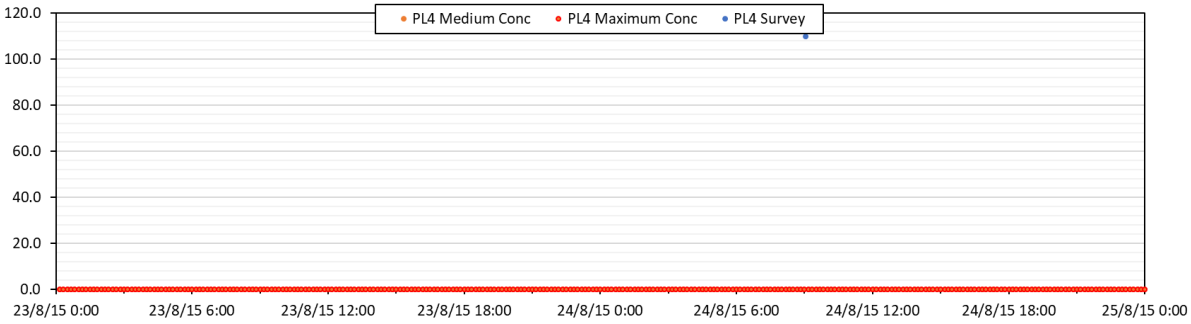

Figure 5.31. Temporal variation of *escherichia coli* concentration in survey point PL4

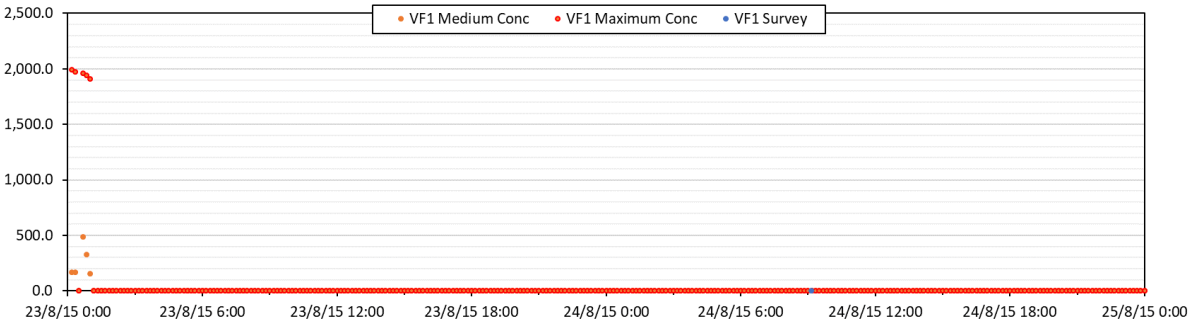

Figure 5.32. Temporal variation of *escherichia coli* concentration in survey point VF1

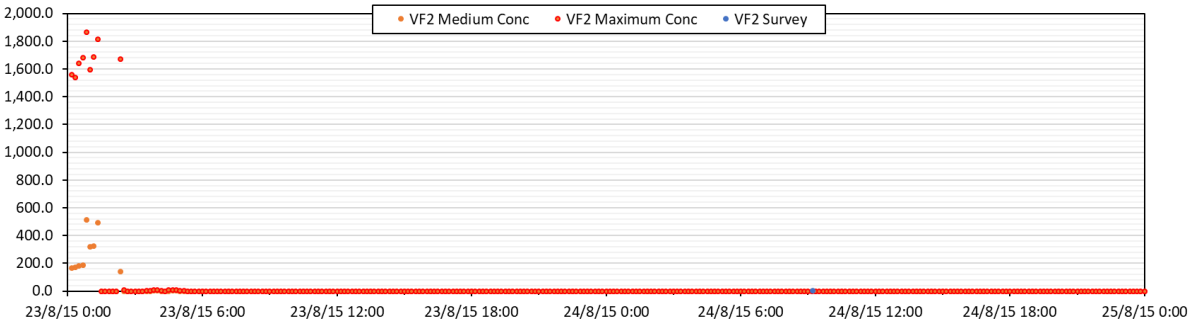

Figure 5.33. Temporal variation of *escherichia coli* concentration in survey point VF2

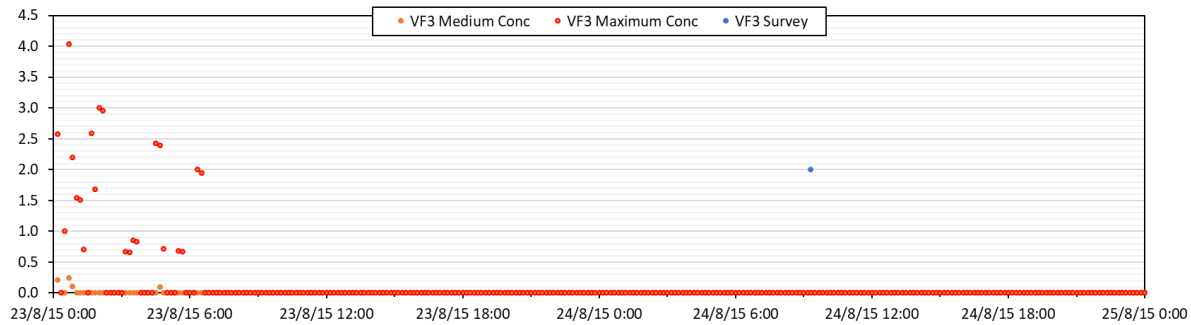

Figure 5.34. Temporal variation of *escherichia coli* concentration in survey point VF3

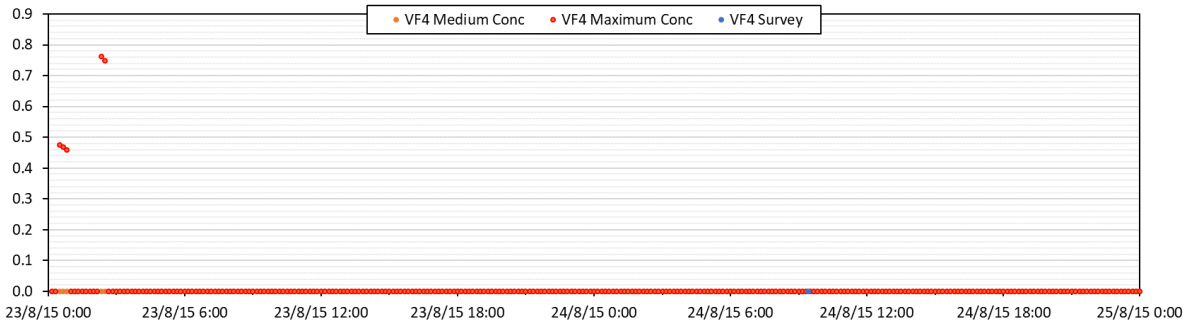

Figure 5.35. Temporal variation of *escherichia coli* concentration in survey point VF4

5.5.2 S1 – Bathing Waters Impact

The Lagrangian tracer results for simulation of bathing water quality impact are displayed from Figure 5.36 to Figure 5.39 with two time instances results that represent the worst case scenario, early in the morning when the sun is still weak and we have an increase in the discharged flows and at the end of the day with the peak flow and low solar radiation.

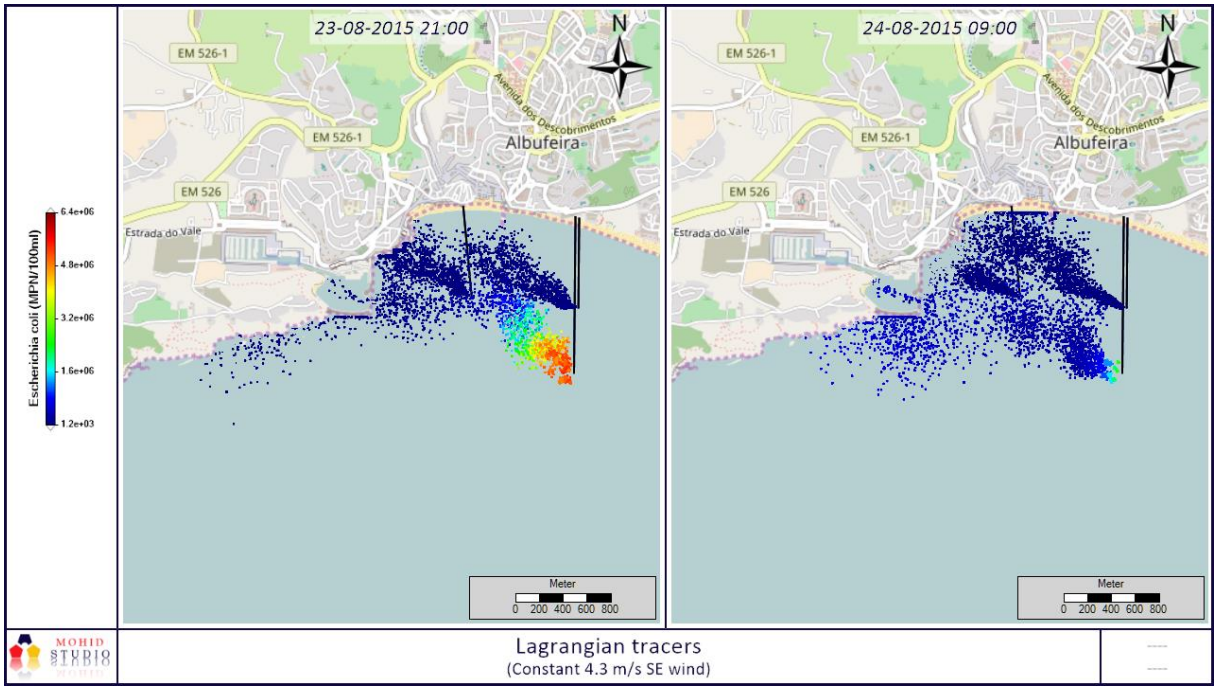

Figure 5.36. Run S1 Lagrangian tracers results with SE wind

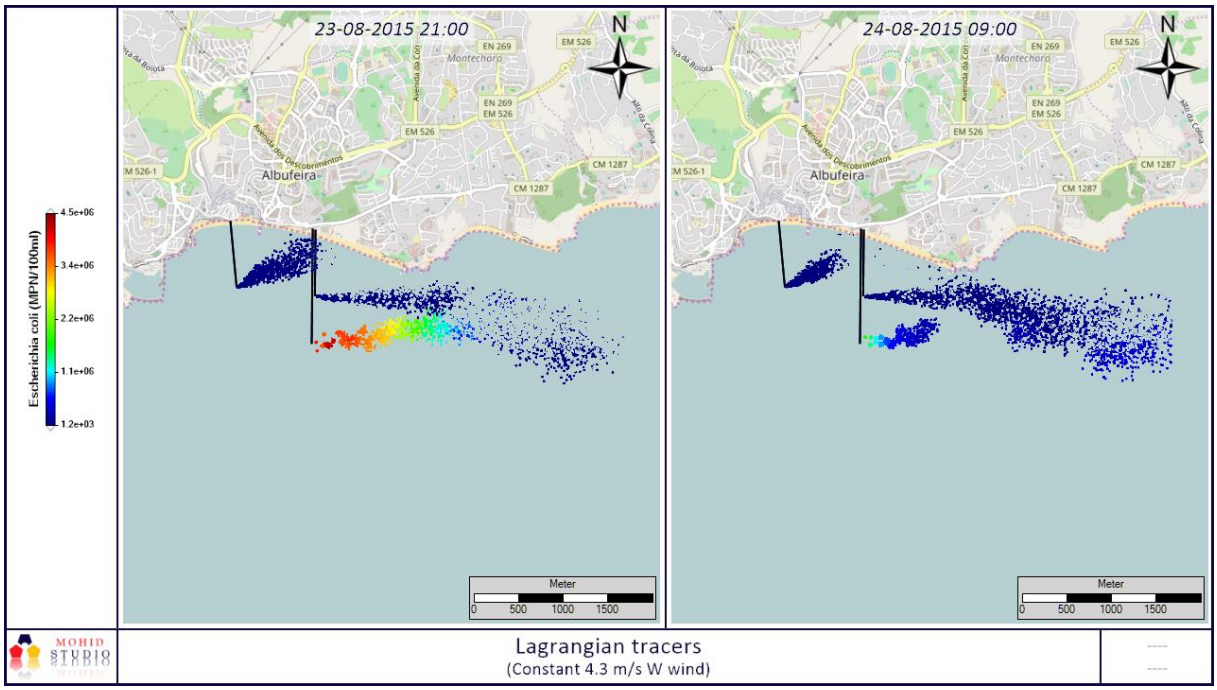

Figure 5.37. Run S1 Lagrangian tracers results with W wind

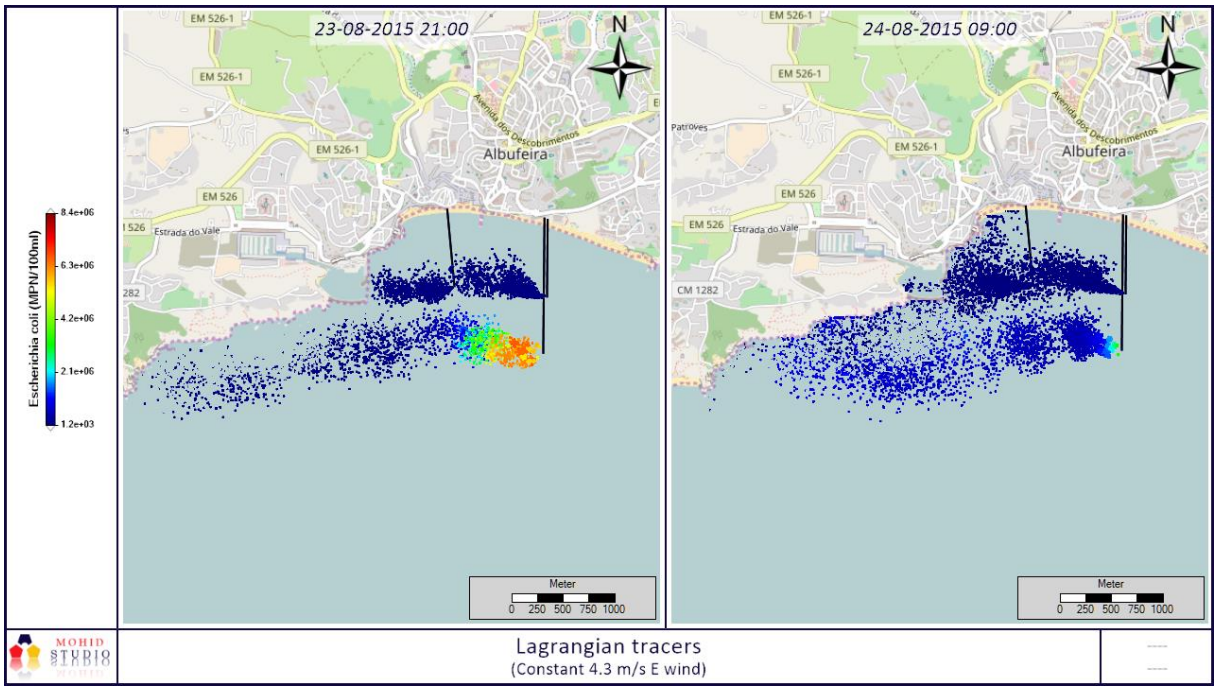

Figure 5.38. Run S1 Lagrangian tracers results with E wind

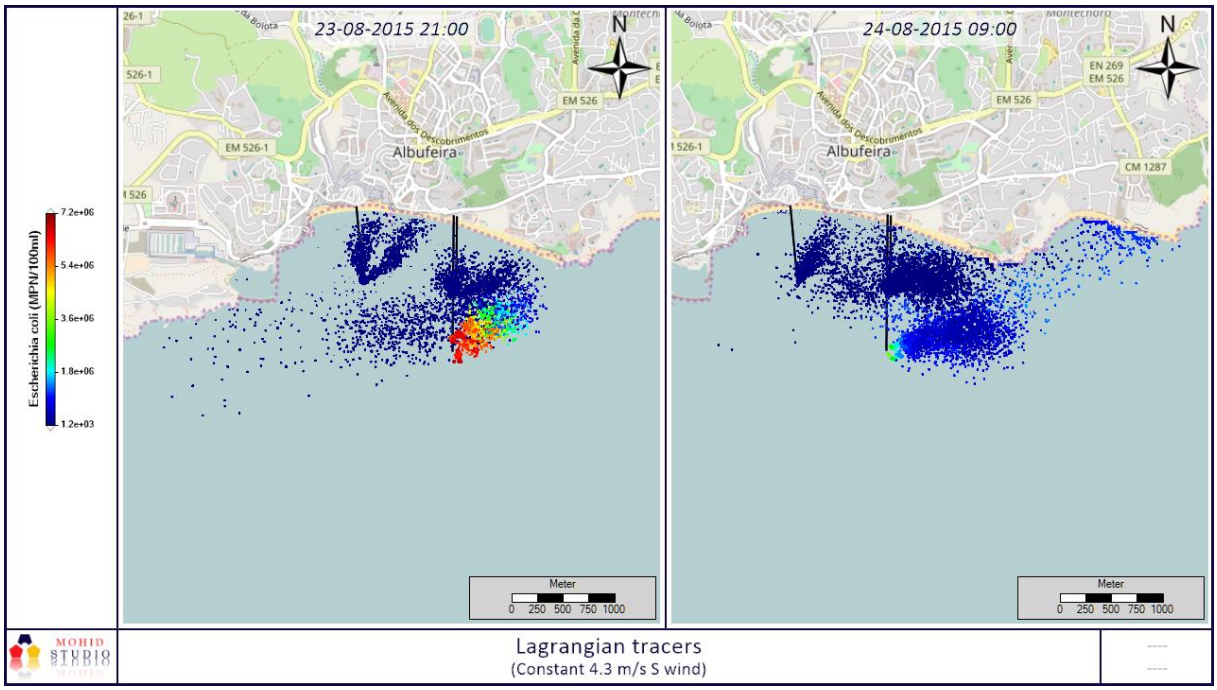

Figure 5.39. Run S1 Lagrangian tracers results with S wind

Figure 5.40 to Figure 5.42 shows the initial dilution given by the MOHIDJET (near-field) module used as an initial condition of Lagrangian tracer's module (far-field).

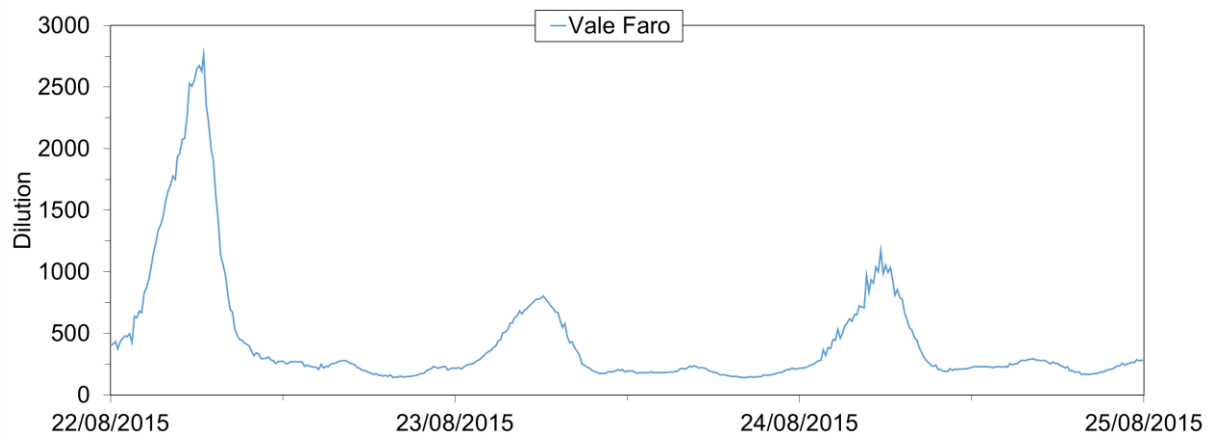

Figure 5.40. Vale Faro outfall initial dilution

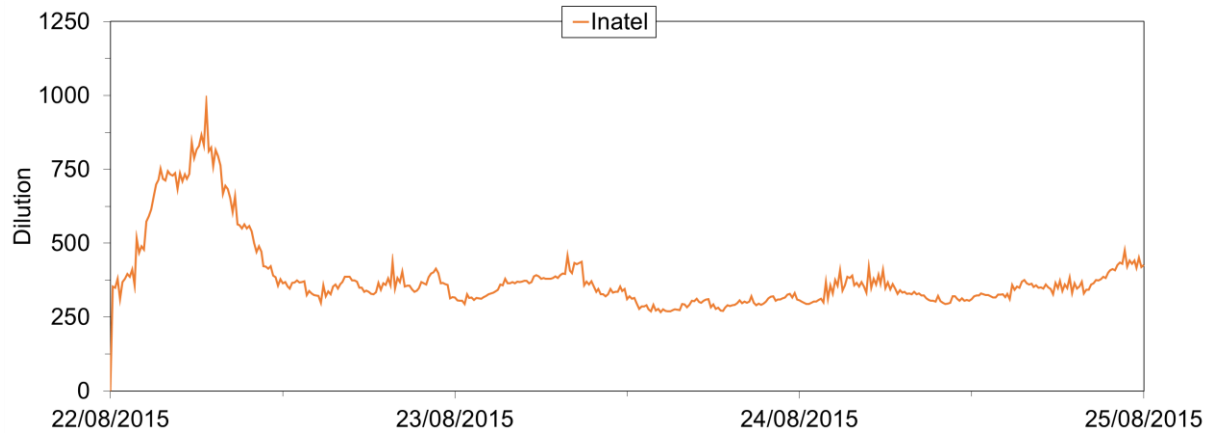

Figure 5.41. Inatel outfall initial dilution

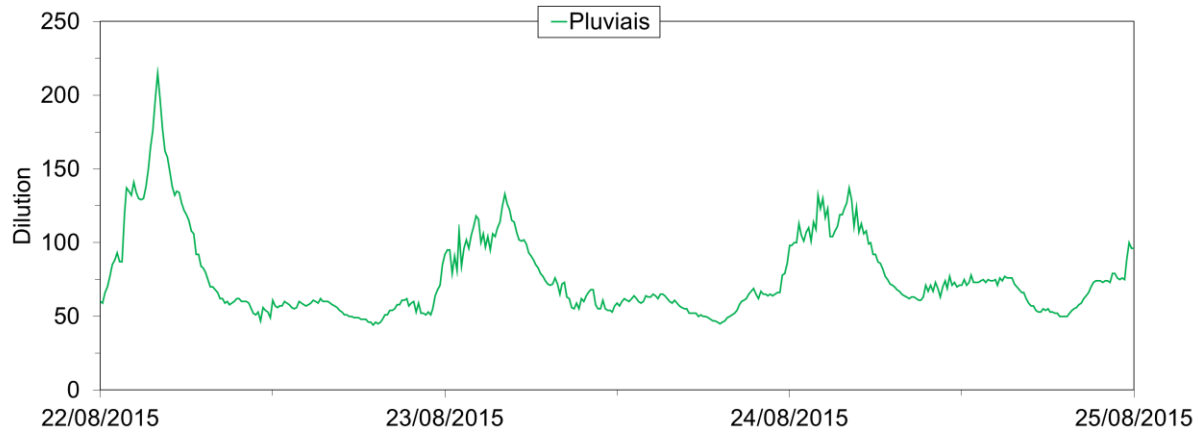

Figure 5.42. Pluviais outfall initial dilution

Figure 5.43 show the results of the velocity modules near the diffuser of each outfall.

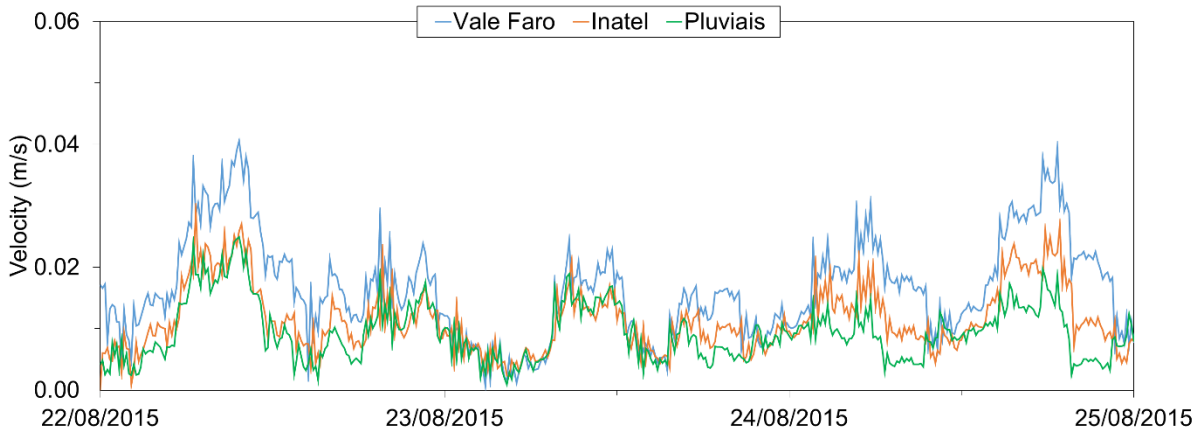

Figure 5.43. Velocity modulus near the outfall diffusers

5.5.3 S2 – Vale Faro WWTP Discharge Limit

The Lagrangian tracer results for simulation of bathing water quality impact with several discharge limits of treated effluent from Vale Faro WWTP and S wind are displayed from Figure 5.44 to Figure 5.47 with two time instances results that represent the worst case scenario, early in the morning when the sun is still weak and we have an increase in the flow and at the end of the day with the peak flow and low solar radiation.

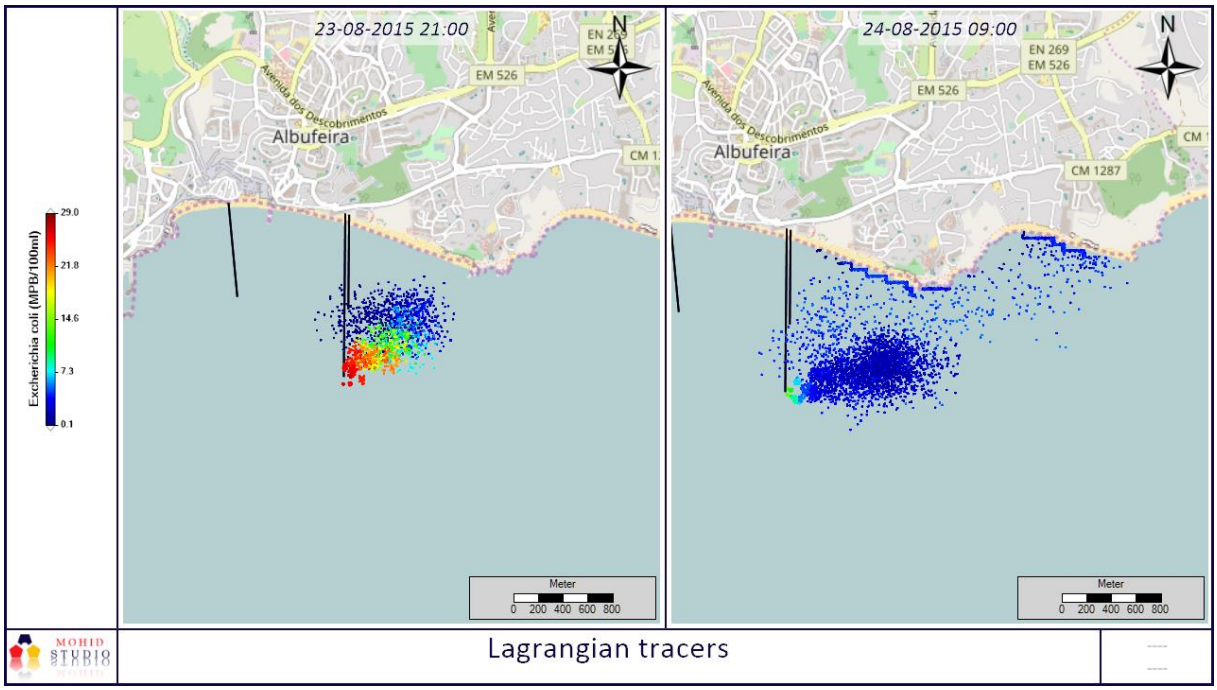

Figure 5.44. Run S2 Lagrangian tracers results with treated effluent discharge of 2×10^3 MPN of *Escherichia coli*

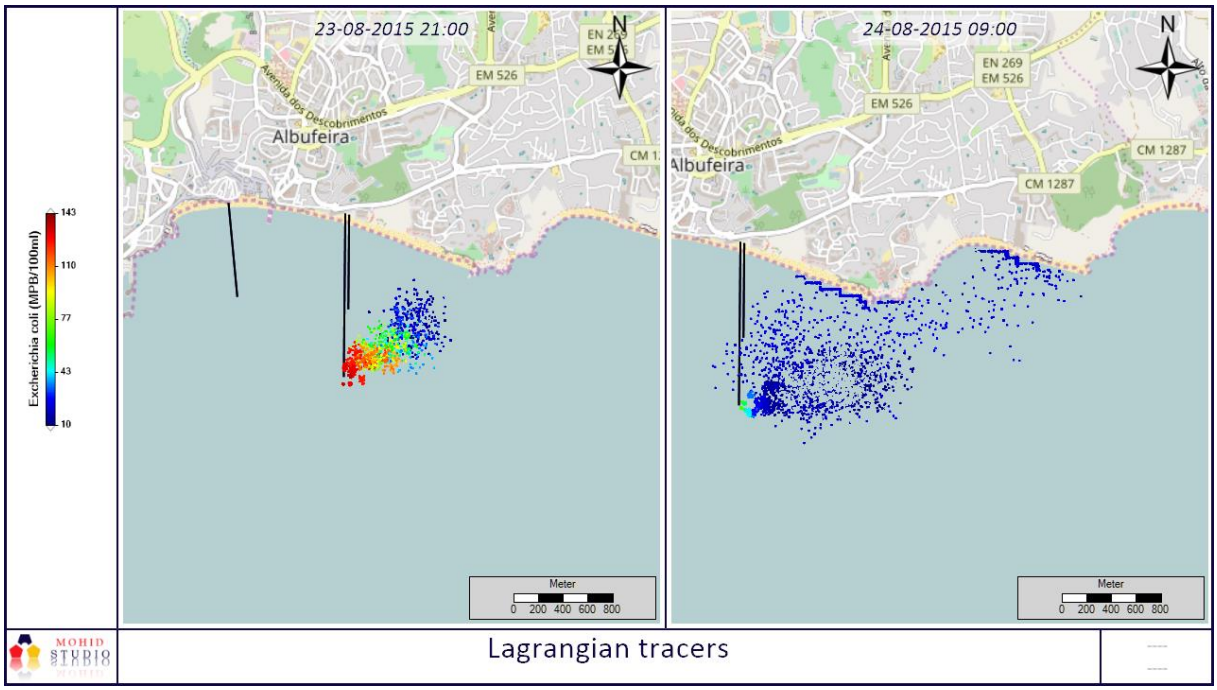

Figure 5.45. Run S2 Lagrangian tracers results with treated effluent discharge of 1×10^4 MPN of *Escherichia coli*

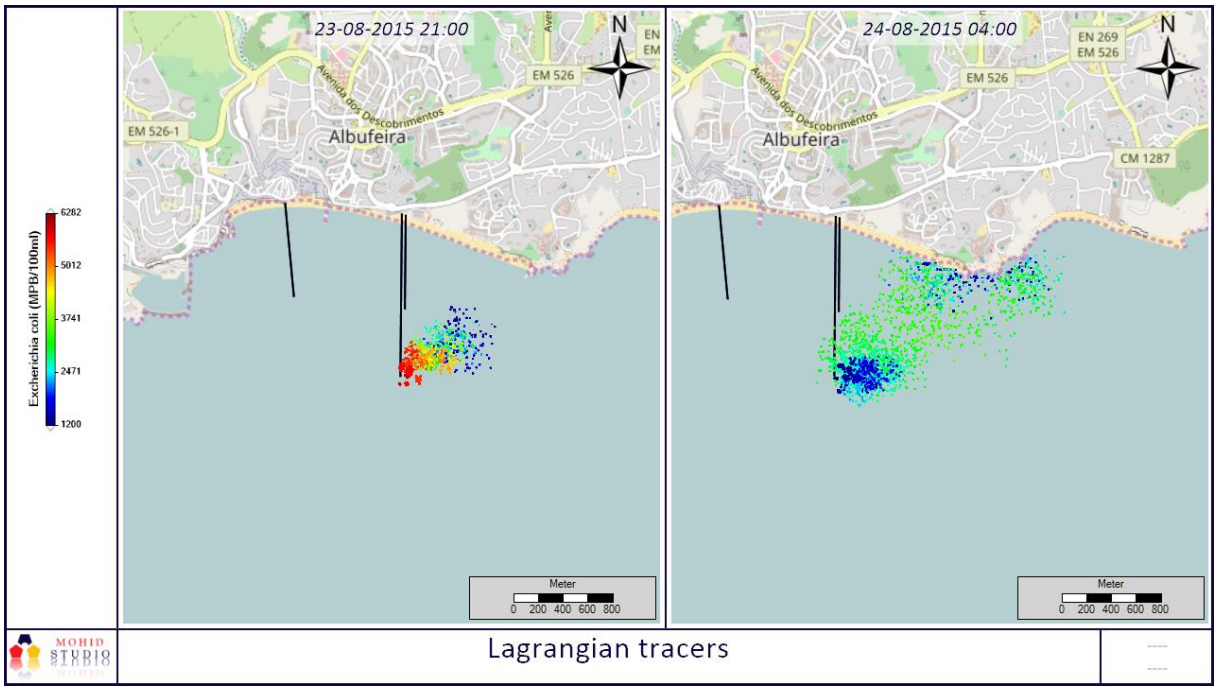

Figure 5.46. Run S2 Lagrangian tracers results with treated effluent discharge of 4.4×10^5 MPN of *Escherichia coli*

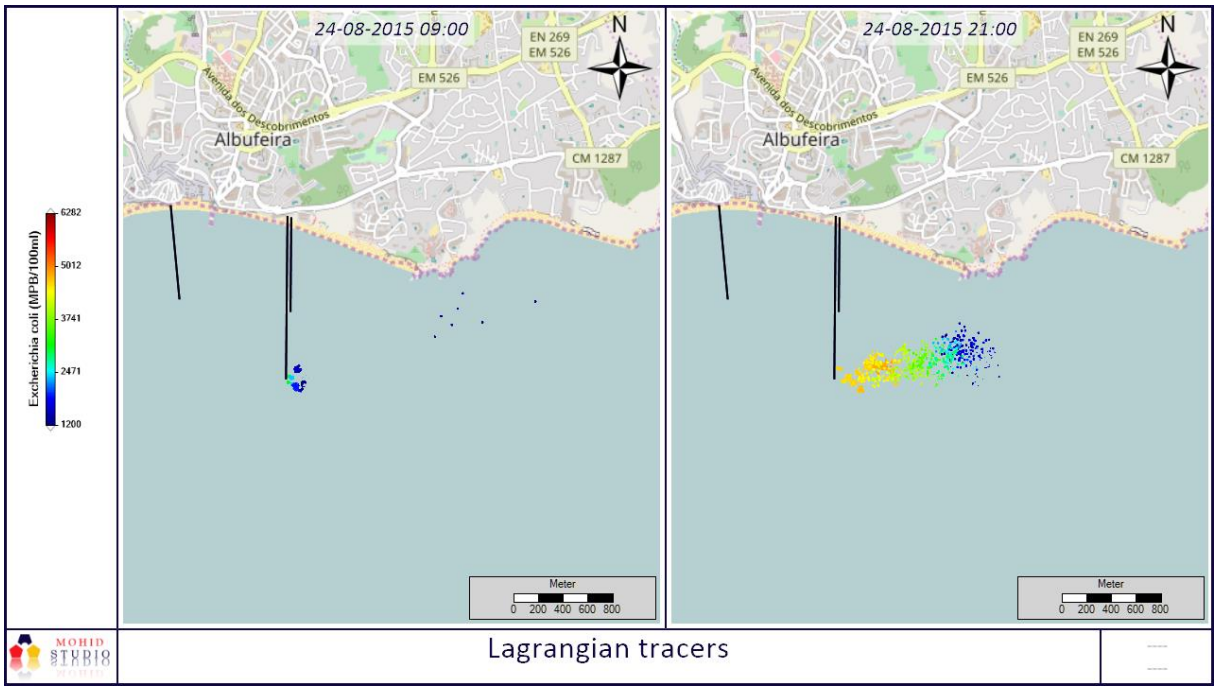

Figure 5.47. Run S2 Lagrangian tracers results with treated effluent discharge of 4.4×10^5 MPN of *escherichia coli*

6 DISCUSSION

6.1 FIELD CAMPAIGNS

The Vale Faro WWTP shows a typical flow pattern of a WWTP in a highly tourism occupied area as there are two peak flows during the day. One early in the morning rising from the minimum flow at about 4:00 AM until the morning peak at about 09:00 AM. The maximum flow occurs at the end of day around 19:00 PM. The flow measurement of Inatel outfall flows are consistent with the flow patterns of the WW infrastructures in the city.

The data gathered in the weather stations allowed to validate the dominant winds in the study area, although with more historical data from the Vale Faro WS it would give better information in the outfalls area of influence. Algoz WS shows a high predominance of north winds in the bathing season as well as outside of the bathing season. Loulé WS shows a predominance of Northwest winds followed by North, East and South-eastern winds outside the bathing season. In the bathing season, the winds of North, Northeast, Northwest and Southwest prevail. Paderne WS that is closest to the study area shows a predominance of South-eastern, Southern and Northern winds during the, and outside the bathing season there is still a Frequency of East and Northeast winds. The Faro airport station has a high predominance of north winds followed by east and west winds outside the bathing season while during the bathing season the prevailing wind was west followed by east-southeast winds. As for the data collected by Vale Faro WS, the predominant wind was from North. Taking in consideration the results from the analysed WS data, the wind directions considered in the simulations were from the West, South, Southeast and East to investigate the impact of the outfall plumes in bathing water quality.

The results of the tide level were obtained by consulting the DGT website as referred to in chapter 4.1.3. A total of 3084 records were obtained between 08/15/2015 00:10 and 08/24/2015 23:58 with 35.7% invalid/null, however, for the period under analysis the records invalid/null records represent 0.7%.

The field results, showed contamination of *escherichia coli* in Pluviais outfall discharge in all field campaigns (24×10^4, 24×10^3 and 24×10^5 MPN/100ml) and in Inatel outfall in the field campaign of 24/08/2015 ($>24\times10^5$ MPN/100ml) and 22/08/2016 ($>24\times10^3$ MPN/100ml) evidencing wastewater contamination upstream of these water lines. In the field campaign of 22/08/2016 shows a value of *escherichia coli* in the Vale Faro outfall bigger then the discharge limit. Despite the discharges from the outfalls higher than the limit value discharge, there was no impact in any of the bathing waters for all field campaigns. Regarding the ocean water

samples, none had values higher than the required limit, with exception of IN2 showing a concentration of 24×10^3 MPN/100ml *escherichia coli* during the field campaign of 24th august, 2015.

6.2 MODEL VALIDATION

The modelling results show realistic solution allowing a characterization of dispersion, its efficiency and the processes controlling it. The model was applied in the Albufeira Bay, obtaining the temporal variation of currents, water levels, salinity, and bacteriological parameters at stipulated points of the analysed domain.

As shown in Figure 5.17, the simulated water level results are in good agreement with the available field data, both in amplitude and phase. The root mean square error (RMSE) is equal to 44 mm for the analysed period and a correlation value of 0.997.

The initial dilution of the wastewater effluent discharged from the ocean outfall in the near field depends primarily on the discharge characteristics, diffuser geometry, the depth of discharge, and the ambient conditions of current and density (Kim et al., 2001). The model showed higher dilution values with smaller flows and the opposite with bigger flows. Despite having the biggest discharged flow, Vale Faro outfall presents better dilution values when compared with Pluviais outfall that has the same diameter but a different diffuser type. In regard of Vale Faro outfall dilution values, it achieved values around 1:200 and 1:1000 during peak flows and values of about 1:5000 with low discharged flows.

The model also shows that the main ambient conditions driving the dispersion are wind and tide. The ocean currents taken in consideration in had a modest contribution to the total dynamics of the area, as wind and tide are the main factors affecting dispersion. The current velocity near the outfalls diffusers follow the same pattern although with different velocity modulus (Figure 5.24). The biggest hydrodynamic velocity near the diffusers is observed in the Vale Faro outfall.

The comparison of the model results for the e*scherichia coli* Lagrangian tracers showed little concordance in *faecal* concentration but a good agreement in the plume direction. This fact may be due to the number of particles used in the calculation method, and in future work, more particles and a computation mesh will be used for the concentration of e*scherichia coli* other than the hydrodynamic mesh. Another situation is the lack of knowledge of the structural condition of the outfalls and diffusers.

6.3 BATHING WATER IMPACT

As expected, the concentration of *escherichia coli* is highest in the early morning and end of the day, decreasing as the solar radiation rises due to strong UV radiation.

The wind conditions simulated show that the risk of bathing water quality impact is higher in the bathing waters of Albufeira city bay (Peneco, Pescadores, Inatel) with SE winds mainly by influence of Vale Faro outfall. West winds push the plumes parallel to the coast with small risk of affecting Inatel bathing water. South winds can affect bathing water quality in a bigger number of bathing waters such as Peneco, Pescadores, Inatel, Aveiros and Oura. The simulations where run with a constant discharge of faecal contamination, therefore real situations of the impact on bathing water quality will always depend on the concentration, flow, time and duration of the discharge.

The results for the simulations with constant wind speed and direction showed lower dilution values for all outfalls as showed in Figure 5.40 to Figure 5.42.

6.4 VALE FARO WWTP DISCHARGE LIMIT

South winds show higher risk of bathing water contamination, for that reason this wind condition was chosen to access a safe discharge limit value of Vale Faro outfall without the need of disinfection, saving operational and maintenance costs in the facility management. Results showed that by obeying the discharge limit of 2000 MPN/100ml *escherichia coli* the risk of affecting bathing water quality is very low with a maximum value verified of about 29 MPN/100ml *escherichia coli* during the entire run near the diffuser early in the morning.

By increasing the limit from 2000 to 1×10^4 MPN/100ml *escherichia coli*, the model achieves a maximum value of about 143 near the outfall diffuser and 10 in the bathing waters of Alemães and Oura, still a very low risk of affecting bathing water quality.

A simulation was run considering the inexistence of disinfection with a concentration of 4.4×10^5 MPN/100ml, showing that the impact in the bathing water can be minimum, with a maximum concentration of about 6282 MPN/100ml *escherichia coli* during the entire simulation and 2471 to 3741 in Alemães bathing water around 4:00 AM.

7 CONCLUSIONS

A three-dimensional hydrodynamic model and a Lagrangian tracer transport model coupled with a near field model MOHIDJET was applied to study the marine outfalls in the Albufeira Bay nested to the Algarve operational model SOMA. The objective is to determine the impact of WWTP discharges in the bathing water quality and the dilution efficiency of submarine outfalls. Data analysis and results of hydrodynamic modelling showed that the wind and tide are the determining factor for the oceanic circulation in the bay. The *escherichia coli* concentrations are also very dependable of the solar radiation time and duration of the discharge.

In order to get more accurate results, and better determination of dynamic characteristics of the discharged effluent and the receiving ambient environment, a weather station was installed in Vale Faro WWTP during this study.

Operational and maintenance costs can be reduced in the Vale Faro WWTP if the discharge limit is raised during the bathing season.

The future work in this study must comprise:

i) The hydrodynamic model showed realistic results in accordance to literature and allowed an characterization of dispersion in the bay with different wind conditions. The model was validated by comparison of the model water level results against measurements in Lagos tide gauge;

ii) The near filed dilution was influenced mainly by outfall diffusers geometry and discharged flows;

iii) In the far field, the results showed that the beaches in the Albufeira Bay are more exposed to possible bathing waters contamination mainly with S winds;

iv) Use an integrated approach in the drainage system, linking a mathematical model in the wastewater and runoff transport infrastructures like EPA SWMM with a mathematical model (GPSX) in the WWTP;

v) A video inspection for accessing the structural conditions of the outfalls and diffusers;

vi) Field campaigns are also planned to execute in the bathing season to continuously access the outfall discharge.

REFERENCES

Allen, C. (1982). Numerical Simulation of Contaminant Dispersion in Estuary Flows. *Proceedings of the Royal Society A: Mathematical, Physical and Engineering Sciences, 381*(1780), 179-194. doi:10.1098/rspa.1982.0064

AVISO+. (2017). Retrieved 04 17, 2017, from http://www.aviso.altimetry.fr/en/data/products/auxiliary-products/global-tide-fes/description-fes2014.html

Baumgartner, D., Frick, W. E., & Roberts, P. (1994). *Dilution models for effluent discharges* (3 ed.). Washington DC, USA: EPA. Retrieved February 23, 2017

Blaustein, R., Pachepsky, Y., Hill, R., Shelton, D., & Whelan, G. (2013). Escherichia coli survival in waters: Temperature dependence. *Water Research, 47*, 569-578.

Chapra, S. (1997). *Surface water-quality modeling* (1 ed.). New York: McGraw-Hill.

Davis, M. (2010). *Water and Wastewater Engineering - Design Principles and Practice.* New York: McGraw-Hill.

Deltares. (2016, January 27). *About Delft3d*. Retrieved January 27, 2016, from Deltares Web site: http://oss.deltares.nl/web/delft3d/about

DGT. (2014). *CAOP*. Retrieved 10 3, 2016, from http://www.dgterritorio.pt/ficheiros/cadastro/caop/caop_download/caop_2014_0/areas fregmundistcaop2014_2

DHI. (2016, January 27). *MIKE 21 & MIKE 3 Flow Model FM: Hydrodynamic Module Short Description.* Retrieved January 27, 2016, from MIKE Powered by DHI Web site: www.mikepoweredbydhi.com/-/media/shared%20content/mike%20by%20dhi/flyers%20and%20pdf/product-documentation/short%20descriptions/mike213_fm_hd_short_description.pdf

Doneker, R., & Jirka, G. (2007). CORMIX user manual: A hydrodynamic mixing zone model and decision support system for pollutant discharges into surface waters. Washington DC, USA: EPA.

EPA. (2002). *User's manual for environmental fluid dynamics code, hydro version (draft).* Atlanta (USA): EPA.

EPA Ireland. (1997). *Wastewater treatment manuals - Primary, Secondary an Tertiary Treatment.* Ireland.

Eregno, F., Tryland, I., Tjomsland, T., Myrmel, M., Robertson, L., & Heistad, A. (2016). Quantitative microbial risk assessment combined with hydrodynamic modelling to estimate the public health risk associated with bathing after rainfall events. *Science of The Total Environment*, 270-279. doi:10.1016/j.scitotenv.2016.01.034

ERTA. (2016, September 24). *História do Concelho de Albufeira - Portal de Turismo do Algarve*. Retrieved September 24, 2016, from Visitalgarve Web site: www.visitalgarve.pt/visitalgarve/vPT/DescubraARegiao/132/Concelhos/Albufeira/Historia

Fernandes, R. (2005). *Modelação Operacional no Estuário do Tejo.* Doctoral Thesis, Universidade Técnica de Lisboa - Instituto Superior Técnico, Lisboa.

Gao, G., Falconer, R., & Lin, B. (2015). Modelling the fate and transport of faecal bacteria in estuarine and coastal waters. *Marine Pollution Bulletin, 100*(1), 162-168. doi:10.1016/j.marpolbul.2015.09.011

Georgiou, S., & Bateman, I. J. (2005). Revision of the EU Bathing Water Directive: economic costs and benefits. *Marine Pollution Bulletin, 50*(4), 430-438. doi:10.1016/j.marpolbul.2004.11.036

Hamrick, J. (1992). *A Three-Dimensional Environmental Fluid Dynamics Computer Code: Theoretical and Computational Aspects.* The College of William and Mary, Virginia Institute of Marine Science.

Henze, M., & Comeau, Y. (2008). Wastewater Characterization. In M. Henze, *Biological Wastewater Treatment: Principles Modelling and Design.* London: IWA.

Hidra. (2016). *Plano Geral de Drenagem de Albufeira.* Relatório de Progresso, Albufeira.

Horikawa, K. (1988). *Nearshore dynamics and coastal processes.* Tokyo (Japan): Univ. of Tokyo Press.

HydroQual, Inc. (2002). A primer for ECOMSED, Version 1.3, User's Manual.

INE. (2012). Retrieved 10 3, 2016, from https://www.ine.pt/xportal/xmain?xlang=en&xpid=INE&xpgid=ine_indicadores&indOcorrCod=0005889&contexto=pi&selTab=tab0

Janeiro, J. (2014). *Development of an operational tool for oil spill forecast: application to oil exposed regions.* Doctoral Thesis, Universidade do Algarve, Faro (Portugal). Retrieved September 27, 2016, from http://hdl.handle.net/10400.1/6865

Janeiro, J., Martins, F., & Relvas, P. (2012). Towards the development of an operational tool for oil spills management in the Algarve coast. *Journal of Coastal Conservation, 16*(4), 449-460. doi:10.1007/s11852-012-0201-8

Janeiro, J., Neves, A., Martins, F., & Relvas, P. (2017). Integrating technologies for oil spill response in the SW Iberian coast. *Journal of Marine Systems, 173*, 31-42. doi:https://doi.org/10.1016/j.jmarsys.2017.04.005

Jasak, H., Jemcov, A., & Tukovic, Z. (2007). OpenFOAM: A C++ Library for Complex Physics Simulations. *International Workshop on Coupled Methods in Numerical Dynamics.* Dubrovnik: IUC. Retrieved August 25, 2016, from http://powerlab.fsb.hr/ped/kturbo/openfoam/papers/CMND2007.pdf

Jirka, G. (1999). Five Asymptotic Regimes of a Round Buoyant Jet in Stratified Crossflow. *28th IAHR Biennial Congress.* Graz (Austria): IAHR.

Jirka, G., Doneker, R., & Hinton, S. (1996). User's manual for CORMIX: A hydrodynamic mixing zone model and decicion support system for pollutant discharges into surface waters. New York: DeFrees Hydraulics Laboratory, Cornell University.

Kallos, G., & the SKIRON group. (1998). *The SKIRON forecasting system: VOL. I: Preprocessing ISBN 960–8468–15–9; VOL. II: Model description ISBN 960–8468–16–7; VOL. III: Numerical techniques ISBN 960–8468–17–5; VOL. IV: Parallelization ISBN 960–8468–18–3; VOL. V: Postprocessing ISBN 960–8468–19* (Vol. I).

Kay, D., Stapleton, C., Wyer, M., McDonald, A., Crowther, J., Paul, N., . . . Gardner, S. (2005). Decay of intestinal enterococci concentrations in high-energy estuarine and coastal waters: towards real-time T90 values for modelling faecal indicators in recreational waters. *Water Research, 39*(4), 655-667. doi:10.1016/j.watres.2004.11.014

Kenov, I. A., Campuzano, F., Franz, G., Fernandes, R., Viegas, C., Sobrinho, J., . . . Neves, R. (2014). Advances in Modeling of Water Quality in Estuaries. In C. Finkl, & C. Makowski, *Remote Sensing and Modeling: Advances in Coastal and Marine Resources* (9, Trans.). Springer.

Lee, J., & Cheung, V. (1990). Generalized Lagrangian Model for Buoyant Jets in Current. *Journal of Environmental Engineering, 116*(6), 1085-1106. doi:10.1061/(asce)0733-9372(1990)116:6(1085)

Leitão, P. (2002). *Integração de Escalas e de Processos na Modelação no Ambiente Marinho.* Doctoral Thesis, Instituto Superior Técnico. Retrieved September 27, 2016, from http://www.mohid.com/Publications/Thesis.asp

Leitão, P., Coelho, H., Santos, A., & Neves, R. (2005). Modelling the main features of the Algarve coastal circulation during July 2004: A downscaling approach. *Journal of Atmospheric & Ocean Science, 10*(4), 421-462. doi:10.1080/17417530601127704

Leitão, P., Neves, R., Braunschweig, F., Leitão, J., & Fernandes, R. (2004). Simulação Integrada da Dispersão de Poluentes no Campo Próximo e no Campo Afastado de um Emissário. *7º Congresso da Água* (pp. 1-15). Lisboa: APRH.

López, I., Álvarez, C., Gil, J., & Revilla, J. (2013). Methodology to elaborate the bathing water profile on urban beaches, according to the requirements of the European Directive 2006/7/EC: the case of Santander beaches (Spain). *Water Science & Technology, 68*(5), 1037. doi:10.2166/wst.2013.342

Mangor, K. (2008). *Currents*. Retrieved 04 17, 2017, from http://www.coastalwiki.org/wiki/Currents

Mangor, K. (2008). *Waves*. Retrieved 04 12, 2017, from http://www.coastalwiki.org/wiki/Waves

Mansilha, C., Coelho, C., Heitor, A., Amado, J., Martins, J., & Gameiro, P. (2009). Bathing waters: New directive, new standards, new quality approach. *Marine Pollution Bulletin, 58*(10), 1562-1565. doi:10.1016/j.marpolbul.2009.03.018

MAOT. (2000). *Plano de Bacia Hidrográfica das Ribeiras do Algarve.*

Marsalek, J., Jiménez-Cisneros, B., Malmquist, P., Karamouz, M., Goldenfum, J., & Chocat, B. (2006). *Urban water cycle processes and interactions.* Retrieved March 6, 2017, from https://hydrologie.org/BIB/Publ_UNESCO/TD_078_2006.pdf

Martins, F. (1999). *Modelação Matemática Tridimensional de Escoamentos Costeiros e Estuarinos usando uma Abordagem de Coordenada Vertical Genérica.* Lisboa: Universidade Técnica de Lisboa - Instituto Superior Técnico.

Martins, F., Janeiro, J., Gabriel, S., Venâncio, A., & Neves, R. (2009). Integrated monitoring of South Portugal water bodies: a methodology towards WFD. *Water Science & Technology, 60*(8), 1979. doi:10.2166/wst.2009.509

Martins, F., Leitão, P., Silva, A., & Neves, R. (2001). 3D modelling in the Sado estuary using a new generic vertical discretization approach. *Oceanologica Acta, 24*(1), 51-62. doi:10.1016/s0399-1784(01)00092-5

Miranda, R., Braunschweig, F., Leitão, P., Neves, R., Martins, F., & Santos, A. (2000). MOHID 2000 - A Coastal Integrated Object Oriented Model. *WIT Transactions on Ecology and the Environment, 40*. doi:10.2495/HY000371

MOHID. (2016, January 27). Retrieved January 27, 2016, from MOHID Web site: www.mohid.com

Naidu, V. (2013). Estimation of Near-Field and Far-Field Dilutions for Site Selection of Effluent Outfall in a Coastal Region - A Case Study. *Journal of Coastal Research, 292*, 1326-1340. doi:10.2112/jcoastres-d-11-00159.1

NASA. (2017). *Ocean in Motion*. Retrieved 6 8, 2017, from http://oceanmotion.org/

National Geographic. (2017, March 6). *Water Currents*. Retrieved from National Geographic: http://voices.nationalgeographic.com/2014/03/19/the-urban-water-cycle-sustaining-our-modern-cities/

NOAA. (2011). *Ocean currents*. Retrieved 04 17, 2017, from http://www.noaa.gov/resource-collections/ocean-currents

Open University. (1999). *Waves, Tides & Shallow-Water Processes* (2 ed.).

Owens, E., Effler, S., Matthews, D., & Prestigiacomo, A. (2013). Evaluation of Offshore Wastewater Outfall and Diffuser for Onondaga Lake, NY. *Journal of Water Resource and Protection, 5*, 1-15. doi:10.4236/jwarp.2013.59A001

Pinardi, N., & Flemming, N. (1998). The Mediterranean Forecasting System Science Plan. *N.º11*. Southampton, UK: EuroGOOS. Retrieved September 27, 2016, from www.vliz.be/imisdocs/publications/260018.pdf

Prinos, P. (2016). *Modelling coastal hydrodynamics*. Retrieved 04 12, 2017, from http://www.coastalwiki.org/wiki/Modelling_coastal_hydrodynamics

Reed, M., Hetland, B., Ditlevsen, M., & Ekrol, L. (2001). DREAM Version 2.0. Dose Related Risk Effect Assessment Model, Users Manual. Trøndheim, Norway: SINEF Applied Chemistry.

Riflet, G. (2010). *Downscaling large-scale ocean-basin solutions in coastal tridimensional hydrodynamic models.* Doctoral Thesis, Instituto Superior Técnico, Lisboa. Retrieved September 27, 2016, from www.mohid.com/PublicData/products/Thesis/PhD-griflet-2010.pdf

Roberts, P., Salas, H., Reiff, F., Libhaber, M., Labbe, A., & Thomson, J. (2010). *Marine Wastewater Outfalls and Treatment Systems.* London: IWA Publishing.

Sabeur, Z., & Tyler, A. (2004). Validation and application of the PROTEUS model for the physical dispersion, geochemistry and biological impacts of produced waters. *Environmental Modelling & Software, 19*(7-8), 717-726. doi:10.1016/j.envsoft.2003.08.006

Sánchez-Arcilla, A., & Lemos, C. (1990). *Surf-zone Hydrodynamics.* Centro Internacional de Métodos Numéricos de Ingeniería.

Santos, C., Barreiros, A., Pestana, P., Cardoso, A., & Freire, A. (2011). Environmental status of water and sediment around submarine outfalls – west coast of Portugal. *Journal of Integrated Coastal Zone Management, 11*(2), 207-217. doi:10.5894/rgci243

Seth / Etermar / Hidrocontrato. (2004). *Projeto de execução da Empreitada de concepção-construção de reforço da etapa de desinfecção da ETAR de Vale Faro, em Albufeira e das correspondentesinfraestruturas de rejeição no mar das águas residuais tratadas.*

Silva, O., Bento, N., Primo, N., & Martins, A. (2013). Otimização do consumo energético associado ao sistema de arejamento da ETAR de Vale Faro. *ENEG.* Coimbra (Portugal).

Tate, P., Scaturro, S., & Cathers, B. (2016). Marine Outfalls. In M. Dhanak, & N. Xiros, *Handbook of Ocean Engineering* (pp. 711-740). New York: Springer.

Tchobanoglous, G., Burton, F., & Stensel, D. (2003). *Wastewater engineering.* New York: McGraw-Hill.

Tucson Water. (2017, March 6). *Our Urban Water Cycle*. Retrieved from City of Tucson: https://www.tucsonaz.gov/water/cycle

UNESCO. (1981). Tenth report of the joint panel on oceanographic tables and standards. *UNESCO Technical Papers in Marine Science, 36*, 24.

Zhao, L., Chen, Z., & Lee, K. (2011). Modelling the dispersion of wastewater discharges from offshore outfalls: a review. *Environmental Reviews, 19*, 107-120. doi:10.1139/a10-025